

# Pattern Matching and Detection in Extremely Resource Constrained Wireless Sensor Networks

**Michael Zoumboulakis**

May 2011

A Dissertation Submitted to  
Birkbeck College, University of London  
in Partial Fulfillment of the Requirements  
for the Degree of Doctor of Philosophy

School of Computer Science & Information Systems  
Birkbeck College  
University of London

# Declaration

This thesis is the result of my own work, except where explicitly acknowledged in the text.

Michael Zoumboulakis \_\_\_\_\_  
May 8, 2011

# Abstract

This thesis investigates the problem of pattern matching and detection in extremely resource constrained Wireless Sensor Networks (WSNs). Specifically, it introduces a collection of in-network methods and algorithms which exploit the observation that processing data inside the network, instead of transmitting it off-network, offers a distinct advantage for sensor node longevity through reduction of network communication.

Operating on windowed sensor observations, we develop temporal domain algorithms that apply symbolic conversion and examine the resulting strings for interesting or unusual patterns with a choice of exact, approximate, non-parametric, probabilistic and multiple pattern matching and detection methods. Precise implementation of the algorithms with integer-only arithmetic, results into a computationally efficient execution profile and modest RAM requirements.

Furthermore, we develop a spatial pattern event location estimation algorithm that combines a geometric method with the application of the Kalman filter to iteratively compute an estimate of the pattern event source location and intensity. This algorithm is decentralised and operates by tasking WSN nodes to collaborate by exchanging information with local neighbours in order to improve estimate accuracy with respect to location and intensity of the spatial pattern event source.

We provide evidence that the proposed algorithms are competitive against alternative methods and validate their operational performance through deployment on WSN nodes and simulations. Overall, we find the proposed algorithms support reactive behaviour in the case of WSNs and align well with the generic goal of preserving resources.

To my parents

# Acknowledgements

I owe my deepest gratitude to my supervisor Dr. George Roussos whose encouragement, guidance and support enabled me to gain a deep understanding of Wireless Sensor Networks and Ubiquitous Computing. I am also indebted to my second supervisor Prof. Alexandra Poulouvassilis for steering my research and providing valuable feedback. Dr. Eleftheria Katsiri deserves special thanks and credit for the idea of an efficient Integer-only Complex Event Detection implementation. I am grateful to Prof. Eamonn Keogh for patiently answering questions about Symbolic Aggregate Approximation and providing relevant test data. I would like to extend my gratitude to Dr. Nigel Martin who provided the valuable support for this research.

On a personal level, my warmest thanks go to my parents and my two sisters whose unconditional love and support made this thesis possible. I am grateful to my Knowledge Lab colleagues Dimitrios Airantzis, Lucas Zamboulis, Rajesh Pampapathi and Jenson Taylor for their help and friendship. Marco Luchini deserves special thanks for financing part of my research in return for (sometimes frightening) work on critical systems. Finally, I am indebted to my friends Vassili, Vasso, Michael, Jack and Helge for their friendship and support throughout the process.

# Contents

<b>Abstract</b>	<b>3</b>
<b>Acknowledgements</b>	<b>5</b>
<b>1 Introduction</b>	<b>14</b>
1.1 Overview and Motivation . . . . .	14
1.1.1 WSN Constraints and Challenges . . . . .	15
1.1.2 Definitions . . . . .	17
1.2 Research Methodology . . . . .	18
1.2.1 Requirements and Research Questions . . . . .	18
1.2.2 Research Methods . . . . .	19
1.3 Contributions . . . . .	20
1.4 Assumptions and Limitations . . . . .	21
1.5 Outline of the Thesis . . . . .	22
<b>2 Pattern Matching and Detection in WSNs and Sensor Data</b>	<b>23</b>
2.1 Environmental Monitoring . . . . .	24
2.2 Data Centre and Structural Monitoring . . . . .	25
2.3 Body Sensor Networks and Context Aware Systems . . . . .	26
2.4 Network Monitoring and Security . . . . .	28
2.5 Spacecraft and Telemetry Pattern Classification . . . . .	30
2.6 Spatial Pattern Location Estimation . . . . .	30
2.7 Generic Approaches and Additional Applications . . . . .	32
2.8 Summary . . . . .	34

<b>3</b>	<b>Pattern Matching and Detection in the Temporal Domain</b>	<b>37</b>
3.1	The Basis for Pattern Matching and Detection . . . . .	37
3.1.1	Advantages of Symbolic Transformation . . . . .	38
3.1.2	An Overview of Symbolic Aggregate Approximation . . . . .	40
3.1.3	Assessing Pattern Similarity and Probability . . . . .	42
3.2	Exact and Approximate Pattern Matching . . . . .	43
3.3	Multiple Pattern Matching . . . . .	44
3.4	Non-Parametric Pattern Detection . . . . .	46
3.5	Probabilistic Pattern Detection . . . . .	46
3.6	Summary . . . . .	48
<b>4</b>	<b>Temporal Algorithms: Evaluation through Emulation</b>	<b>50</b>
4.1	Methodology and Experimental Setup . . . . .	50
4.2	Case Study 1: Indoor Deployment . . . . .	52
4.2.1	Evaluation of Exact and Approximate Matching . . . . .	52
4.3	Case Study 2: Seismic and Acoustic Data . . . . .	58
4.3.1	Evaluation of Non-Parametric Pattern Detection . . . . .	58
4.3.2	The Effect of Measurement Noise to NPPD . . . . .	64
4.4	Case Study 3: Physiological Data . . . . .	66
4.4.1	Evaluation of NPPD and PPD . . . . .	67
4.5	Summary of Findings . . . . .	72
<b>5</b>	<b>Temporal Algorithms: Evaluation through Deployment</b>	<b>73</b>
5.1	Execution Profile of Temporal Domain Algorithms . . . . .	73
5.1.1	Refactoring of Pattern Matching and Detection Algorithms	74
5.2	Dynamic Sampling Frequency Management (DSFM) Algorithm .	81
5.2.1	Data Centre WSN Deployment . . . . .	83
5.3	Integration with Publish/Subscribe . . . . .	90
5.4	Observations from Further Deployments . . . . .	91
5.5	Summary of Findings . . . . .	92

<b>6</b>	<b>Pattern Location Estimation in the Spatial Domain</b>	<b>94</b>
6.1	The Location Estimation Problem . . . . .	94
6.2	Kalman Filter Properties . . . . .	95
6.3	Spatial Pattern Location Estimation (SPLE) Algorithm . . . . .	98
6.4	Summary . . . . .	103
<b>7</b>	<b>Spatial Algorithm: Evaluation through Simulation</b>	<b>104</b>
7.1	Methodology and Simulation Set-up . . . . .	104
7.1.1	Maximum Selection Algorithm . . . . .	105
7.1.2	Dispersion Model . . . . .	105
7.1.3	Kalman Filter Initial Parameters . . . . .	106
7.1.4	Topology Generation . . . . .	107
7.2	Evaluation of Spatial Pattern Location Estimation . . . . .	108
7.2.1	Metrics . . . . .	108
7.2.2	Grid Topology . . . . .	108
7.2.3	Random Topology . . . . .	110
7.3	Summary of Findings . . . . .	114
<b>8</b>	<b>Conclusions and Future Work</b>	<b>118</b>
8.1	Summary of the Thesis . . . . .	118
8.2	Summary of Contributions . . . . .	121
8.3	Critical Appraisal . . . . .	122
8.4	Directions for Future Research . . . . .	122
	<b>Bibliography</b>	<b>129</b>
	<b>A Publications</b>	<b>147</b>
	<b>B Example of Multiple Pattern Matching</b>	<b>149</b>
	<b>C Software Development Timing Model</b>	<b>152</b>
	<b>D Maximum Selection Spatial Location Algorithm</b>	<b>154</b>

# List of Figures

1.1	Typical WSN nodes: TMote Sky and TI ez430-rf2500 . . . . .	16
1.2	Power draw of a TMote Sky . . . . .	17
3.1	Scale-independent pattern matching example . . . . .	39
3.2	Symbolic conversion example . . . . .	41
4.1	Emulating data acquisition in MATLAB . . . . .	51
4.2	Case study 1: APM example . . . . .	57
4.3	Case study 2: NPPD example . . . . .	62
4.4	Case study 2: NPPD compared to EWMA . . . . .	63
4.4	Case study 2: NPPD compared to RSAM . . . . .	64
4.5	Case study 2: Impact of signal noise to NPPD . . . . .	66
4.6	Case study 3: NPPD example on ECG data . . . . .	70
4.7	Case study 3: PPD example on EMG data . . . . .	71
5.1	APM/EPM Runtime comparison . . . . .	79
5.2	Runtime comparison of MPM and Linear Search. . . . .	80
5.3	Node locations from data centre deployment . . . . .	85
5.4	DC deployment: detected patterns . . . . .	89
6.1	The Kalman filter loop . . . . .	96
6.2	Estimate propagation example . . . . .	101
6.3	Example of the SPLE geometric computation . . . . .	102
7.1	Dispersion plume and concentration intensities . . . . .	110

7.2	Geometric computation example (a) . . . . .	115
7.2	Geometric computation example (b) . . . . .	116
7.2	Geometric computation example (c) . . . . .	117

# List of Tables

2.1	Comparison of alternative event detection methods . . . . .	35
2.1	Comparison of alternative event detection methods (cont'd) . . .	36
3.1	Sample distance lookup table for 10-letter alphabet . . . . .	42
4.1	Mean number of false positives for APM Algorithm . . . . .	55
4.2	Mean number of false positives for EPM Algorithm . . . . .	56
4.3	NPPD performance compared to EWMA and RSAM . . . . .	61
4.4	The effect of noise to NPPD performance . . . . .	65
4.5	Detection latency on ECG data . . . . .	69
5.1	Floating Point runtime for EPM and APM Algorithms . . . . .	77
5.2	Integer-only runtime for EPM and APM Algorithms . . . . .	78
5.3	Integer-only runtime for NPPD Algorithm . . . . .	79
5.4	Runtime comparison of MPM and Linear Search . . . . .	80
5.5	Detection summary from data centre deployment . . . . .	88
7.1	Parameter values for gas dispersion model . . . . .	106
7.2	Kalman filter initial parameters . . . . .	107
7.3	SPLE performance (4,900-node WSN, grid placement) . . . . .	111
7.4	SPLE performance (1,024-node WSN, grid placement) . . . . .	112
7.5	SPLE performance (5,000-node WSN, random placement) . . . . .	113
7.6	SPLE performance (1,000-node WSN, random placement) . . . . .	113
A.1	Publications related to this thesis . . . . .	148

B.1	Outline of merging and pruning of the array structures . . . . .	150
B.2	Example of Binary Search over a (Pruned) Suffix Array . . . . .	151
C.1	A timing model as a WSN development guide . . . . .	153

# List of Algorithms

3.1	Exact Pattern Matching (EPM) Algorithm . . . . .	44
3.2	Approximate Pattern Matching (APM) Algorithm . . . . .	45
3.3	Multiple Pattern Matching (MPM) Algorithm . . . . .	46
3.4	Non-Parametric Pattern Detection (NPPD) Algorithm . . . . .	47
3.5	Probabilistic Pattern Detection (PPD) Algorithm . . . . .	48
5.1	Dynamic Sampling Frequency Management (DSFM) Algorithm .	82
6.1	Spatial Pattern Location Estimation (SPLE) Algorithm . . . . .	99
D.1	Maximum Location Estimation Algorithm . . . . .	155

# Chapter 1

## Introduction

In this thesis, we introduce methods and algorithms that provide pattern matching and detection functionality in Wireless Sensor Networks (WSNs). The context for this work is set by reactive applications which have to respond to interesting or unusual changes in the underlying monitored process, phenomenon or structure. This chapter provides an outline of the problem together with the research framework and the contributions of the proposed solution.

Section 1.1 offers a brief overview and motivation for the selected problem and specifically presents characteristics and constraining factors of WSNs. Section 1.2 identifies requirements and research questions and outlines methods employed in addressing those questions. Section 1.3 presents contributions made in this thesis, Section 1.4 states the assumptions and limitations of the proposed solution and Section 1.5 outlines the structure of the thesis.

### 1.1 Overview and Motivation

Wireless Sensor Networks (WSNs) are often deployed for the purpose of detecting significant events or anomalies in the monitored phenomenon, process or structure (henceforth, *monitored object*) [BPC<sup>+</sup>07, AK04, ASSC02]. Such *reactive* systems typically collect and process sensor observations to programmatically classify the real world state of the monitored object into one or more classes and take the

necessary actions accordingly. For example, in a structural health monitoring system, a building is monitored for structural faults by comparing a seismic response signal to known stress patterns.

Matching or detecting patterns in sensor observations is a common requirement in a number of domains (reviewed in Chapter 2) yet the problem of computationally efficient approaches has attracted less attention in comparison with research in network layer protocols. Moreover, solutions are often based on transmitting observations outside the network or to a tier of high capability devices for processing.

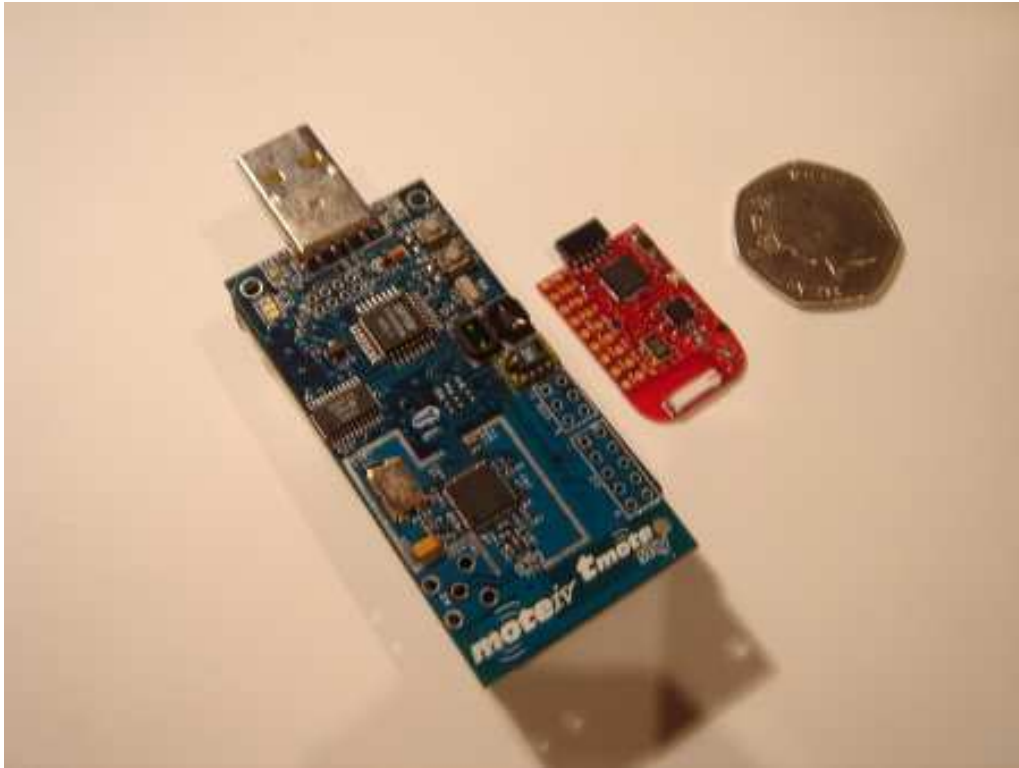
In this thesis, we assume a homogeneous WSN comprised of resource limited devices (henceforth, *nodes*) and we attempt to solve the problem of pattern matching and detection inside the network. Apart from the ubiquity of the problem, we are motivated by the benefit of an in-network solution, namely prolonged lifetime resulting from reduction of radio communication [MGH09, ZG09, TE07, CES04, GKW<sup>+</sup>02].

### 1.1.1 WSN Constraints and Challenges

We target the extremely resource constrained end of the Wireless Sensor Network (WSN) spectrum that comprises nodes such as those shown in Figure 1.1. The constraining factors that differentiate such nodes from other distributed systems are:

- (i) *Limited power resources.* Typically, nodes are powered by batteries which limit their useful lifetime and specify an energy budget that, in most applications, must be extended as much as possible. Radio communication, sensing and processing share this budget and pose a challenge to developers who must serve the application's purpose and, at the same time, maximise node lifetime.
- (ii) *Restricted functionality.* Embedded microcontrollers (MCUs), limited RAM and — in the vast majority of cases — lack of Floating Point Units (FPUs)

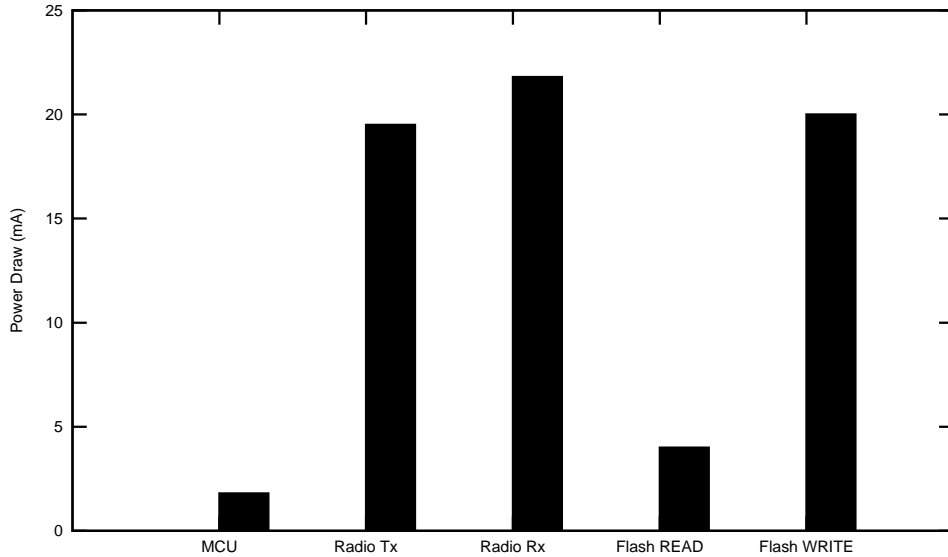
Figure 1.1: Extremely resource constrained WSN nodes: the TelosB / TMote Sky (left) and the newer ez430-rf2500 (middle). The former features 10KB RAM and 48KB Flash on a 8MHz MCU with active draw  $300\mu\text{A}$  while the latter features 1KB RAM and 32KB Flash on a 16MHz MCU with respective draw of  $270\mu\text{A}$ .



set a limit on the complexity of computations that can be executed on nodes. Algorithms with complex state and long running computations are not suitable for this execution environment [ZG09, PLPG06] since they can consume the nodes' limited resources and shorten their useful lifetime.

- (iii) *Costly radio communication and limited bandwidth.* The fabric that interconnects nodes in a WSN is also the most expensive component with respect to power draw; typical consumption is shown in Figure 1.2. Minimising the amount and range of communications, can prolong the lifetime of a WSN [WDWS10, FCG10, ZG09, GJV<sup>+</sup>05, Kri05, AY05, SMP<sup>+</sup>04, HHM03, ASSC02, PK00]. As a rule of thumb, a bit of data transmitted by radio can cost as much as executing 1,000 MCU instructions [MFHH03].

Figure 1.2: Per-component power-draw of a TMote Sky WSN node [Ins06]. Note the high cost of radio communication in relation to the cost of MCU.



Further to the above constraints, WSN application designers are challenged by limited support for software development and a tight coupling between application and system layers [ZG09].

### 1.1.2 Definitions

We define a *pattern* as an ordered list of sensor observations revealing interesting or unusual activity in the monitored object. We use the term *pattern* as a synonym to event or pattern event. We define *spatial patterns* as patterns with position and direction in physical space.

We use *pattern matching* to refer to the problem of finding occurrences of one or more user-submitted template patterns in the stream of sensor observations. Similarly, we use *pattern detection* to refer to the problem of discovering *sustained* changes or local anomalies [Han02] in the stream of sensor observations after an unsupervised learning period. We define a sustained change as one that manifests in more than two sensor observations [MPL<sup>+</sup>07] within a time interval (window).

## 1.2 Research Methodology

We propose pattern matching and detection algorithms and conduct experimental evaluation to assess their accuracy and operational profile. Evaluation through deployment demonstrates suitability of our algorithms for the target platform. Evaluation through simulation investigates the performance of the proposed algorithms under varying parameters and compares their pattern matching and detection accuracy against competitive techniques.

The following sections state the goals of this thesis and discuss methods employed in addressing the research questions.

### 1.2.1 Requirements and Research Questions

We identify the following requirements for a solution that addresses the problem of in-network pattern matching and detection:

- (i) It should cater for a variety of usage scenarios such as matching user submitted template patterns and also detecting unusual patterns without relying on prior user information.
- (ii) It should reduce network communication for pattern matching and detection, and only engage in localised communication when required.
- (iii) It should execute efficiently on extremely resource constrained WSN nodes.
- (iv) It should be compatible with existing WSN paradigms and not require change of underlying communication protocols to accommodate pattern matching and detection functionality.
- (v) It should accommodate WSN applications with different sampling frequency requirements performing pattern matching and detection in a timely manner, as close to real time as possible.

The thesis addresses the following questions:

- 
- (R1.) Is there a class of algorithms that make in-network pattern matching and detection feasible for extremely resource constrained nodes?
  - (R2.) How is the algorithms' matching/detection performance affected by different choice of algorithm parameters?
  - (R3.) Is this class of algorithms a viable alternative in comparison to other event detection methods?
  - (R4.) Are the requirements, as stated above, satisfied by such pattern matching and detection algorithms?

Question R1 is addressed with the algorithms of Chapter 3 and answered through deployment in Section 5.1. Question R2 is answered initially through emulation (Section 4.2) and findings are validated through deployment (Section 5.2.1). Question R3 is answered through emulating sensor node streaming data acquisition in software, and specifically by comparing the temporal domain pattern detection algorithm against two competitive techniques (Section 4.3.1). Lastly, R4 is answered with the algorithms of Chapters 3 and 6 which are evaluated with a combination of deployment and simulation.

### 1.2.2 Research Methods

After reviewing literature related to the problem of pattern matching and detection, evaluation of the proposed solution was conducted through implementation and deployment on WSN nodes to assess suitability for the extremely resource constrained execution environment and compatibility with existing WSN communication protocols.

Simulation experiments were conducted to evaluate the performance of the algorithms with respect to the rate of true and false positives in the temporal domain, and pattern event location estimation accuracy in the spatial domain.

Data and tools used in evaluation of the proposed algorithms are widely available, and our experimental setup is described — Sections 4.1, 5.1 and 7.1 — to encourage peer review of our findings from the WSN community. The software

developed in this thesis is used by fellow researchers and is publicly available together with data collected from our deployments to encourage reproducibility of experiments.

### 1.3 Contributions

The work described in this thesis makes contributions that address the WSN application issue of pattern matching and detection, and offers a computationally efficient implementation of reactive functionality. Moreover, it limits radio communication and MCU active time in order to complement the generic goal of prolonged WSN lifetime. Specifically, we make the following contributions:

- (i) Develop temporal domain in-network pattern matching and detection algorithms that reduce network communication. Described in Chapter 3, the algorithms cater for exact, approximate, multiple, non-parametric and probabilistic pattern matching and detection.
- (ii) Provide evidence that the proposed algorithms produce consistently good results in three case studies (Chapter 4) with respect to matching/detection accuracy. The case studies evaluate different aspects of the algorithms such as the impact of different parameters to false positives and accuracy in comparison with other event detection techniques.
- (iii) Demonstrate that the algorithms are suitable for extremely resource constrained nodes by integer arithmetic refactoring and deployment (Chapter 5). Suitability is further demonstrated by incorporating dynamic sampling frequency adjustments to reduce MCU active time, and integrate the proposed algorithms with a Publish/Subscribe (Pub/Sub) interface that employs standard TinyOS communication protocols.
- (iv) Introduce an iterative algorithm, based on a geometric computation and a Kalman filter (Chapter 6), that engages in localised communication to

estimate the location of a spatial event inside the network in a collaborative manner.

- (v) Evaluate the estimation performance of the spatial algorithm and, in particular, investigate the impact of WSN topology and node placement to the estimation performance in comparison with a competitive approach (Chapter 7).

We believe that the above contributions provide a competitive pattern matching and detection family of algorithms that can be used in a variety of reactive WSN applications.

## 1.4 Assumptions and Limitations

The work proposed in this thesis makes the following assumptions:

- Homogeneous network comprised of extremely resource constrained nodes with characteristics outlined in Section 1.1.1.
- For location estimation, the single pollutant source and WSN nodes are stationary. The nodes are aware of their location coordinates which are accurate and error-free.

The first assumption means that the proposed algorithms are not dependent on a base station, high capability nodes or centralised coordination.

We recognise the following limitations with respect to the proposed algorithms:

- They do not cater for cross correlated matching and detection of patterns in multiple dimensions (sensed modalities).
- They operate on windowed observations and are not designed to detect outliers or single data point events.
- They do not provide historic pattern matching and detection for past events since nodes, by default, do not store sensor observations.

- They do not take into account dynamic metadata that can change the interpretation of observations and consequently the outcome of matching and detection.
- The spatial domain algorithm cannot, in its present form, cater for multiple, mobile sources and dynamic environmental conditions.

A subset of the above limitations is addressed in directions for future work explored in Section 8.4.

## 1.5 Outline of the Thesis

Chapter 2 offers a literature review of event detection and pattern classification methods for WSNs and sensor data. Temporal pattern matching and detection algorithms are introduced in Chapter 3 and evaluation through emulation is conducted in Chapter 4. The latter work can be divided in two categories: investigation of the effect of algorithm parameter selection to pattern matching and detection and comparison against competitive methods. Chapter 5 describes the practical work undertaken for the evaluation of the temporal domain algorithms through full implementation and deployment. Specifically, it presents the refactoring of our algorithms and associated timing measurements obtained from WSN nodes that demonstrate suitability for extremely resource constrained nodes. Furthermore, it presents the dynamic sampling frequency extension to non-parametric pattern detection, and discusses field validation through a data centre deployment. Chapter 6 introduces the spatial domain algorithm that targets location estimation of a pollutant-emitting source and Chapter 7 presents related findings obtained from simulation experiments that include a comparison to a competitive maximum selection algorithm. Finally, the thesis concludes in Chapter 8 with a critical appraisal and a detailed plan for future work.

## Chapter 2

# Pattern Matching and Detection in WSNs and Sensor Data

Pattern matching and detection can be addressed with a variety of techniques such as clustering, density estimation, probabilistic matching, Kalman filtering, expert systems and string matching. In this chapter, we review techniques that target WSNs or sensor data and present approaches categorised per application domain.

Techniques for event detection in environmental monitoring applications are reviewed in Section 2.1, and Section 2.2 presents approaches for data centre and structural health monitoring. Section 2.3 reviews pattern matching and detection in body sensor networks and context aware computing. Network monitoring and security applications are reviewed in Section 2.4. Approaches for pattern matching and detection in spacecraft image and telemetry data are discussed in Section 2.5. Spatial pattern location estimation approaches are reviewed in Section 2.6 and generic approaches are presented in Section 2.7. Finally, we summarise our findings in Section 2.8.

## 2.1 Environmental Monitoring

*Lance* [WADHW08] addresses resource prioritisation and bandwidth allocation in WSNs. It is a volcano monitoring application where an unusual pattern is a signal segment denoting activity that may lead to an eruption. *Lance* caters for correlated pattern event detection and it employs an Exponentially Weighted Moving Average (EWMA) method to detect patterns that trigger data upload to a base station. In Section 4.3, we conduct a comparison between the proposed Non-Parametric Pattern Detection algorithm and EWMA with data from the deployment of *Lance*.

The approach described in [BRR08] presents a model-based system that aims to detect and predict river flood pattern events in developing countries. The suggested model is based on statistical methods such as linear regression. This approach assumes a tiered architecture where resource-constrained sensor nodes transmit summaries and statistics of raw observations to a set of high capability computation nodes. The latter determine data correctness, feed it to the model for event detection/prediction and possibly request additional data from sensors to reduce uncertainty. PRESTO [DGL<sup>+</sup>05] is another tiered system based on an ARIMA (Auto Regressive Integrated Moving Average) forecasting model that detects unusual patterns by comparing predicted values to sensor observations.

The work described in [KSW<sup>+</sup>08] employs the symbolic conversion algorithm SAX [LKLC03], also used by temporal domain algorithms proposed in this thesis, to obtain a discretised version of Electrical Penetration Graph (EPG) data relating to the behaviour of insects. Specifically, the authors developed a constant-time version of the Time Series Bitmap (TSB) [KLK<sup>+</sup>05] algorithm that can be used on constrained devices for real-time EPG classification. Their aim is to improve unsupervised classification of insects' lifecycle data in experimental conditions. The work does not provide implementation details but a deployment is mentioned in their future plans.

The approach described in [BHL07] presents a distributed algorithm for detecting ecological anomalies as well as estimating erroneous or missing data. The

proposed method performs automatic inference and prediction based on statistical distributions of differences in observations between a node and its neighbours. Nodes compute the distribution of differences to perform a *p-test* that determines the likelihood of an observation exceeding a significance level. One drawback of this approach is the radio communication overhead required to compute the distribution of spatial differences.

## 2.2 Data Centre and Structural Monitoring

Research described in [PMSR09] proposes a temporal data mining solution to optimise the performance of data centre chillers. Sensor nodes deployed in data centres observe temperature and humidity data that varies according to the load of individual servers, storage and networking equipment. This system illustrates the operation a Wireless Sensor Actuator Network (WSAN): depending on observed patterns, a decision must be made to turn on/off chillers, select a utilisation range and react to cooling demands. The authors focus on *motif mining*, which is the identification of frequently occurring temporal patterns. First, a string representation of the sensor observations is generated with the symbolic aggregate approximation (SAX) [LKLC03] algorithm. A Run-Length Encoding (RLE) of the symbolic sequence records transitions from one symbol to another. Frequent episode mining is conducted over the sequence of transitions to identify the underlying efficiency profile of the data centre under different environmental circumstances.

The work described in [XLCL06] employs contour map matching to determine whether a user-supplied pattern matches sensor produced observations. The application scenario is event detection in coal mines, monitoring gas, dust and water leakage events as well as high/low oxygen density regions. A limitation is that it assumes users capable of describing the pattern of interest as distributions of an attribute over space and variations of this distribution over time. A related approach [LLC07], targeting gas leakage events in mines, tasks nodes to construct 3-dimensional gradient data maps which are transmitted to a sink and compared

to predefined patterns.

*Wisden* [XRC<sup>+</sup>04] is a system that employs a wavelet integer lifting transform to detect patterns in structural health monitoring applications. It uses wavelet compression to store vibration data locally and transmits a lossy version to the base station. Its pattern detection component operates as follows: if samples within a window are comparable in value and of low magnitude then the structure is perceived to be in a quiescent state. Such windows are considered normal and compressed using RLE, in contrast to pattern events which are transmitted uncompressed. One strength of this approach is that the computational efficiency of the event detection mechanism is verified through deployment.

The system presented in [LKQ<sup>+</sup>03], aims to detect patterns in order to diagnose potential damages that could affect the integrity of filament wound composite structures such as solid rocket motors and liquid fuel containers. It uses actuator nodes either embedded in the structure or placed on its surface, to emit a diagnostic stress wave signal. A neighbouring sensor node captures the signal and compares it to a baseline normal signal. If a difference is observed, it indicates change in the surface of the structure that can be attributed to damage. One challenge with this described method is difficulty of generalisation — for instance, stress layers' placement had a significant impact to detection accuracy — although there is mention of expanding the work such that it applies on other structures and different materials.

## 2.3 Body Sensor Networks and Context Aware Systems

The approach described in [HJCX08] introduces wavelet-based ECG data mining for Body Sensor Networks (BSNs). The system targets remote patient monitoring through a combination of resource constrained nodes and offline processing. Nodes are responsible for ECG noise filtering and periodic transmission of ECG

waveforms to a central server for processing. The server employs feature extraction with wavelet transforms and the Local Holder Exponent (LHE) function. Support Vector Machines (SVMs) are used for classification of ECG signal fragments. In contrast to our methods that process data inside the network, this approach incurs the communication cost of transmitting observations to a base station.

*BiosensorNET* [KHW<sup>+</sup>07] is a BSN comprising resource constrained nodes for near real-time heart rate variability analysis of ECG signals. It is based on two algorithmic layers: a real-time layer extracts the QRS complex which is the significant part of the ECG signal. It passes the QRS to a near real-time layer that performs variability analysis on the frequency domain and invokes further processing only if it determines that the QRS is significant. To our knowledge, this is one of the first efforts to address both pattern detection and implementation for extremely resource constrained nodes in the field of BSNs.

The work described in [SRT07] employs the symbolic aggregate approximation SAX [LKLC03] algorithm for string conversion of gesture data obtained by accelerometers and gyroscopes worn by human subjects. Gestures are characterised by the movement of limbs in Cartesian space and their identification and classification through wearable sensors can assist in determining the context and activity of persons. The proposed approach, similar to our work, offers approximate pattern matching with a different distance metric, the *edit* distance. Although they target real-time gesture classification in constrained sensor nodes, the work lacks WSN deployment evidence and performance results are collected in a desktop-class machine. A related system [WYC<sup>+</sup>06] targets human activity recognition from sensor accelerometer observations using decision trees, neural networks and Support Vector Machines (SVMs).

A method aimed at pattern matching over trajectory data is described in [BCFL09] where authors propose a distance metric to determine similarity between trajectory subsequences. Recognising patterns in trajectory data has applications ranging from remote monitoring of elderly patients to military detection of enemy movements. Pattern detection is performed by testing whether a time

window has fewer than a predetermined number of neighbours in its left and right sliding windows. Experimental results show efficiency with respect to processing time measurements, however evaluation is conducted offline lacking validation on WSN nodes.

The approach of [HMBE06] targets context-aware computing and specifically mining for unusual patterns in observations representing human interactions with their environment. The authors propose the use of a *Suffix Tree* data structure to encode the structural information of activities and their event statistics at different temporal resolutions. The method aims to identify unusual patterns that either consist of structural differences to normal behaviour or differences based on the frequency of occurrence of motifs. The approach relies on training data to construct the dictionary of legitimate behaviour and sequences are classified as unusual using a match statistic computed over the suffix tree. The strength of the approach is that suffix tree traversal requires linear time, however dynamic suffix tree construction and update is not always suitable to platforms with severe resource constraints due to dynamic memory allocation demands of such operations.

## 2.4 Network Monitoring and Security

The approach described in [WDWS10] presents a system for distributed pattern event detection using training data or statistical means. The system is based on feature extraction by discretisation in time intervals and computation of the difference between minimal and maximal observations for each interval. The output is a feature vector that is compared in terms of Euclidean distance against a number of prototype vectors. One strength of this approach is that it has been evaluated through a deployment in a security application detecting trespassing at a construction site. However, unlike our approach, training requires considerable memory and processing resources and is performed on a desktop-class machine rather than on WSN nodes.

The work described in [DSS07] introduces Artificial Immune Systems (AIS)

for misbehaviour detection. AIS are inspired from the human immune system and its ability to detect harmful agents such as viruses and infections. The method facilitates local learning and detection with a gene-based approach. Each node maintains a local set of detectors produced by negative selection from a larger set of randomly generated detectors tested on a set of self strings. The detectors test new strings that represent local network behaviour, and detect non-self strings denoting unusual patterns. The approach has been evaluated using MAC layer messages and targets detection of local patterns that indicate misbehaviour over a layer of the OSI reference model stack.

The approach described in [HGH<sup>+</sup>06], proposes a Principal Component Analysis (PCA) method for detecting unusual patterns with complex thresholds in a distributed manner. Nodes transmit observations to a coordinator responsible for firing a trigger based on the aggregate behaviour of a subset of nodes. The individual nodes perform filtering such that they transmit only when observations deviate significantly from the last transmitted data. Detection is accomplished with two window triggers that fire on persistent threshold violations over a fixed or varying window of observations. Although the approach is aimed at detecting unusual network traffic patterns, it can generalise to other WSN applications. The main criticism is that coordinator nodes introduce single points of failure in the detection scheme.

A related approach [LNL06], considers intrusion detection in WSNs from samples of routing traffic. First, feature selection of traffic and non-traffic related data is performed in order to learn the distribution of values affecting routing conditions and traffic flows. Second, pattern detection is performed locally by comparing a window of observations to previously collected normal data. This window contains samples mapped to points in a feature space and are analysed together with their surrounding region. If a point lies in a sparse region of space is classified as unusual using a fixed-width clustering algorithm. The method is capable of locally detecting novel patterns, but it is limited by the number of modelled attacks.

## 2.5 Spacecraft and Telemetry Pattern Classification

In [CWC<sup>+</sup>07], the authors describe mining scientific data on-board a spacecraft in order to react to dynamic patterns of interest as well as to provide data summaries and prioritisation. Three image pattern recognition algorithms are presented that were employed on board the Mars Odyssey spacecraft to detect polar cap edges and atmospheric opacity events.

The approach described in [SOM07] presents three unsupervised pattern recognition algorithms evaluated offline using historical data obtained from a space shuttle main engine, comprising up to 90 sensors, for the objective of future inclusion in the Ares *I* and Ares *V* launch systems. The algorithms employ Support Vector Machines (SVMs), clustering and nearest neighbour for pattern classification.

A system aimed at automatic satellite reliability monitoring is described in [DTP91]. The diagnosis of faults from, sometimes limited, sensor data is performed by an expert system. The authors describe how the expert system was built even with limited knowledge and its ability to perform inexact reasoning to accommodate sparse sensors. A disadvantage is inherited from expert systems and is attributed to the supervised learning required to describe possible fault states.

## 2.6 Spatial Pattern Location Estimation

The approach described in [CYR<sup>+</sup>08] addresses an instance of the spatial location estimation problem considered in Chapter 6. The authors address spatial pattern location estimation of a radioactive source using an iterative pruning data fusion algorithm tolerant of measurement noise. The system is based on the ratio-of-square-distance (RoSD) location estimation algorithm that uses observations from three nodes and improves estimation accuracy as more nodes become

available. The outcome of RoSD algorithm is fed into an iterative pruning clustering algorithm that provides a geometric solution to the location estimation problem. Two strengths of this approach is the evaluation of realistic noise and error conditions, and the implementation on WSN nodes.

The work described in [GJV<sup>+</sup>05] proposes *VigilNet*, a hierarchical system for in-network detection and classification of vehicles and persons. Using a combination of magnetometers, motion sensors, and microphones, lower tier nodes apply a moving average aggregation scheme and forward their summaries to dynamic cluster heads. The cluster heads examine spatio-temporal correlations, compute confidence scores over the aggregate data and forward the outcome to a base station. The base station finalises classification results with linear regression and estimates metadata such as target location and velocity. One strength of this system is that it validates spatial pattern detection through deployment on extremely resource constrained nodes.

The distributed Kalman filter proposed in [SOSM05] targets location estimation in WSNs with imperfect communication links based on an iterative spatial averaging algorithm. It introduces a transfer function that describes the error behaviour of the distributed Kalman filter in the case of stationary noise processes. The authors focus on location estimation of sonic sources using acoustic sensors and claim that their method generalises to other domains. Evaluation is conducted through simulation and the description lacks WSN implementation details.

We adopt the gas distribution and sensor response model of Ishida [INM97], described in Section 7.1. In this work, the authors deploy a mobile robot that detects the concentration of gas in the atmosphere and moves to appropriate locations in an attempt to estimate the source location. Achieved through fitting the gas distribution model to the sensor response at each location, they provide a sensing algorithm that is also capable of estimating the release rate of the gas pollutant.

Generic coarse grained location estimation techniques include the *Centroid Calculation* or Point-in-Triangle (PIT) methods [Kri05]. A variation of the former

is employed in the geometric computation described in Section 6.3 and used by our spatial location estimation algorithm. A refinement of the PIT technique is the Approximate Point in Triangle (APIT) described in [HHB<sup>+</sup>03]. A geometric approach based on the circles of Apollonius is described in [CP07]. A family of methods based on Time Difference of Arrival (TDOA) with geometric and numerical solutions, can be found in [MPR03], [Rao06], and [XRS07].

## 2.7 Generic Approaches and Additional Applications

In [RBLP09] the authors propose a pattern detection system based on elliptical anomalies which are defined by the ellipsoid or hyperellipsoid caused by the region of distance around the mean of two or more monitored variables. Given a set of column vectors representing sensor observations, the aim is to partition the set into normal and unusual observations. The algorithms for first and second order elliptical anomaly detection can be fully distributed in the network. A drawback is that computational cost on WSN nodes is not evaluated, although the authors assume resource constrained nodes.

The approach presented in [SWJR07] targets the problem of pattern detection using a density test for distributional changes. Possibly multidimensional sensor observations are tested against a baseline data set with a statistical test that determines whether data points in the set of observations were sampled from the same underlying distribution that produced the baseline set. The test statistic is distribution-free and based on kernel density estimation and Gaussian kernels. The baseline distribution is inferred using a combination of the kernel density estimator with an Expectation Maximisation (EM) algorithm. The capability of recognising patterns occurring at multiple data dimensions simultaneously is a strength of this approach. However it lacks implementation details for WSN nodes and is only evaluated through simulation.

The approach described in [MP03] proposes online novelty detection on temporal sequences with Support Vector Regression (SVR). A confidence score indicating degree of novelty is used for detection. The method depends on pattern duration that is not always known in advance, and detection accuracy under different duration settings is not examined.

The work presented in [SG07] employs a combination of wavelets and neural networks in order to predict pattern event occurrences. Their approach allows for Dynamic Power Management (DMP) by alternating sleep states of nodes in times of inactivity. Similar work presented in [KDS05] employs wavelets and neural networks for classification of sensor observations. A weakness of both approaches is that they are evaluated through simulation and lack implementation on WSN nodes.

The work described in [IPV07], computes anomaly scores from signals when they differ from reference states. The application scenario is sensor validation — the task of ensuring correct operation by detecting unexpected behaviour. Once an unusual pattern is detected, change analysis is performed by pinpointing the variables causing the change. The system employs a stream of weighted graphs where each signal corresponds to a node and edges are weighted by the similarity between a pair of data fragments. Each sensor node produces a dissimilarity matrix of multi-variate observations in a streaming fashion and compares it against a reference dissimilarity matrix. The anomaly analysis is conducted by graph and distribution comparison. An approach also targeting validation is presented in [GN03] where the feasibility of artificial intelligence techniques for the diagnosis of acceleration sensor faults is investigated.

Localisation Anomaly Detection (*LAD*) [DFN06] is aimed at detecting anomalies in localisation schemes typically caused by adversaries, for example enemies in military applications deployed in hostile environments. The authors propose a number of threshold techniques to infer whether localisation is compromised. The drawback is that they do not offer implementation evidence with respect to the computational efficiency of the techniques on WSN nodes.

An algorithm that detects intrusion in WSNs based on statistical information of network packets is presented in [PHCL06]. The approach proposed in [CPGM06] considers spectral anomaly detection in combination with in-network fusion to detect attacks or malfunctions. The work presented in [BGG09], describes a framework that incorporates in-network processing for spatio-temporal event detection and state estimation with a focus on applications from the aerospace domain. Approaches such as [HCM08], that are not limited to WSNs, suggest the use of machine learning techniques and specifically a dynamic version of predictive coding. *DEAMON* [STKC09] is an approach capable of monitoring complex conditions based on distribution and assignment of composite event expressions in the network.

## 2.8 Summary

In this chapter, we reviewed alternative approaches for pattern matching and detection from a range of application domains that address the problem with different techniques, summarised in Table 2.1. The range of applications highlights the wide scope of the pattern matching and detection problem. However, a number of the reviewed systems are limited because of:

- Lack of operational validation with implementation evidence for extremely resource constrained WSNs.
- Off-network processing or tiered models that transmit observations for analysis by high capability nodes.

The first issue casts doubt on the feasibility of these techniques for extremely resource constrained nodes, and the second point often accelerates resource consumption as a consequence of engaging in radio communication.

In the next chapter, we describe our proposed solution to in-network pattern matching and detection using computationally efficient methods and algorithms.

Approach	Basis	Application	Strength	Weakness
<b>MOVING AVERAGE</b>				
[WADHW08]	EWMA	Seismic & Acoustic data	Lightweight approach	Dependence on fixed threshold
[GJV <sup>+</sup> 05]	Moving Averages	Target Detection and Classification	In-network solution evaluated on real nodes	Dependence on tuning several parameters
<b>SYMBOLIC</b>				
[PMSR09]	Symbolic conversion/Run-length encoding	Data centre monitoring	Dynamic modelling of data centre chillers	Lack of implementation evidence
[CLD08]	Symbolic conversion & TSB	EPG Data/Insect monitoring	Approximate matching	Lack of WSN implementation evidence
[HMBE06]	Subsequence matching using Suffix Trees	Context-aware computing	Linear time matching	Not suitable for dynamic tree updates
<b>REGRESSION ANALYSIS &amp; MODEL-BASED</b>				
[BRR08]	Linear regression model	River flood pattern events	Distributed data-driven model	Assumes presence of a resource-rich tier
[BHL07]	Bayesian classification	Ecological anomaly detection	Automatic Inference & Prediction	Radio communication cost involved in classifier
[MP03]	Support Vector Regression	Abstract/Temporal sequences	Confidence score	High computational costs for large training windows
<b>KALMAN FILTER &amp; DENSITY ESTIMATION</b>				
[SWJR07]	Kernel density estimators	Abstract/Multidimensional data	Detects patterns occurring at multiple dimensions simultaneously	Performance not evaluated
[SOSM05]	Kalman Filter	Sonic source localisation	Distributed operation	Lack of WSN implementation evidence
[INM97]	Distribution fitting	Gas source localisation	Estimates gas release rate	Assumes knowledge of gas distribution model
<b>EXPERT SYSTEMS &amp; GRADIENT MAP MATCHING</b>				
[DSS07]	Artificial Immune Systems (AIS)	Misbehaviour detection on network data	Efficiency of local detectors	Not clear whether generalisable
[XLCL06]	Contour-map matching	Coal-mine monitoring	SQL extensions allows users to specify events as pattern	Relies on prior-distribution knowledge by user
[DTP91]	Expert System	Satellite telemetry data	Inexact reasoning	Knowledge acquisition bottleneck of Expert Systems

Table 2.1: Comparison of selected pattern matching and detection methods for WSNs and sensor data

Approach	Basis	Application	Strength	Weakness
<b>NEAREST NEIGHBOUR &amp; CLUSTERING</b>				
[WDWS10]	Feature extraction & NN	Trespassing detection	Evaluated through deployment	Training relies on desktop-class machine
[BCFL09]	NN/Clustering	Trajectory pattern recognition	Efficient processing time for classifying new observations	Lack of WSN implementation evidence
[SOM07]	NN/Clustering/SVMs	Spacecraft engine data	Pattern mining in data from up to 90 sensors	Detection accuracy relies on thresholds
[IPV07]	Stochastic nearest neighbour	Sensor Validation	Multidimensional data & change analysis	Lack of WSN implementation evidence
[LNLP06]	Fixed-width clustering	Network Intrusion Detection	Can detects novel patterns	False negatives of slow-occurring events
<b>WAVELETS &amp; SVMs</b>				
[HJCX08]	Wavelets	ECG data mining with SVMs	Considers info. security	Offline processing
[SG07]	Wavelets and neural networks	Abstract	Dynamic power management	Lack of WSN implementation evidence
[XRC <sup>+</sup> 04]	Wavelets	Structural Health Monitoring (SHM)	Evaluated through implementation	Event data on flash can be overwritten rapidly
<b>THRESHOLDING</b>				
[STKC09]	Composite event algebra	Abstract	Energy efficiency through predicate distribution	Comp. cost not bounded
[CWC <sup>+</sup> 07]	Dynamic Thresholding and SVMs	Spacecraft image data	Respects resource constraints	Suitability for WSN nodes not demonstrated
[DPN06]	Dynamic Thresholding	Localisation Anomalies	Inference capability	Lack of WSN implementation evidence
<b>SIGNAL &amp; PRINCIPAL COMPONENT ANALYSIS</b>				
[KHW <sup>+</sup> 07]	Two-phase variability analysis	Near real-time ECG mining	Evaluated through implementation	Detection latency of second phase
[HGH <sup>+</sup> 06]	Principal Component Analysis (PCA)	Distributed network pattern recognition	Source-side filtering	Relies on coordinator node (SPoF)
[LKQ <sup>+</sup> 03]	Scatter signal analysis	SHM of rocket motors and fuel containers	No false positives	Dependence on sensor/actuator placement
<b>GEOMETRIC</b>				
[CYR <sup>+</sup> 08]	TDOA & RSoD	Radioactive source localisation	Comparative Evaluation	Lack of evaluation on random topologies
[RBLP09]	Elliptical Anomalies	Abstract/Environmental data	Distributed solution with same accuracy as centralised	Comp. cost not explicitly modelled

Table 2.1: Comparison of selected pattern matching and detection methods for WSNs and sensor data

# Chapter 3

## Pattern Matching and Detection in the Temporal Domain

This chapter introduces algorithms for in-network pattern matching and detection in the temporal domain. The algorithms process incoming sequences of streaming sensor observations, transform them to a symbolic representation and determine whether the resulting string matches one or more user-submitted template patterns or, in lieu of the latter, classify it as normal or unusual. All the algorithms presented in this chapter are autonomous by design and do not rely on network communication for pattern matching and detection.

We first provide an overview of symbolic conversion, in Section 3.1, which forms the basis for our algorithms. The pattern matching and detection algorithms are presented in Sections 3.2 to 3.5, and a summary of their characteristics is presented in Section 3.6.

### 3.1 The Basis for Pattern Matching and Detection

The algorithms proposed in this chapter employ an in-network transformation phase where numeric sensor observations are discretised to produce a symbolic

representation. A sliding window is applied to transform numeric observations to strings with the Symbolic Aggregate Approximation algorithm (SAX) [LKLC03]. Pattern matching and detection is performed in-the-network by operating on the symbolic representation alone.

Two broad usage scenarios are considered: first, a matching case where a sensor-produced string (henceforth, *sensor string*) is compared to one or more user submitted template patterns (henceforth *templates*) and, second, a detection case where templates for comparison are unavailable and nodes must classify incoming sensor strings following an unsupervised learning phase.

### 3.1.1 Advantages of Symbolic Transformation

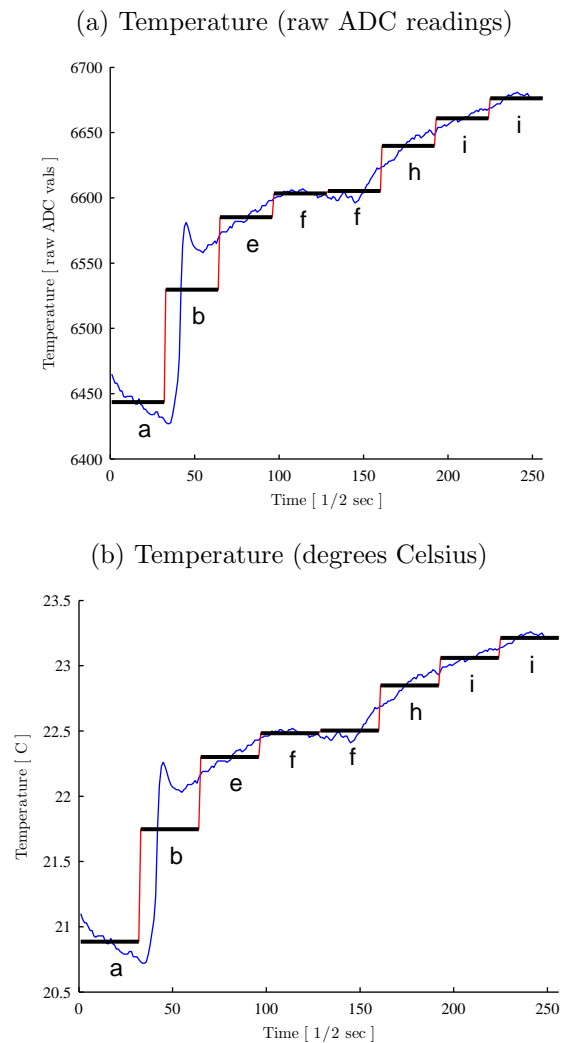
Transforming numeric sensor observations to sequences of symbols offers the following advantages:

- It fixes the computational cost of pattern matching and detection to a value known at compile-time (explored further in Chapter 5). This type of operational predictability is desirable in WSNs since it makes application behaviour deterministic [LGH<sup>+</sup>05].
- It allows the application of well-known techniques, from the fields of bioinformatics, probability theory and data mining, that can be combined to meet the requirements of pattern matching and detection.
- It allows pattern similarity to be assessed independently of magnitude of numeric observations, since it converts numeric sequences to strings of a finite, and typically small (under 15 characters), alphabet. An example of scale independence is shown in Figure 3.1.

Further to the above advantages, we specifically considered variants of the SAX algorithm because it has a proven track record in data mining across a number of related domains ranging from biometric recognition [CMY05] to anticipating the formation of tornadoes [MRK<sup>+</sup>07]. It has desirable properties such as dimensionality and numerosity reduction as well as a distance metric that is guaranteed to

lower bound the Euclidean distance. Moreover, in Chapter 5 we find that SAX is a relatively computationally lightweight approach thus likely to be a good fit for the resource constrained nature of WSN nodes.

Figure 3.1: Example of assessing pattern similarity independently of observation magnitude. Figure (a) shows raw ADC readings of temperature and figure (b) shows the same data converted to degrees Celsius. The two patterns match, since they result to the same string (shown in both figures).



### 3.1.2 An Overview of Symbolic Aggregate Approximation

The proposed algorithms treat SAX as a black box that takes a numeric sensor sequence of observations as input and returns a reduced string representation as output. Symbolic conversion takes place in three phases:

- (i) Normalise the sequence  $u$  of numeric sensor observations to a centred, scaled version where the  $i$  element is given by:

$$\frac{u_i - \mu}{\sigma}, \quad (3.1)$$

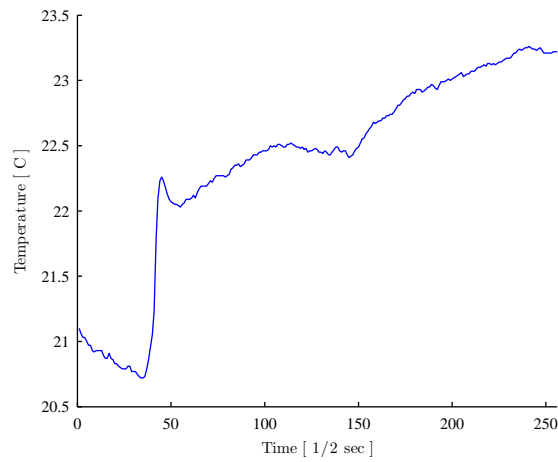
where  $\mu$  is the mean of  $u$  and  $\sigma$  is the standard deviation.

- (ii) Transform the normalised sequence to a Piecewise Aggregate Approximation (PAA) representation. PAA reduces the length of the sequence using piecewise polynomial approximation which is compression with a numerosity reduction technique that divides the sequence into  $w$  equal-sized frames. The mean value of data falling within a frame is computed and a vector of these values comprises the data-reduced PAA representation.
- (iii) The final step of the conversion process is a table lookup operation. The lookup table is a two-dimensional tiling of a sorted list of numbers  $B = \beta_1, \beta_2, \dots, \beta_{\alpha-1}$  such that the area under a  $N(0, 1)$  Gaussian curve from  $\beta_i$  to  $\beta_{i+1}$  is equal to  $\frac{1}{\alpha}$  where  $\alpha$  is the size of the alphabet  $\Sigma$ . It is assumed that  $\beta_0$  and  $\beta_\alpha$  are  $-\infty$  and  $+\infty$  respectively. A sample table for a 10-letter alphabet is shown in Table 3.1.

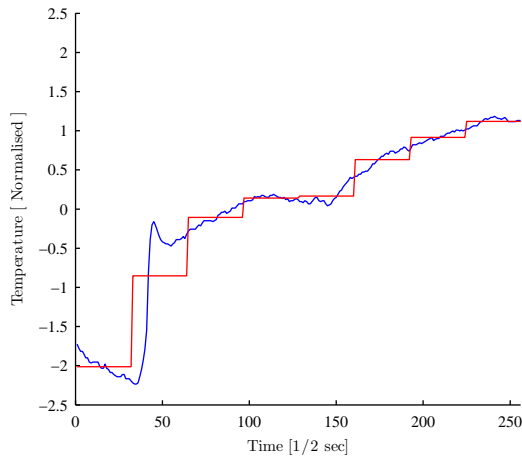
The transformation process is depicted in Figure 3.2; Figure 3.2a shows the numeric sequence prior to normalisation, Figure 3.2b shows the intermediate PAA representation and Figure 3.2c shows the final string. The interested reader can refer to the literature [KLF05, KLR04, LKLC03] on SAX for a more detailed treatment of the conversion process.

Figure 3.2: Example of symbolic conversion of a sensor sequence, to Piecewise Aggregate Approximation (PAA) and to the final string.

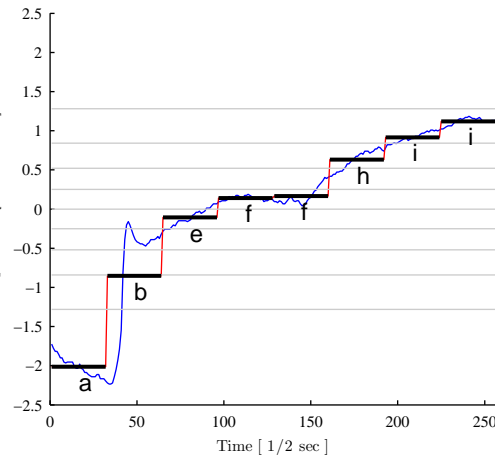
(a) Numeric temperature sequence from data centre deployment (Section 5.2.1)



(b) PAA approximation of the numeric sequence.



(c) Final string mapping of PAA approximation.



### 3.1.3 Assessing Pattern Similarity and Probability

With the exception of the probabilistic detection and multiple matching algorithms (Sections 3.3 and 3.5), we employ a distance function to quantify the difference between two string representations  $\bar{u}$  and  $\bar{r}$ . Assuming  $\bar{u}$  is the sensor string and  $\bar{r}$  is the template, the calculation depends on a lookup table (Table 3.1) and the below equation:

$$\|\bar{u} - \bar{r}\|_S = \sqrt{\frac{|u|}{|\bar{u}|}} \sqrt{\sum_{i=1}^{|\bar{u}|} (dist(\bar{u}_i, \bar{r}_i))^2}, \quad (3.2)$$

where  $|u|$  denotes the length of the input window representing the length of the numeric sensor sequence,  $|\bar{u}|$  denotes the length of its corresponding string representation, and  $dist(\bar{u}_i, \bar{r}_i)$  denotes a lookup to the table (Table 3.1) for characters  $i$  of strings  $\bar{u}$  and  $\bar{r}$ , for instance  $dist(a, c) = 0.1936$ .

The two mutually exclusive labels assigned in classification of incoming strings with the matching algorithms are *interesting* and *normal*. Similarly, the pattern detection algorithms classify a sensor string as either *unusual* or *normal*. The matching and detection outcomes depend on which of the proposed algorithms is chosen, and are obtained in the following manner:

- (i) In the case of matching, a sensor string  $\bar{u}$  is accepted as a pattern event and classified as *interesting* **if**  $\|\bar{u} - \bar{r}\|_S = 0$  (exact match) **or**  $\|\bar{u} - \bar{r}\|_S \leq \theta$  (approximate match) **or**  $\bar{u}$  is a substring of  $\bar{r}$  (multiple match), where  $\theta$  stands for a user-supplied distance threshold.
- (ii) In the case of inverted matching, a sensor string is rejected (not pattern

	a	b	c	d	e	f	g	h	i	k
a	0	0	0.1936	0.5776	1.0609	1.6384	2.3409	3.24	4.4944	6.5536
b	0	0	0	0.1024	0.3481	0.7056	1.1881	1.8496	2.8224	4.4944
c	0.1936	0	0	0	0.0729	0.2704	0.5929	1.0816	1.8496	3.24
d	0.5776	0.1024	0	0	0	0.0625	0.25	0.5929	1.1881	2.3409
e	1.0609	0.3481	0.0729	0	0	0	0.0625	0.2704	0.7056	1.6384
f	1.6384	0.7056	0.2704	0.0625	0	0	0	0.0729	0.3481	1.0609
g	2.3409	1.1881	0.5929	0.25	0.0625	0	0	0	0.1024	0.5776
h	3.24	1.8496	1.0816	0.5929	0.2704	0.0729	0	0	0	0.1936
i	4.4944	2.8224	1.8496	1.1881	0.7056	0.3481	0.1024	0	0	0
k	6.5536	4.4944	3.24	2.3409	1.6384	1.0609	0.5776	0.1936	0	0

Table 3.1: Sample Distance Lookup Table for a 10-letter Alphabet.

event) and classified as *normal* **if**  $\|\bar{u} - \bar{r}\|_S \neq 0$  (inverted exact match) **or**  $\|\bar{u} - \bar{r}\|_S > \theta$  (inverted approximate match) **or**  $\bar{u}$  is not a substring of  $\bar{r}$  (inverted multiple match). For inverted detection, the most recent sensor string  $\bar{u}_t$  is rejected (not pattern event) and classified as *normal* **if**  $\|\bar{u}_t - \bar{u}_{t-1}\|_S \leq \theta$  (inverted non-parametric detection) **or**  $P(\bar{u}_t) \neq 0$  (inverted probabilistic detection), where  $\bar{u}_t$  is the string obtained at time  $t$  (similar for  $t - 1$ ),  $\theta$  is obtained as a maximum learnt distance between temporally adjacent strings, and  $P(\bar{u}_t)$  is the path probability of string  $\bar{u}_t$ .

- (iii) In the case of detection, the most recent sensor string  $\bar{u}_t$  is accepted as a pattern event and classified as *unusual* **if**  $\|\bar{u}_t - \bar{u}_{t-1}\|_S > \theta$  (non-parametric detection) **or**  $P(\bar{u}_t) = 0$  (probabilistic detection).

In summary, a sensor string is classified as *interesting* if it matches a template exactly or approximately, otherwise it is classified as *normal*. Multiple pattern matching assumes  $|\bar{r}| \gg |\bar{u}|$ , where  $|\bar{r}|$  is the cumulative length of the templates (henceforth, the *text*) and  $|\bar{u}|$  is the length of the sensor string. In this case, classification reduces to an exact string matching problem that classifies the string as *interesting*, if  $\bar{u}$  is a substring of  $\bar{r}$ . Non-parametric pattern detection compares temporally adjacent sensor strings and classifies the most recent as *unusual* if it exceeds a maximum distance learnt during a training phase. Probabilistic pattern detection computes the path probability of  $P(\bar{u}_t)$ , given some learning data, and classifies a sensor string as *normal* if it has a non-zero probability of occurrence, or otherwise *unusual*.

## 3.2 Exact and Approximate Pattern Matching

Exact and approximate pattern matching assumes that users are able to describe patterns of interest. An example is a user with observations from past or related deployments, submitting one or more ordered subsets of observations as templates. A WSN node receives a template, stores it and attempts matching against incoming sensor strings. However, due to node storage access costs and

---

**Algorithm 3.1** Exact Pattern Matching (EPM) Algorithm

---

**Require:** `template`  $\neq \varepsilon$

- 1: **if** `template` is numeric **then**
- 2:    $\bar{r} \leftarrow \text{int\_sax}(\text{template})$
- 3: **else**
- 4:    $\bar{r} \leftarrow \text{template}$
- 5: **end if**
- 6: **repeat**
- 7:    $\bar{u}_r \leftarrow \text{int\_sax}(\text{sensor-values}[\ ])$
- 8:    $\delta \leftarrow \|\bar{u}_t - \bar{r}\|_S$
- 9: **until**  $\delta == 0$
- 10: call Notify and **goto** line 6

---

limitations, historic searches are not supported — a node cannot match a user-submitted template against past sensor strings as the nodes do not, by default, store past strings. Instead, they apply a sliding window over the stream of observations, convert them to a string and attempt to match against user-submitted templates, close to real-time.

Matching, shown in lines 8-9 of Algorithms 3.1 and 3.2, is performed as a distance calculation between two strings: the user-submitted template and the sensor string. The distance is calculated using a character look up table and the SAX distance metric, both discussed in Section 3.1.3. Matching is not tightly-coupled with the specific distance metric and alternative metrics are possible.

The approximate matching algorithm is a variation on exact pattern matching. In order to determine whether the sensor string matches a template, the output of the distance calculation  $\|\bar{u} - \bar{r}\|_S$  is compared to a threshold  $\theta$  (line 9 of the algorithms) as described previously (Section 3.1.3). The threshold value depends on desired matching sensitivity and is application dependent.

### 3.3 Multiple Pattern Matching

The scenarios for multiple pattern matching are: (a.) one or more users interested in exact occurrences of smaller substrings in much longer text, and

---

**Algorithm 3.2** Approximate Pattern Matching (APM) Algorithm

---

**Require:** `template`  $\neq \varepsilon$   
**Require:** `theta`  $\neq \varepsilon$   
1: **if** `template` is numeric **then**  
2:    $\bar{r} \leftarrow \text{int\_sax}(\text{template})$   
3: **else**  
4:    $\bar{r} \leftarrow \text{template}$   
5: **end if**  
6: **repeat**  
7:    $\bar{u}_t \leftarrow \text{int\_sax}(\text{sensor-values} [])$   
8:    $\delta \leftarrow \|\bar{u}_t - \bar{r}\|_S$   
9: **until**  $\delta \leq \theta$   
10: call Notify and **goto** line 6

---

(b.) a number of users submitting numerous templates of arbitrary length for matching. Both cases are accommodated in a computationally space and time efficient manner, owing to the use of a *Suffix Array* [Gus97] data structure.

The Suffix Array is defined as an array of integers in the range 0 to  $|\bar{r}| - 1$ , specifying the lexicographic order of the  $|\bar{r}|$  suffixes of text (user-submitted templates). The array requires  $O(|\bar{r}|)$  space and can be searched in  $O(|\bar{u}| \log |\bar{r}|)$  time [MM90], where  $|\bar{u}|$  is the length of the sensor string and  $|\bar{r}|$  is the length of the text. The array enables sensor nodes to determine whether their produced string matches stored user-submitted templates, maintaining theoretical search efficiency as the size of stored templates grows. A sensor string that is a substring of the text is classified as *interesting*.

The procedural steps for MPM are outlined in Algorithm 3.3. Although the listed algorithm does not show how the suffix array can be updated — for instance, if a user submits a new pattern at runtime — this can be achieved using the procedure described in [SLLM09]. An extended example that highlights the array construction and search process can be found in Appendix B, Tables B.1 and B.2, respectively.

---

**Algorithm 3.3** Multiple Pattern Matching (MPM) Algorithm

---

**Require:** `templates[]`  $\neq \varepsilon$

- 1: **for**  $i = 0$  **to** `Length(templates[])` **do**
- 2:   Construct Array for Suffixes of `templates[i]` with suffix length  $\geq$  min length of `templates[]`
- 3: **end for**
- 4: `SuffixArray`  $\leftarrow$  merge Arrays dropping duplicate Suffixes
- 5: **loop**
- 6:    $\bar{u}_t \leftarrow \text{int\_sax}(\text{sensor-values}[])$
- 7:   Index  $\leftarrow$  call `BinarySearch(SuffixArray,  $\bar{u}_t$ )`
- 8:   **if** Index  $\geq 0$  **then**
- 9:     call `Notify` and **goto** line 5
- 10:   **end if**
- 11: **end loop**

---

### 3.4 Non-Parametric Pattern Detection

The Non-Parametric Pattern Detection (NPPD) algorithm can classify sensor strings as *unusual* without relying on user-submitted templates. The typical use case involves users who wish to be informed of sustained unusual changes in the monitored object but are unable to quantify or describe changes in a manner that can be translated to one or more pattern matching expressions or templates.

Algorithm 3.4 shows the procedural steps for learning that takes place in lines 2-10. The rate of change of the monitored object is computed by comparing the string distance of temporally adjacent sensor strings. As the rate of change in the monitored object decreases, the distance between temporally adjacent strings approaches zero. With learning completed, a node stores the maximum witnessed change perceived normal as a string distance (line 7), to be used later (line 15) as a threshold value. Distance between two temporally adjacent sensor strings that exceeds the maximum learnt distance, results in the classification of the most recent sensor string as *unusual*.

### 3.5 Probabilistic Pattern Detection

---

**Algorithm 3.4** Non-Parametric Pattern Detection (NPPD) Algorithm

---

**Require:** learnPeriod  $\neq \varepsilon$

- 1:  $max_\delta, learnCounter \leftarrow 0$
- 2: **while** learnCounter  $\leq$  learnPeriod **do**
- 3:  $\bar{u}_t \leftarrow \text{int\_sax}(\text{sensor-values}_t [])$   
    {sensor-values<sub>t</sub> is a window with the most recent observations}
- 4:  $\bar{u}_{t-1} \leftarrow \text{int\_sax}(\text{sensor-values}_{t-1} [])$   
    {sensor-values<sub>t-1</sub> is a window temporally shifted by one time unit}
- 5:  $\delta \leftarrow \|\bar{u}_t - \bar{u}_{t-1}\|_S$
- 6: **if**  $\delta > max_\delta$  **then**
- 7:      $max_\delta \leftarrow \delta$
- 8: **end if**
- 9:     Increment learnCounter by 1
- 10: **end while**
- 11: **loop**
- 12:  $\bar{u}_t \leftarrow \text{int\_sax}(\text{sensor-values}_t [])$
- 13:  $\bar{u}_{t-1} \leftarrow \text{int\_sax}(\text{sensor-values}_{t-1} [])$
- 14:  $\delta \leftarrow \|\bar{u}_t - \bar{u}_{t-1}\|_S$
- 15: **if**  $\delta > max_\delta$  **then**
- 16:     call Notify and **goto** line 11 {Current distance is greater than max distance learnt}
- 17: **end if**
- 18: **end loop**

---

Probabilistic Pattern Detection (PPD) (Algorithm 3.5) is procedurally similar to non-parametric detection, in that it also undergoes a learning phase. The difference is that PPD does not employ the distance metric of Equation 3.2 to determine similarity between strings. Instead, it relies on a Markov model to compute the probability of occurrence of a sensor string, given symbol transitions observed during training.

PPD handles symbolic conversion as a Markov process where the set of states equals the size of the alphabet. If the process outputs  $\bar{u}_i$  at time  $t$  and then moves to  $\bar{u}_j$  at time  $t + 1$ , the probability for this transition is represented by  $p_{ij}$  and a state transition from state  $i$  to  $j$  is observed. To encode symbol transitions, a square matrix called the *transition matrix* is populated. For simplicity, we employ a Markov chain of order one, however higher order (memory) Markov chains can

---

**Algorithm 3.5** Probabilistic Pattern Detection (PPD) Algorithm

---

**Require:** learnPeriod,  $\theta \neq \varepsilon$

- 1: learnCounter  $\leftarrow$  0
- 2: TransitionMatrix[] []  $\leftarrow$  0
- 3: **while** learnCounter  $\leq$  learnPeriod **do**
- 4:    $\bar{u} \leftarrow \text{int\_sax}(\text{sensor-values}[])$
- 5:   **for**  $i = 0$  to  $|\bar{u}|$  **do**
- 6:     Update TransitionMatrix[] [] {Update state transition probabilities}
- 7:   **end for**
- 8:   Increment learnCounter by 1
- 9: **end while**
- 10: **loop**
- 11:    $\bar{u}_t \leftarrow \text{int\_sax}(\text{sensor-values}[])$
- 12:   **if**  $P(\bar{u}_t) \leq \theta$  **then**
- 13:     call Notify and **goto** line 10
- 14:   **end if**
- 15: **end loop**

---

be used.

Path probabilities are computed using the Markov model built during the learning phase (line 12). A path probability is a realisation of a Markov chain as a path in time through its state space [Nor97]. Such a probability for path  $(\bar{u}_1, \bar{u}_2 \dots \bar{u}_t)$  is given by:

$$P(\bar{u}_t) = p_{\bar{u}_1 \bar{u}_2} p_{\bar{u}_2 \bar{u}_3} \dots p_{\bar{u}_{t-1} \bar{u}_t}$$

A zero probability for a sensor string results in its classification as *unusual* since the individual transitions in the string were improbable, given the learning data that populated the transition matrix.

## 3.6 Summary

In this chapter we introduced a collection of algorithms that provide pattern matching and detection functionality. The basis for the algorithms is SAX, a symbolic conversion method employed to transform sliding windows of sensor

observations to strings such that pattern matching and detection can be accomplished using the strings alone.

The proposed algorithms cater for the following situations:

- (i) Exact pattern matching, that matches a sensor string against a user submitted template.
- (ii) Approximate pattern matching, that offers similarity searches between sensor strings and templates.
- (iii) Multiple pattern matching, that implements exact pattern matching with theoretical search efficiency when the cumulative length of templates is much larger than the sensor string.
- (iv) Non-parametric pattern detection, that learns the normal rate of change between temporally adjacent sensor strings, and uses it to classify new strings as normal or unusual.
- (v) Probabilistic pattern detection, similar to the above, classifies a sensor string according to the path probability of the string given a transition matrix populated during learning.

In the next chapter we evaluate the performance of our algorithms, with respect to true and false positives, in real world sensor data sets.

# Chapter 4

## Temporal Algorithms: Evaluation through Emulation

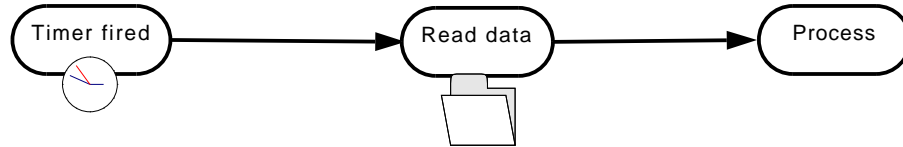
In this chapter, we initiate the performance evaluation of the pattern matching and detection algorithms introduced in Chapter 3. The aim is twofold: first, to assess matching and detection accuracy across a selection of real-world sensor data and different choice of algorithm parameters, and second, to compare the algorithms with competitive methods for event detection. Evaluation is performed by *emulation*, a type of simulation where a computer program imitates functions of another device [Jai91], in our case a WSN node — we defer discussion of practical evaluation through deployment to Chapter 5.

We begin with a discussion of methodology and experimental setup in Section 4.1 which is common across all the experiments described in this chapter. We categorise experiments in three broad case studies (Sections 4.2 to 4.4) examining data from different sensors and summarise findings in Section 4.5.

### 4.1 Methodology and Experimental Setup

We emulate the data acquisition process as it would be typically implemented in a WSN setting: sensors are sampled at a specific (configurable) frequency and observations are processed by our algorithms. The sequence, shown in Figure 4.1,

Figure 4.1: Emulating data acquisition in MATLAB: the loop of a timer firing, data read from a file, and data processed by one of the pattern matching and detection algorithms.



involves the following tasks:

- (i) A *virtual* sensor node's timer firing, for instance signalling the `fired()` event in TinyOS [STG07].
- (ii) A callback function sampling a hypothetical sensor which in this case is a call to fetch the next value from a data file.
- (iii) A processing task, which is a call to our temporal pattern matching and detection algorithms, posted once the function from the previous step has returned the value representing the sensor observation.

The experiments described in this chapter were conducted using implementations of the temporal pattern matching and detection algorithms in MATLAB R2008b [Mat10]. We employ the MATLAB `timer` object [Mat08d] to emulate the streaming nature of data acquisition in WSNs. The timer object reproduces sensor data, stored in a file, at the original sampling frequency using the `timer.Period` property.

For each matched or detected pattern, the emulation program displays a message in the MATLAB command window indicating that a pattern has been matched against a user-submitted template or detected/discovered. In addition, an entry is written to an experiment log file indicating the data file name supplying the sensor observations and the relative time point in the data file corresponding to match/detection. A plot of the sensor data is generated and contains a visual marker denoting the starting time point of detection or a user-submitted template overlaid on the sensor data. Plots were used in conjunction with the log files for counting true and false positives.

To validate the emulated implementation in MATLAB, experiments were reproduced on the WSN-specific TOSSIM [LLWC03] simulator. Verification was performed by tasking a TOSSIM-simulated node to execute the same steps as the MATLAB program and confirm pattern classification by displaying the relative timestamp (in timer ticks) of match/detection on the command window. This process confirmed that the relative time point of match/detection by MATLAB emulation was identical with that reported by TOSSIM.

## 4.2 Case Study 1: Indoor Deployment

The experiments of this case study were conducted on data from the indoor deployment [Int04] of 54 nodes at the Intel Lab, Berkeley. This data set was selected for the following reasons:

- It is representative of the class of applications we are targeting with characteristics specific to indoor deployments.
- It contains imperfections, in the form of outliers and missing values, that were not corrected to assess detection performance under realistic data characteristics.

The data set contains approximately 2.3 million observations of temperature, humidity, light, and voltage sampled at a frequency of 0.031Hz. The data is made available as a single file with timestamped observations.

### 4.2.1 Evaluation of Exact and Approximate Matching

In this section we evaluate Algorithms 3.1 and 3.2 which require the input of a specific template pattern by a user for matching against strings obtained by symbolic conversion of the sensor stream.

## **Metric**

We employ the mean number of false positives per node to characterise the impact of symbolic conversion parameters to the number of incorrect pattern matches reported by the exact and approximate matching algorithms of Chapter 3.

## **Hypothesis**

There are values of symbolic conversion parameters — alphabet size, window length and compression ratio — that reduce false positives reported by the exact and approximate pattern matching algorithms, on data from different sensors.

## **Experiments**

For this series of experiments, the data set was divided to observations per node in order to emulate data acquisition in MATLAB in the manner described previously. To simulate users interested in pattern events, template patterns were supplied by extracting sequences of data and providing them as input to the algorithms for matching. An example of a user-submitted template pattern employed in the experiments is the sustained increase in temperature observed between 7.00 am and 7.20 am, possibly due to the effect of sunrise or automated heating system.

The expected behaviour of exact pattern matching is to identify an occurrence of the user-submitted template pattern. As described in Section 3.2, the algorithm positively matches a sensor string to the template pattern when the distance between the two strings is zero. False positives are counted when the exact pattern matching algorithm produces a zero distance between the template pattern and a sensor string that does not correspond to the template pattern. Using the early morning sustained increase in temperature as a template pattern example, a false positive is counted if the algorithm matches with zero distance this template to a sensor string from a different time of day.

The expected behaviour of approximate matching is to identify similarities between user supplied template patterns and sensor strings. This translates to positively matching a sensor string to a template pattern when the distance between them is zero *or* below a user-supplied threshold. This user-supplied threshold determines the desired similarity between the template and the sensor strings. For the purpose of the experiment, appropriate values for thresholds were selected by specifying that the template pattern and the sensor string can have up to 10% of their symbols at most 2 characters apart. For instance, in this experiments the template pattern “*aabbccdde*“ would approximately match the sensor string “*abb**b**ccdd**d**e*“, with their character differences highlighted in bold typeface. A false positive is counted when the algorithm matches with distance below the threshold a pattern template to a sensor string from a different time of day. Figures 4.2a and 4.2b show examples of approximate pattern matching with windows of varying sizes.

The experiment was conducted over temperature, humidity, light, and voltage sensor data and different symbolic conversion parameter values were explored. Specifically, input window lengths of 28, 40, 160, 496, 836 and 1260 were tested as these values represent a choice likely to cater for a variety of both short and long duration pattern events. Finally, a range of symbolic conversion compression ratios (1/1, 2/1, 4/1, and 6/1) and alphabets (5, 10, 15 and 20 characters) were tested to explore the effect of string approximation information content to false positives.

## Findings

The main finding of this experiment is that the number of false positives reported by the exact and approximate pattern matching algorithms depend on symbolic conversion parameters such as compression ratio, input window length and type of sensor data. For instance, Table 4.1 shows that increasing the window length from 40 sensor readings to 160 sensor readings with a symbolic compression ratio of 2/1, reduces false positives from 13 to 3. We believe that this is a positive result as three false positive reports in a 30-day deployment period incurs only a

		Window length				Comp. Ratio
		40	160	486	836	
		<i>Mean False Positives</i>				
<b>Alphabet Size</b>	<b>5</b>	11	6	2	0	None
		17	8	4	2	2/1
		34	29	26	23	4/1
<b>Alphabet Size</b>	<b>10</b>	2	1	0	0	None
		13	3	3	1	2/1
		22	16	15	9	4/1
<b>Alphabet Size</b>	<b>15</b>	1	1	0	0	None
		13	3	3	1	2/1
		21	16	16	9	4/1

Table 4.1: Relationship of alphabet size, window length and compression ratio with the mean number of false positives (per node) reported by the Approximate Pattern Matching (APM) algorithm on the temperature attribute over a data set spanning a period of 30 days.

moderate use of the radio, for instance only three notifications transmitted.

We find that longer windows are necessary in order to reduce false positives for data with less smooth changes such as light. The average values of false positives over the light attribute are shown on Table 4.2 and their relationship to window length is in agreement with the observations made in [KLF05], in particular the view that larger windows are necessary for data with a high degree of variability. Moreover, increasing the alphabet size above 10 characters does not significantly reduce the number of false positives.

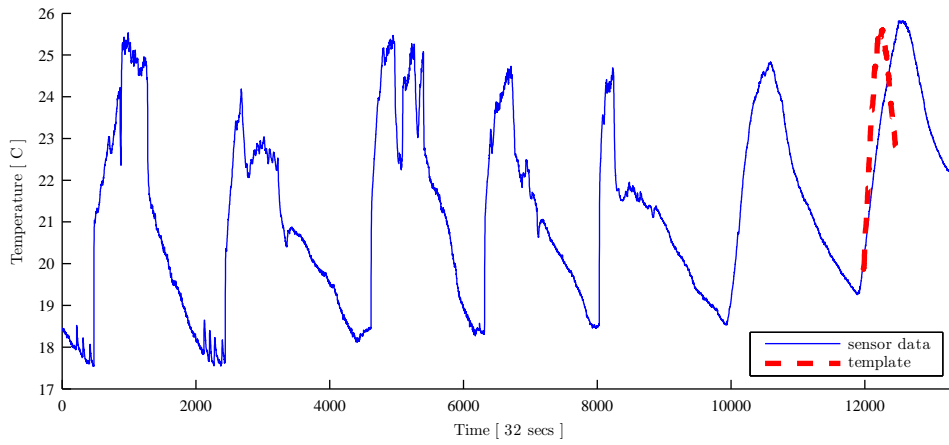
Overall, our hypothesis was confirmed as there are certain symbolic conversion parameter values that reduce the number of false positives. Specifically, we settle on an alphabet size of 10 characters, compression ratio of 2/1 or 4/1 and input window lengths of 40 and above. Although the pattern matching algorithms can use default values for these parameters, there is some benefit for users who choose to fine tune compression ratio and window length — either at pre-deployment or at runtime — according to characteristics of the sensed data such as variability and sampling frequency.

		Window length				Comp. Ratio
		40	160	486	836	
		<i>Mean False Positives</i>				
<b>Alphabet Size</b>	<b>5</b>	67	55	32	6	None
		113	98	67	29	2/1
		119	101	74	34	4/1
<b>Alphabet Size</b>	<b>10</b>	44	37	16	5	None
		87	66	41	18	2/1
		91	72	50	28	4/1
<b>Alphabet Size</b>	<b>15</b>	44	37	16	3	None
		79	64	41	18	2/1
		90	72	49	28	4/1

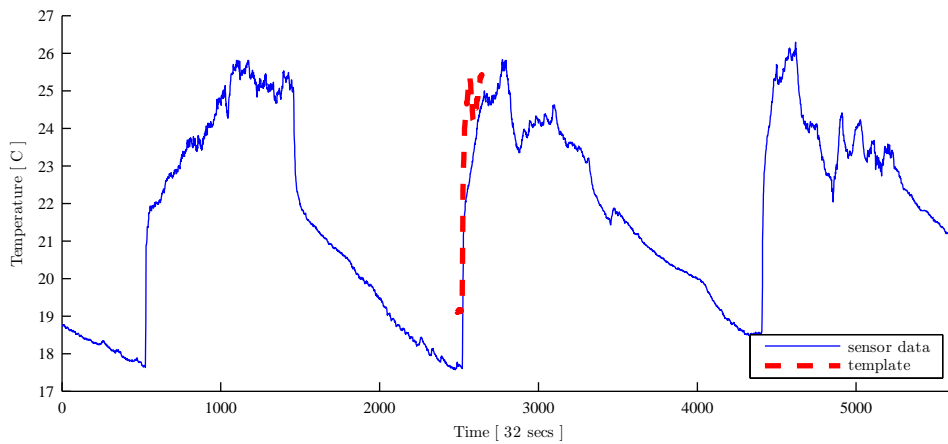
Table 4.2: Relationship of alphabet size, window length and compression ratio with the mean number of false positives (per node) reported by the Exact Pattern Matching (EPM) algorithm on the light attribute over a data set spanning a period of 30 days.

Figure 4.2: Case study 1: Approximate Matching on the Intel Data Set.

- (a) A pattern event of 486 data points (from 20/03 08:00am) is submitted for approximate matching in the week 01/03-07/03 (Node 10). A similar pattern is identified at point 11,976, with string distance 0.5.



- (b) A pattern event of 160 observations (from 17/03 06:30am) is submitted for approximate matching in the three days 01/03-03/03 (Node 3). A similar pattern from the morning spike in temperature on the 2nd of March is identified at point 2485 with string distance 0.19.



## 4.3 Case Study 2: Seismic and Acoustic Data

The purpose of this case study is to conduct an accuracy comparison of the Non-Parametric Pattern Detection (NPPD) algorithm with two alternative techniques, and to perform a preliminary study of the effects of measurement noise to detection accuracy.

The experiments were carried out on data from the volcanic monitoring deployment [WALJ<sup>+</sup>06] at Reventador, an active volcano in Ecuador. The data set was selected for the following reasons:

- It is also representative of a class of reactive environmental applications aimed at detecting unusual activity, which is a good fit with our research goals.
- It contains a large number of pattern events recorded in two sensing modalities: seismic and acoustic.

According to [WALJ<sup>+</sup>06], the deployment comprised 16 sensor nodes that sampled seismic and acoustic data at a frequency of 100Hz for a 19-day period in 2005. The data is made available as a collection of 1,209 files out of which we identified 947 contained pattern events while the rest were either data segments without unusual patterns or noise possibly due to faulty sensors. Each file includes a header section with the timestamps of the data sample including the time length of the pattern event.

### 4.3.1 Evaluation of Non-Parametric Pattern Detection

The experiments of this section compare the accuracy of the Non-Parametric Pattern Detection (NPPD) algorithm (Section 3.4) against two competitive techniques:

- *Exponentially Weighted Moving Average* (EWMA) according to the implementation details described in [WALJ<sup>+</sup>06].

- *Real-time Seismic Amplitude Measurement* (RSAM), which is an alternative method for detecting unusual volcanic activity [EM91].

The first technique was employed by the researchers who carried out the data collection while the second technique is an alternative method for measuring volcanic activity.

### Metrics

To characterise the accuracy of the pattern detection algorithm with respect to true positives, we employ the *sensitivity* [WF05] metric given by:

$$S = \frac{TP}{TP + FN}, \quad (4.1)$$

where  $TP$  is the total number of true positives classified by a pattern matching and detection method and  $FN$  is the total number of false negatives. In addition, we use the *false positive rate* which is given by:

$$FPR = \frac{FP}{TP + FN}, \quad (4.2)$$

where  $FP$  is the total number of false positives or patterns misclassified as *unusual* by our algorithm.

### Hypothesis

The Non-Parametric Pattern Detection (NPPD) algorithm (Section 3.4) can perform competitively against EWMA and RSAM.

### Experiments

The process followed measures the accuracy of NPPD by counting the number of true and false pattern event occurrences reported by the algorithm and comparing it against the corresponding figures for EWMA and RSAM. To investigate the impact of algorithmic parameters to pattern detection accuracy we conduct the

experiments using two settings: *high sensitivity* aiming to make pattern detection more sensitive to seismic events of relatively small magnitude and *low sensitivity* for detecting seismic disturbances of relatively higher magnitude. For NPPD the choice of high/low sensitivity was represented by the symbolic conversion compression ratios of 2/1 and 4/1. In the case of EWMA and RSAM, high/low sensitivity was implemented by selecting different values for the thresholds.

For this case study, NPPD uses a window length of 128 readings and a 10-letter alphabet. The values for these parameters relate to the symbolic conversion component of the NPPD algorithm and were obtained during earlier empirical studies, discussed in Section 4.2.1. The NPPD algorithm was trained on a subsequence of 1,024 data points that did not contain any pattern events. Distances were computed using Equation 3.2 for the comparison of adjacent strings obtained by transforming temporally adjacent numeric sensor observations using the algorithm of Section 3.4.

Both EWMA and RSAM rely on a threshold to determine whether the underlying activity of the monitored process is unusual. In the case of EWMA, the ratio of two exponentially-weighted moving averages (EWMAs) over the input signal is compared to the threshold. The short-term average (STA) contained 30 observations, the long-term average (LTA) contained 300 observations and the threshold was set to 0.3 and to 0.25 to represent low and high sensitivity respectively. We obtained values for STA/LTA window lengths, weights and thresholds empirically after testing numerous alternatives on a 1/4 of the data <sup>1</sup>.

RSAM [EM91] is similar to EWMA, but instead of operating on ratios of averages it sums the mean amplitude of the signal during a given interval to provide a measure of the level of activity. When the RSAM amplitude exceeds a threshold an event is triggered. We employed an interval of 3,000 observations and thresholds of 0.02 and 0.01 to represent low and high sensitivity respectively.

---

<sup>1</sup>We attempted to communicate with the authors of the original work [WALJ<sup>+</sup>06, WADHW08] to enquire about their choice of parameter values but unfortunately we did not receive a reply.

	NPPD		EWMA		RSAM	
	<i>TP</i>	<i>FP</i>	<i>TP</i>	<i>FP</i>	<i>TP</i>	<i>FP</i>
Low Sensitivity	77.4%	3.8%	76.8%	8.2%	56.9%	1.06%
High Sensitivity	92.7%	18.9%	91.9%	20.2%	84.5%	2.2%

Table 4.3: Summary of detection accuracy results of NPPD compared with EWMA and RSAM. *TP* stands for *True Positives* and *FP* stands for *False Positives*.

## Findings

The main findings of the experiments are summarised in Table 4.3. We found that NPPD detected 92.7% or 878 of the total 947 events with a false positive ratio of 18.9% or 179 patterns falsely classified as *unusual*. These results are on par with the accuracy of EWMA that detected 91.9% or 870 events with a false positive ratio of 20.2% or 192 events. RSAM performed less well in detection, with true positive rate of 84.48% or 800 events, but produced a significantly lower number of false positives (2.2% or 21 events).

To highlight the type of seismic events contained in the data set we show two examples in Figure 4.3. We also show how these patterns are detected by NPPD with both low (4/1 compression ratio) and high sensitivity (2/1 compression ratio) detection depicted as vertical lines marking the starting point of the most recent unusual pattern. Similarly, Figure 4.4 shows an example of a seismic event and corresponding summarised seismic amplitude using the EWMA and RSAM methods.

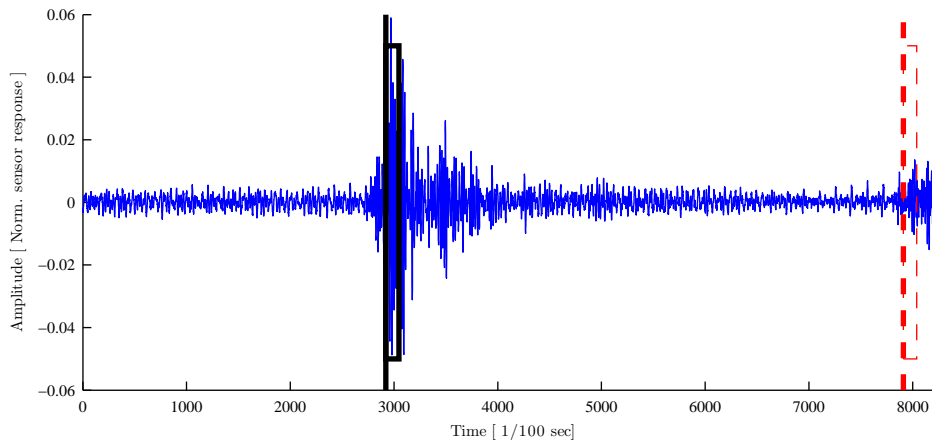
In line with our expectations, decreasing compression ratio produces better approximations of the numeric sensor data. This improves the rate of true positives detected by NPPD since relatively smaller changes in seismic activity are represented by different symbols causing higher distances between temporally adjacent sensor strings. This illustrates the tradeoffs between low and high sensitivity: for both NPPD and EWMA, high sensitivity increases the true positive rate (from 77.4% to 92.7% for NPPD) but there is a corresponding rise in the number of false positives (from 3.8% to 18.9%). RSAM performed better in that

respect as the rate of growth in false positives was much smaller — from 1% with low sensitivity to 2.2% with high sensitivity.

In summary, the hypothesis that NPPD can perform competitively against EWMA and RSAM was confirmed by the experimental results of this case study.

Figure 4.3: Case study 2: Examples of seismic pattern events detected by NPPD with two sensitivity levels and corresponding compression settings. The solid vertical line denotes 4/1 compression and the dashed line denotes 2/1 ratio.

- (a) Seismic events at node 200 (13/08/2005, 12.29). The rectangle shows the length of the unusual pattern.



- (b) Seismic events at node 209 (16/08/2005, 04.04). The rectangle shows the length of the unusual pattern.

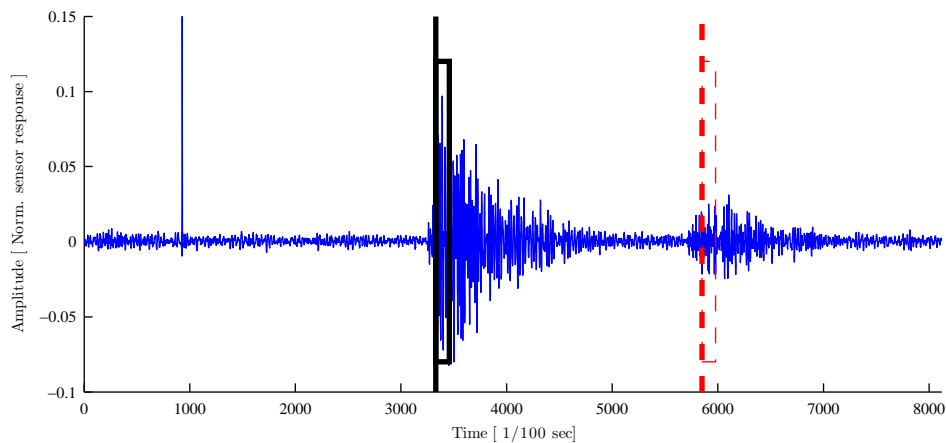
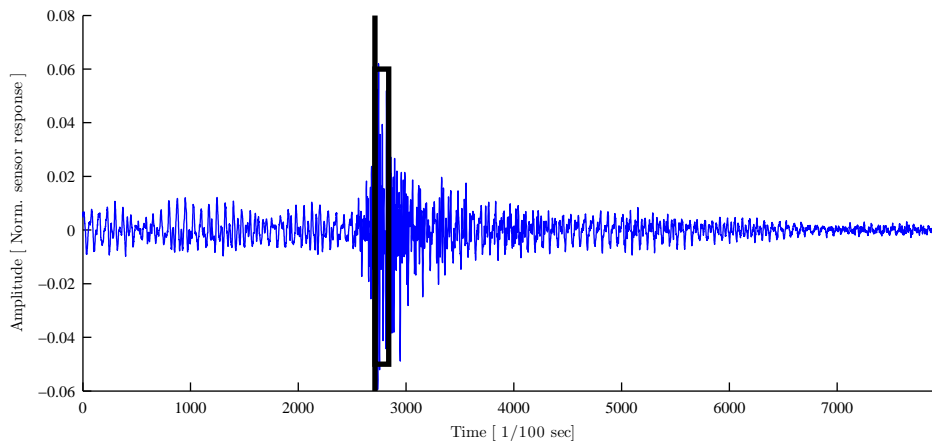


Figure 4.4: Case study 2: A comparison of pattern detection using NPPD with EWMA and RSAM. In Figure 4.4a, the vertical line (node 201, 14/08/2005, 01.50) denotes the beginning of the unusual pattern and the rectangle shows the pattern length (128). Figure 4.4b shows the EWMA ratio of averages with a horizontal line representing the threshold.

(a) Pattern detected as unusual (denoted by the vertical line) using NPPD



(b) Seismic activity summarisation with EWMA, denoted by the STA/LTA ratio, and event detection shown by the STA/LTA ratio crossing the horizontal threshold line

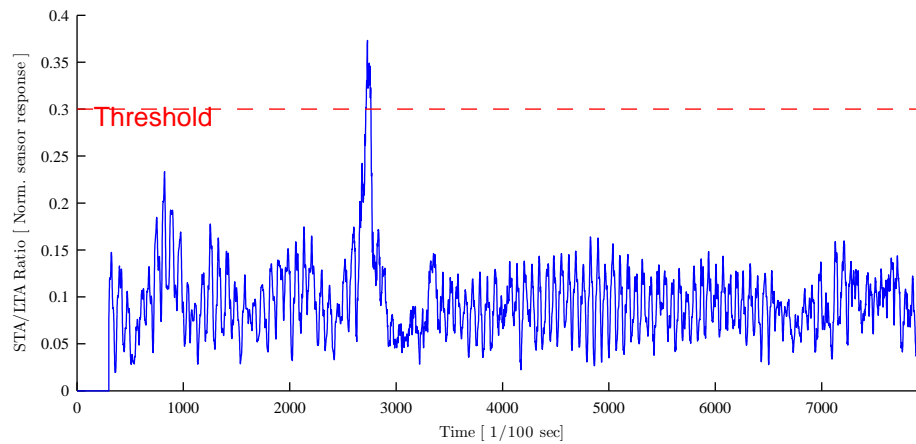
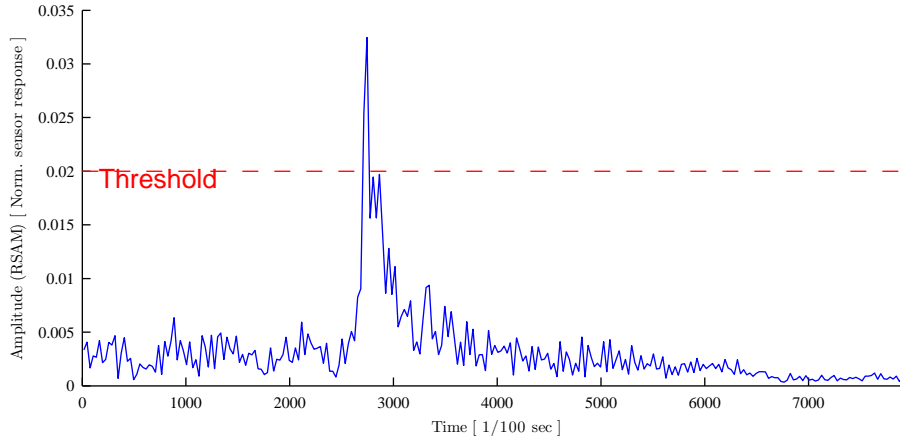


Figure 4.4: Case study 2: Figure 4.4c shows the RSAM measure with the horizontal line representing the threshold.

- (c) Seismic amplitude summarisation with RSAM, denoted by the RSAM measure, and event detection shown by the summarised amplitude crossing the horizontal threshold line



### 4.3.2 The Effect of Measurement Noise to NPPD

This experiment is a preliminary investigation into the effect of measurement noise to pattern detection accuracy. It employs a simplified additive noise model and aims to provide an insight in the noise magnitude tolerated by the NPPD algorithm.

#### Hypothesis

Sensitivity and false positive rate of the NPPD algorithm degrade gracefully with respect to increasing signal noise.

#### Experiments

We focus on a subset of the entire data set, specifically the data from an active volcanic day with 90 natural events — the 14th of August 2005 from 00:58 to 21:08. Observations are corrupted by additive random noise of progressively

Mean SNR	Mean SNR (dB)	True Positives	False Positives
1	0	87.78%	14.44%
0.87	-0.6048	87.78%	7.78%
0.73	-1.3668	86.52%	6.74%
0.49	-3.098	83.33%	6.67%
0.36	-4.437	76.67%	4.44%
0.17	-7.6955	60.00%	3.33%
0.09	-10.4576	18.89%	7.78%

Table 4.4: The effect of additive random noise to NPPD detection accuracy, represented by sensitivity and false positive rate.

higher magnitudes obtained by MATLAB’s `randn` function [Mat08c] that generates pseudorandom values drawn from the standard normal distribution.

The Signal-to-Noise Ratio (SNR) for each experiment was calculated as the power ratio of the signal over the noise [Byr05], and specifically using the following formula over the square amplitude ratio:

$$SNR = \left( \frac{A_{Signal}}{A_{Noise}} \right)^2,$$

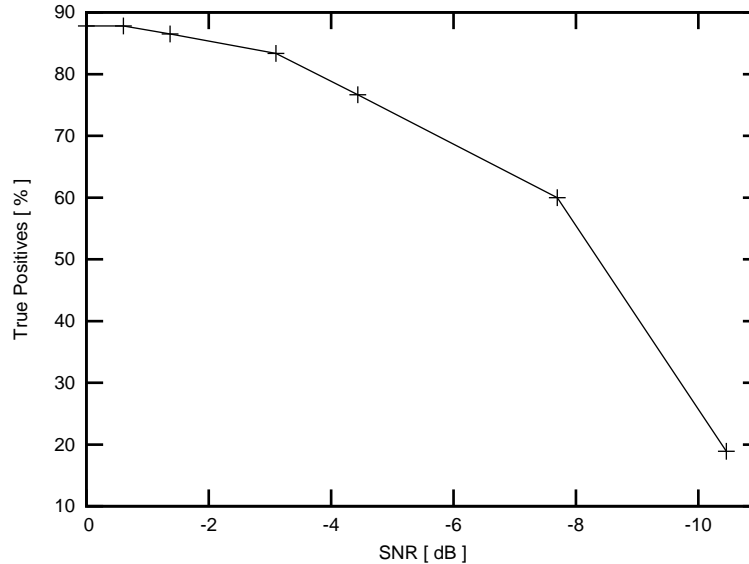
where  $A_{Signal}$  stands for the amplitude of the signal and  $A_{Noise}$  stands for the amplitude of the noise. The symbolic conversion component of the NPPD algorithm employed similar parameters to the previous experiment: a window length of 128, compression ratio of 2/1 and alphabet size of 10.

## Findings

As seen in Table 4.4 and Figure 4.5, we find that detection accuracy degrades gracefully in relationship to decreasing SNR: deteriorating the signal to a mean SNR of 0.73 reduced sensitivity from 87.78% to 86.52%. NPPD accuracy, represented by true positive rate, reduces to 83.33% even when signal is corrupted with mean SNR of 0.49.

One, perhaps unexpected, result is that a mean SNR of 0.73 reduced the number of false positives from 14.44% to 6.74%. This reduction is attributed to variations in signal amplitude, previously falsely detected as unusual patterns

Figure 4.5: Impact of Signal to Noise Ratio (SNR) on true positives.



which, in this case, become less prominent as they are surrounded by similar variations caused by noise.

These preliminary findings confirm the hypothesis that the NPPD algorithm can tolerate a degree of additive noise in the signal without significantly compromising pattern detection accuracy.

## 4.4 Case Study 3: Physiological Data

This data set was obtained from the UCR Time Series Data Mining archive [UoC08] and contains Electrocardiography (ECG) and Electromyography (EMG) data. It was selected for the following reasons:

- It is representative of a large class of systems, such as body sensor networks, targeted by our approach.
- It incorporates pattern events with different characteristics than the other case studies: specifically changes tend to be in signal periodicity rather than in sensor reading magnitude.

The ECG data contains segments of 512 normal observations sampled at 128Hz that change to supraventricular and malignant ventricular — both different types of arrhythmias — for the remaining 512 observations. The EMG data contains two sets of 30,000 observations sampled at 1KHz of an athlete’s Gluteus Maximus activity during the last 30 seconds of a 3 min exercise on a treadmill at 3.72 m/s for the first set and 4.56 m/s for the second set.

#### 4.4.1 Evaluation of Non-Parametric and Probabilistic Pattern Detection

The purpose of this experiment is to evaluate the detection latency of non-parametric and probabilistic pattern detection, Algorithms 3.4 and 3.5 of the previous chapter respectively.

##### Metric

To characterise the delay in pattern detection, we employ detection latency as the time elapsed, in seconds, between the starting point of a pattern event and the time point that the pattern was classified as unusual by the algorithms. This metric is important in the context of medical applications since timely notification of pattern events concerning the health status of a patient can be critical [MFjWM04].

##### Hypothesis

Non-parametric and probabilistic algorithms are capable of detecting patterns in high frequency physiological data with relatively low detection latency.

##### Experiments

To simulate an ECG pattern event, we append segments from supraventricular and malignant ventricular ECG data to normal ECG data. There are 18 ECG segments of normal data, 30 segments of supraventricular and 22 segments of

malignant ventricular. The experiment tests 52 combinations of normal ECG changing to either supraventricular or malignant ventricular. For EMG data we append two sets recording muscular activity from the same athlete on a treadmill workout with different speed settings.

For NPPD, a window length of 128 observations was used with compression ratio of 2/1, alphabet size of 10 and training data set to a 1/4 of each data set.

The PPD algorithm does not require any parameters apart from a learn counter which was set to a 1/4 of each data set or 128 and 7,500 observations, for ECG and EMG respectively. Recall that detection occurs when distance between temporally adjacent strings exceeds the maximum learnt distance in the case of NPPD, and for PPD, when the path probability for observed strings obtained from symbolic conversion of numeric observations is equal to zero.

## Findings

Table 4.5 summarises the minimum, maximum and average latencies over the 52 ECG experiments. These findings confirm the hypothesis and show relatively low NPPD mean latency: 0.086 seconds for normal ECG turning to malignant ventricular and 0.102 seconds for normal ECG turning to supraventricular. Corresponding times for the detection latency of the PPD algorithm, were 0.047 and 0.109 seconds. We believe that the worst-case scenario with maximum detection latency of 0.797 seconds shows a delay that could satisfy bounds of time critical medical applications.

Examples of pattern detection for ECG data and the NPPD algorithm are shown in Figures 4.6a (malignant ventricular) and 4.6b (supraventricular).

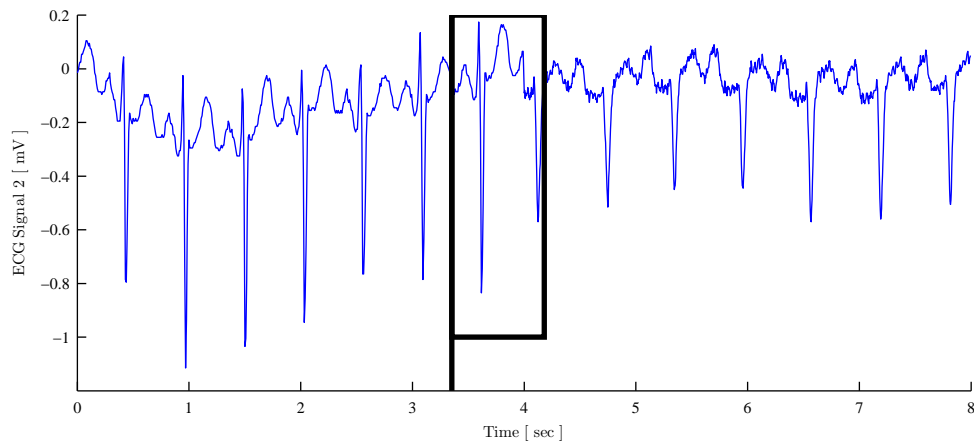
Due to lack of additional data, the EMG evaluation consisted of only one experiment where the PPD algorithm flagged a string of length 512 with 0-probability at time 30.412 shown in Figure 4.7 — a latency of 0.412 seconds.

	<b>Pattern Detection Latency (secs)</b>		
	Min	Max	Mean
	<i>Non Parametric Pattern Detection</i>		
Normal ECG changing to Malignant Ventricular	0.055	0.492	0.086
Normal ECG changing to Supraventricular	0.062	0.797	0.102
	<i>Probabilistic Pattern Detection</i>		
Normal ECG changing to Malignant Ventricular	0.039	0.156	0.047
Normal ECG changing to Supraventricular	0.07	0.359	0.109

Table 4.5: Minimum, maximum and mean detection latency (in seconds) over 52 experiments of NPPD and PPD algorithms on ECG data. Learning counter was set to 1/4 of the data set, or exactly 1 second. Latency is the elapsed number of seconds from the time of the pattern event (exactly at 4 seconds) to the time of detection.

Figure 4.6: Case study 3: Example of NPPD on ECG data: the ECG changes from normal to arrhythmic at precisely 4 seconds. The vertical line denotes the beginning of an unusual pattern detected and the rectangle denotes the length of the pattern (128 data points).

- (a) ECG — normal turning to Malignant Ventricular (trial 12). The change happens at precisely 4 seconds. The pattern is identified at 4.18.



- (b) ECG — normal turning to Supraventricular (trial 1). The change occurs at precisely 4 seconds. The pattern is identified at 4.38.

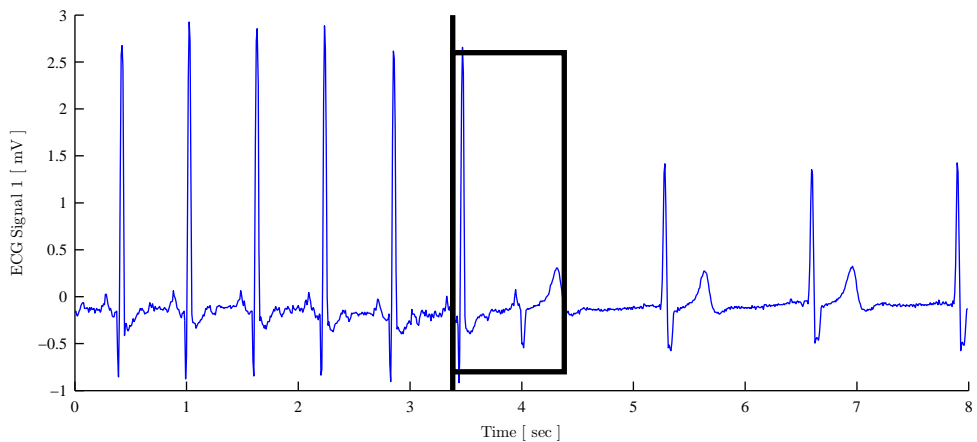
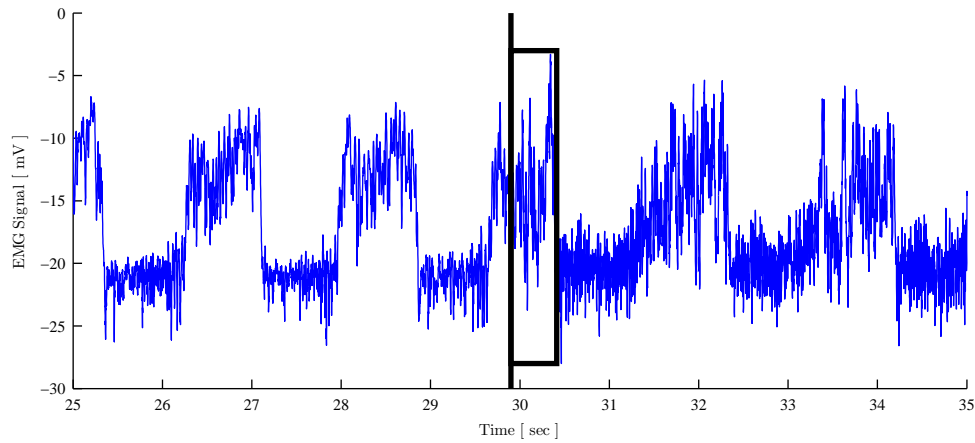


Figure 4.7: Case study 3: Example of PPD on EMG Data — a string of length 512 is classified as unusual with a zero path probability at time point 30.412. The change occurs at precisely 30 seconds. The vertical line denotes the beginning of an unusual pattern and the rectangle denotes the length of the pattern (512 data points).



## 4.5 Summary of Findings

We conducted evaluation of the temporal pattern matching and detection algorithms on three data sets and the following eight sensing modalities: seismic, acoustic, temperature, humidity, voltage, light, ECG and EMG. The data sets were selected to represent target reactive applications that can benefit from pattern matching and detection functionality.

We found the following:

- (i) Symbolic conversion parameter values play a role in the number of false positives reported by the exact and approximate pattern matching algorithms. Longer input windows reduce false positives especially on data with a high degree of variability.
- (ii) The non-parametric pattern detection algorithm is competitive with other techniques such as EWMA and RSAM. NPPD provides higher detection sensitivity (true positive rate) than both EWMA and RSAM.
- (iii) NPPD sensitivity degrades gracefully with respect to increasing signal noise: detection accuracy remains over 80% even with a mean SNR of 0.49.
- (iv) Both NPPD and PPD algorithms show relatively low detection latency — approximately a tenth of a second on average — on physiological data such as ECG and EMG.

We continue the evaluation of the temporal algorithms in the next chapter with a discussion of findings obtained through deployment.

# Chapter 5

## Temporal Algorithms: Evaluation through Deployment

This chapter analyses the runtime behaviour and operational profile of the proposed temporal domain algorithms, and shows their suitability for the extremely resource constrained execution platform through deployment on real WSNs.

First, Section 5.1 demonstrates execution efficiency through measurement of the algorithms' runtime on WSN nodes. Second, Section 5.2 introduces a dynamic sampling frequency management method that allows nodes to reduce MCU workload during periods of inactivity. Third, Section 5.3 describes integration with a Publish/Subscribe system that provides the user interface to the pattern matching and detection algorithms. Finally, Section 5.4 illustrates suitability for a novel type of node that lacks on-board power source and Section 5.5 summarises findings from deployments.

### 5.1 Execution Profile of Temporal Domain Algorithms

The vast majority of extremely resource constrained WSN nodes lack floating point units (FPUs) forcing floating point operations to be executed in software

penalising performance and accuracy of arithmetic results [Gol91, Hig02]. The floating point arithmetic impact identified in conventional computing as capable of reducing system performance by half [OF02], is magnified in WSNs since apart from affecting performance it can consequently reduce useful node lifetime.

Motivated by the dependence of symbolic conversion and distance calculation components of the temporal algorithms on floating-point operations, we initiated a study into their execution profile. We identify the cost of floating point operations involved in the temporal algorithms, and we refactor such that they use exclusively integer arithmetic. To this effect, we employ a combination of scaling, fixed-point arithmetic, bitwise techniques and related optimisations such as loop unrolling. In the following sections, we show the runtime savings achieved through the application of these techniques. A detailed discussion of methods and techniques employed can be found in [ZR09d].

Timing measurements reported in this chapter are collected on TMote Sky/TelosB [Sen08] nodes running TinyOS 2 [LBC<sup>+</sup>08] applications compiled with msp430-gcc 3.2.3. Execution times are measured at entry and exit points of functions with the `Timer` [STG07] component of TinyOS and specifically the `startOneShot` and `stop` commands. Elapsed execution times for blocks of code under investigation are reported using the TinyOS `printf` library.

### 5.1.1 Refactoring of Pattern Matching and Detection Algorithms

The purpose of this experiment is to profile the pattern matching and detection algorithms in order to show that they are suitable for extremely resource constrained WSN nodes. For reference, we first identify (Appendix C) the relative cost of different arithmetic operations on the target platform. The outcome is a timing model (cf. Table C.1) used as a guide in the software development process of the integer-only pattern matching and detection algorithms.

## Metrics

The execution profile of the pattern matching and detection algorithms is characterised by:

- Total processing runtime (in milliseconds) required by the pattern matching and detection algorithms.
- Total RAM usage (in bytes) occupied by the program image.

## Hypothesis

There are significant runtime savings to be gained from the application of integer arithmetic combined with related optimisations to the pattern matching and detection algorithms.

## Experiments

We compare the execution time required for our temporal algorithms between floating point and integer arithmetic implementations. We use an alphabet of 10 characters and compression ratio of 2/1, as these are typical parameter choices established in the last chapter. Time requirements for exact and approximate matching are identical since they involve the same procedural steps.

For the Multiple Pattern Matching (MPM) algorithm, we implement a linear search algorithm (cf. [Gus97] for a description of linear search algorithms on strings) as a basis for comparison with respect to search costs, for example searching whether a sensor string exists among a collection of user submitted templates. We collect timing measurements for MPM from nodes that produce strings of length 20 from numeric sensor observations of length 40.

We begin our analysis by profiling operations, through execution time measurement, involved in a floating-point implementation of the pattern matching algorithm. The execution profile shows that the larger share of processing time is attributed to normalisation of numeric sensor values according to the formula:

$$\frac{u_i - \mu}{\sigma}$$

where  $\mu$  is the mean and  $\sigma$  is the standard deviation of the sequence of numeric sensor values  $u$ . To reduce this cost attributed to floating point division and subtraction, we replace floats with integers and eliminate division altogether. Instead, we scale<sup>1</sup> the row of breakpoints — (Table 3.1, in Chapter 3) corresponding to alphabet size — by integer  $\sigma$ . To operate on numbers of the same magnitude, we multiply the intermediate Piecewise Aggregate Approximation (PAA) representation by the same scaling factor. The number of multiplications required, is equal to the length of the resulting string representation. Scaling the breakpoints involves 10 — the length of breakpoints and typical size of alphabet — multiplications compared to 40 or more — the length of the numeric sequence — divisions previously required to standardise  $u$ .

We introduce an integer square root is for computation of standard deviation  $\sigma$ . Substituting integer square root for operating on numbers of higher magnitude requiring 64-bit types is a costly decision according to Table C.1 (Appendix C) which shows 64-bit division requiring almost as much MCU time as floating point division. With integer square root and the maximum value produced by the Analog-to-Digital Converter (ADC), 32-bit numbers are sufficient for representing the maximum values of scaled results.

## Findings

The main finding of this experiment is the improved execution time of the integer pattern matching algorithm, shown in Figure 5.1, in comparison with a floating point implementation. Table 5.1 shows a more detailed account of the timing measurements for operations involved in a floating-point implementation of pattern matching. The corresponding timing measurements for the integer-only implementation of the exact and approximate algorithms are shown in Table 5.2:

---

<sup>1</sup>We use binary scaling with a scaling factor of 2048.

Operation	Number of data points in input window					
	40		80		120	
	Time (ms)	% of total time	Time (ms)	% of total time	Time (ms)	% of total time
NORMALISATION						
a. Mean	12	(10.34%)	24	(10.3%)	37	(10.72%)
b. Std Dev	42	(36.21%)	81	(34.76%)	120	(34.78%)
c. Subtract & Divide	25	(21.55%)	53	(22.75%)	78	(22.61%)
PAA TRANSFORM	24	(20.69%)	48	(20.6%)	73	(21.16%)
SYMBOLIC TRANSFORM	10	(8.62%)	20	(8.58%)	28	(8.12%)
DISTANCE CALCULATION	3	(2.59%)	7	(3.0%)	9	(2.61%)
<b>Total Time</b>	116ms		233ms		345ms	
RAM Image Size (Bytes)	766		846		926	

Table 5.1: Performance Times (in ms) for Exact Pattern Matching (EPM) and Approximate Pattern Matching (APM) algorithms implemented in floating point operations.

the process of converting a window of 40 data points to a string and then matching against a user-submitted template takes 11.74ms compared to 116ms for the floating point pattern matching algorithms, a factor of ten improvement.

To illustrate the difference in current consumption, the floating point pattern matching algorithm requires 60.3mA<sup>2</sup> while its integer-only counterpart requires 8.43mA, based on a sampling frequency of 1Hz and input window of 40 data points. Apart from the direct benefit of reducing power draw due to reduced MCU workload, reduced execution times also allow WSN application designers to shut off node components for longer achieving further savings in resources.

The runtime performance of the Non-Parametric Pattern Detection (NPPD) algorithm is comparable with exact and approximate pattern matching since it

<sup>2</sup>Calculated consulting the datasheet power draw for active and idle MCU time [Sen08].

Operation	Number of data points in input window					
	40		80		120	
	Time (ms)	% of total time	Time (ms)	% of total time	Time (ms)	% of total time
NORMALISATION	5.96	(51.95%)	9.97	(50.87%)	15.59	(49.36%)
PAA TRANSFORM	4.13	(35.97%)	6.81	(34.74%)	11.41	(36.13%)
SYMBOLIC TRANSFORM	0.92	(7.99%)	1.81	(9.23%)	2.91	(9.21%)
DISTANCE CALCULATION	0.47	(4.1%)	1.01	(5.15%)	1.67	(5.3%)
<b>Total Time</b>	11.74ms		19.6ms		31.58ms	
RAM Image Size (Bytes)	1180		1371		1591	

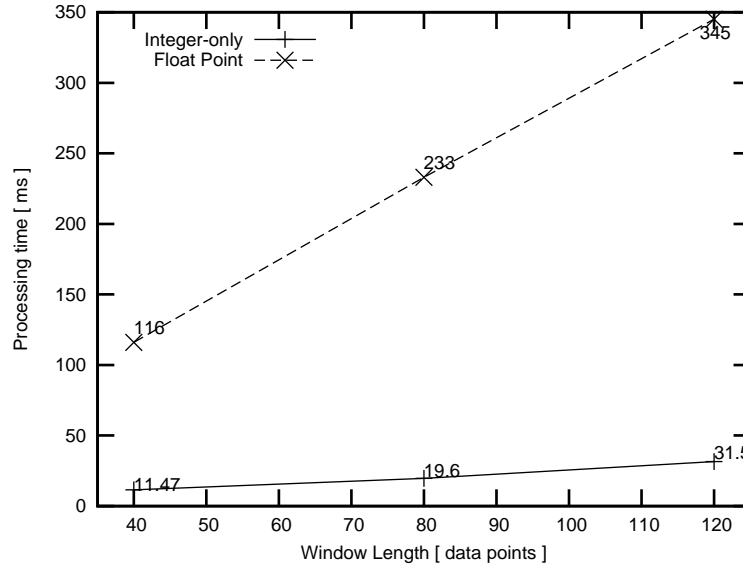
Table 5.2: Performance Times (in ms) for Exact Pattern Matching (EPM) and Approximate Pattern Matching (APM) algorithms implemented in integer arithmetic.

involves similar procedural steps. However, NPPD requires two calls to symbolic conversion to convert the temporally adjacent windows of numeric sensor observations to strings. The execution times for NPPD are shown in Table 5.3.

For Multiple Pattern Matching (MPM), Table 5.4 shows the comparison in terms of the runtime cost of matching a sensor produced string in the collection of user-submitted patterns against a linear search approach. MPM requires 8ms to search for a sensor string of length 20 in a collection of templates of cumulative size of 256, compared to 14ms for the linear search. None of the test cases represent a worst-case for linear search, that is when the sensor string is not found at all in the user-submitted collection of templates.

These findings confirm the hypothesis as there is a factor of ten improvement in runtime performance achieved through precise implementation of the temporal domain algorithms with integer arithmetic and related optimisations.

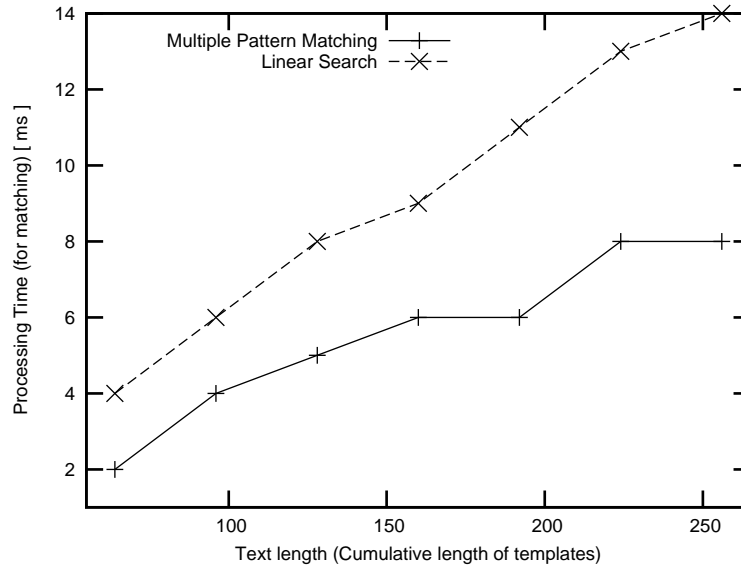
Figure 5.1: Runtime comparison of floating-point and integer-only APM/EPM algorithm implementations on a TMote Sky /TelosB.



Operation	Number of data points in input window					
	40		80		120	
	Time (ms)	% of total time	Time (ms)	% of total time	Time (ms)	% of total time
NORMALISATION	6.23	(47.13%)	11.96	(49.83%)	18.11	(50.11%)
PAA TRANSFORM	5.09	(38.5%)	8.92	(37.17%)	13.23	(36.6%)
SYMBOLIC TRANSFORM	1.43	(10.82%)	2.11	(8.79%)	3.13	(8.66%)
DISTANCE CALCULATION	0.47	(3.56%)	1.01	(4.21%)	1.67	(4.63%)
<b>Total Time</b>	13.22ms		24.0ms		36.14ms	
RAM Image Size (Bytes)	1941		2620		3210	

Table 5.3: Performance Times (in ms) for Non-Parametric Pattern Detection (NPPD) algorithm implemented in integer arithmetic.

Figure 5.2: Comparison of MPM with linear search. The MPM search is for a sensor string of length 20 in the cumulative text of templates.



Cumulative Length of template patterns	Time (ms)		RAM (bytes)	
	<i>MPM</i>	<i>Linear</i>	<i>MPM</i>	<i>Linear</i>
64	2	4	728	591
96	4	6	776	623
128	5	8	824	655
160	6	9	872	688
192	6	11	920	721
224	8	13	968	754
256	8	14	1016	786

Table 5.4: Search cost execution times (in ms) and RAM usage (in bytes) for MPM compared to linear search. The MPM search is for a sensor string of length 20 in the collection of user-submitted template patterns.

## 5.2 Dynamic Sampling Frequency Management (DSFM) Algorithm

Dynamic Sampling Frequency Management (DSFM) extends Non-Parametric Pattern Detection (NPPD) by allowing WSN nodes to automatically adjust their sampling frequency according to the rate of change of the monitored object. The aim of DSFM is to reduce resource expenditure attributed to MCU and sensor acquisition during periods of relative stability of the monitored object.

The procedural steps for DSFM are listed in Algorithm 5.1 and are similar to Non-Parametric Pattern Detection (cf. Section 3.4) involving an identical learning phase. When learning completes, a node progressively reduces its sampling frequency until the minimum allowed sampling frequency is achieved. If a node observes a distance greater than the maximum distance learnt caused by a pattern classified as *unusual*, the maximum allowed sampling frequency is restored.

We recognise that certain WSN applications have strict sampling frequency requirements dictated by signal periodicity. If these requirements can be specified as a sampling frequency interval, DSFM selects and adjusts sampling frequency within the interval relaxing the need for pre-deployment signal analysis.

---

**Algorithm 5.1** Dynamic Sampling Frequency Management (DSFM) Algorithm

---

**Require:** learnPeriod  $\neq \varepsilon$ **Require:** min-sampling-frequency, max-sampling-frequency

```

1:  $max_\delta, learnCounter \leftarrow 0$ 
2: while learnCounter  $\leq$  learnPeriod do
3:    $\bar{u}_t \leftarrow \text{int\_sax}(\text{sensor-values}_t [])$ 
     {sensor-valuest is a window with the most recent observations}
4:    $\bar{u}_{t-1} \leftarrow \text{int\_sax}(\text{sensor-values}_{t-1} [])$ 
     {sensor-valuest-1 is a window temporally shifted by one time unit}
5:    $\delta \leftarrow \|\bar{u}_t - \bar{u}_{t-1}\|$ 
6:   if  $\delta > max_\delta$  then
7:      $max_\delta \leftarrow \delta$ 
8:   end if
9:   Increment learnCounter by 1
10: end while
11: loop
12:    $\bar{u}_t \leftarrow \text{int\_sax}(\text{sensor-values}_t [])$ 
13:    $\bar{u}_{t-1} \leftarrow \text{int\_sax}(\text{sensor-values}_{t-1} [])$ 
14:    $\delta \leftarrow \|\bar{u}_t - \bar{u}_{t-1}\|$ 
15:   if  $\delta \geq max_\delta$  then
16:     Call Notify
17:     if sampling-frequency  $<$  max-sampling-frequency then
18:       sampling-frequency  $\leftarrow$  max-sampling-frequency
       {Set sampling frequency to maximum allowed}
19:     end if
20:   else
21:     if sampling-frequency  $>$  min-sampling-frequency then
22:       if sampling-frequency  $\times .9 >$  min-sampling-frequency then
23:         sampling-frequency  $\leftarrow$  sampling-frequency  $\times .9$ 
         {Reduce sampling frequency by 10%}
24:       else
25:         sampling-frequency  $\leftarrow$  min-sampling-frequency
26:       end if
27:     end if
28:   end if
29: end loop

```

---

### 5.2.1 Data Centre WSN Deployment

To assess the operation of Dynamic Sampling Frequency Management (DSFM), we deploy the algorithm on a network of seven TMote Sky/TelosB nodes in a commercial data centre.

#### Context and Deployment Details

The deployment was commissioned by a global telecommunications company as a proof of concept for a data centre monitoring solution. It was carried out at the company's London headquarters in a data centre hosting over 200 servers and associated storage and networking equipment.

The most common type of failures observed by this company are due to cooling problems that cause, sometimes unrecoverable, hardware failures. These cooling failures are usually attended by a dedicated team of four facilities employees. A Building Management System (BMS) with wired sensors is responsible for detecting increases in temperature and notifying the facilities team. However, in the last two years technical employees noticed a large number of BMS false negatives where sustained high temperature events were not identified. A number of servers equipped with built-in sensors and management agents periodically alert on high inlet or ambient temperature observations without a corresponding alert from the BMS.

On the 2nd of May 2010, the company experienced a substantial failure of one of the two air conditioning units in its London data centre. The failure reduced the cooling capacity to half and caused concern for critical systems hosted in the data centre. The facilities team investigated the problem and found that the failed cooling unit was in need of complete replacement. While waiting for the purchase, delivery and replacement of the faulty unit, the facilities team decided to temporarily reduce rising temperatures by opening windows, to facilitate cold air circulation, and deploying several portable air-conditioning units. In hindsight, the open windows adversely affected the operation of computing equipment and caused latent failures, due to dust particles gathering on air ducts

of sensitive hardware.

### Metric

In order to assess the benefit of the DSFM algorithm the metric of MCU workload saving is introduced as the number of timer ticks saved due to DSFM in comparison with operating under constant sampling frequency.

### Hypothesis

The DSFM algorithm can reduce MCU workload, expressed as total number of timer ticks, by autonomously adjusting node sampling frequency without compromising detection of pattern events.

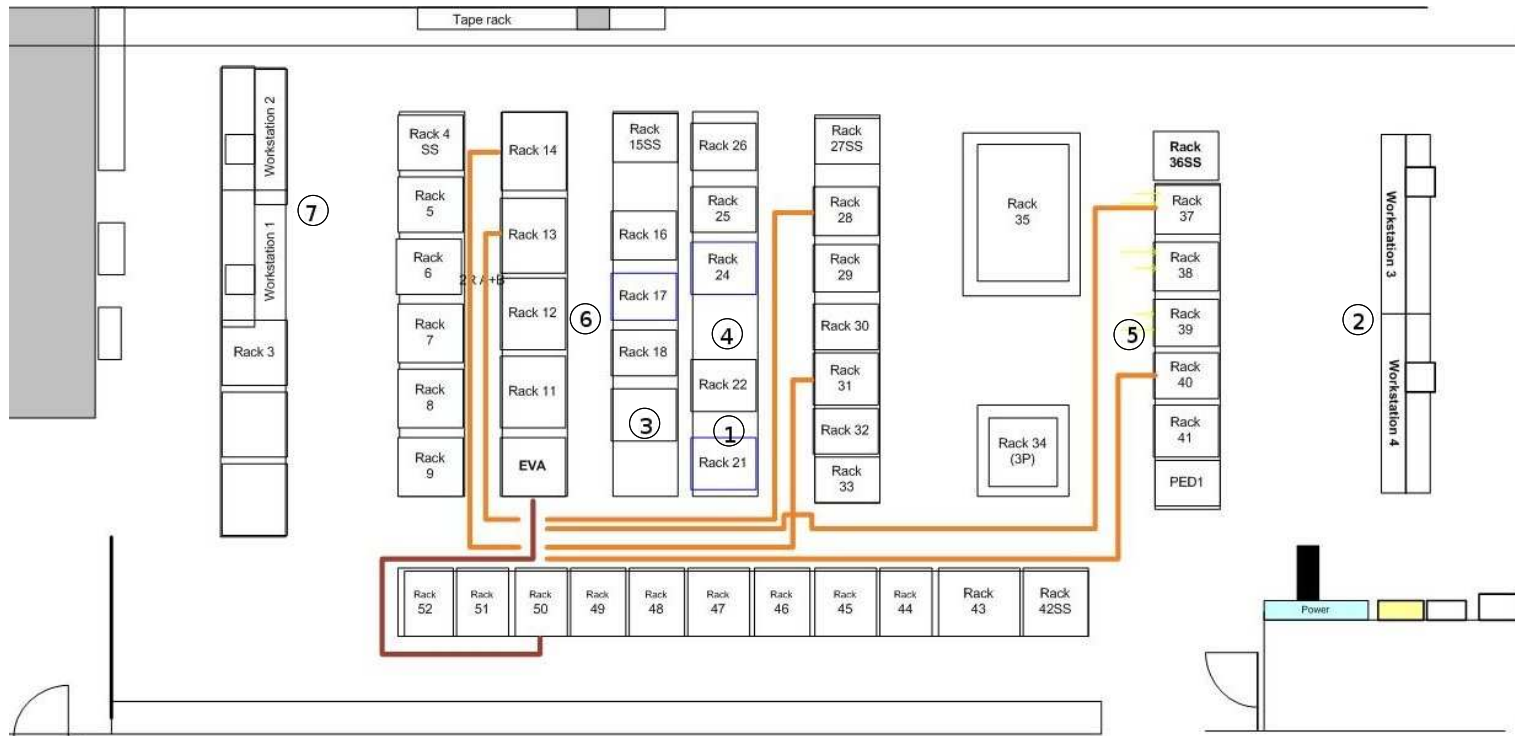
### Experiments

During the time of the cooling failure, we were asked to deploy a WSN for a week with an application objective of alerting upon any significant and sustained changes in temperature or humidity. This offered us the opportunity to validate the operation of DSFM.

The floor plan and deployed nodes are shown in Figure 5.3 with the circled numbers representing node IDs and locations. Nodes 1, 3 and 4 were located on top of equipment racks at a height of 215cm, nodes 5 and 6 were placed on the middle of racks at approximate height of 110cm and nodes 2 and 7 were placed on workbench surfaces at a height of 105cm. Node 1 is the base station, running the TinyOS `BaseStation` utility, and the only node powered by a USB/serial connection to a computer, with the latter used to log notification packets received from nodes 2 – 7 via node 1. Instead of running DSFM, it passively collects temperature and relative humidity at a constant frequency of 0.5Hz.

Nodes 2–7 run the DSFM algorithm and employ an alphabet of 10 characters for pattern detection and a compression ratio of 2/1. DSFM requires a sampling frequency interval with minimum and maximum sampling frequencies acceptable by the user. The interval is specified as  $[0.5, 0.125]$ Hz (or  $[2048, 8192]$  sampling

Figure 5.3: Node locations from data centre deployment. Circled numbers represent node IDs.



period using TinyOS Timers' binary milliseconds [STG07]). WSN nodes were tasked with different symbolic input window lengths, specifically: 128 data points for nodes 3 and 6, 256 data points for nodes 4 and 5 and 512 data points for nodes 2 and 7.

Nodes 2–7 initiate learning the normal rate of change by monitoring distances between temporally adjacent strings as described in Section 3.4. Learning duration was set to the first day of deployment or (approximately) 43,200 timer ticks. When learning completes, nodes let DSFM manage the sampling frequency using the TinyOS `stop` and `startPeriodic` timer commands. There are two separate independent timers for each monitored attribute (temperature and humidity). Whenever DSFM adjusts the frequency, it sends a packet to the base station to notify the relative time of adjustment (in timer ticks), the string distance causing the adjustment, the name of the timer monitored attribute and old and new sampling frequencies. In practice, transmission is not necessary and was used for experiment verification purposes.

During the deployment, there was one natural pattern event caused by a thunderstorm that triggered a rise in relative humidity spanning a period of over 12 hours. Such external events do not usually impact ambient temperature and indoor humidity, however this was not the case during the deployment since data centre windows were ajar.

The DSFM algorithm detected two and five pattern events over relative humidity and temperature attributes respectively. Except one, all patterns detected on the relative humidity attribute were during and after the thunderstorm which caused an approximately 7% increase of relative humidity. Nine pattern events were triggered during the drop in relative humidity after the thunderstorm. There was one false positive triggered by node 3. In line with the emulation results of Section 4.2.1, the number of patterns classified as unusual reduced as the window length increased. Although all the detected patterns refer to the same physical event that spanned several hours, the algorithms detected 22 patterns that represent changes in the signal spanning, at most, a few minutes.

On the temperature attribute, there was a total of five pattern events, out

of which two were false positives. Nodes with input window lengths above 128 did not report false positives, in line with expectations from results described in Section 4.2.1. The remaining three unusual patterns coincided with increases and sustained high observations. True and false positives were confirmed by technical engineers of the company, and the three true temperature pattern events were matched with notifications by the BMS<sup>3</sup> and alerts sent from server management agents. An example of the data, as recorded by the base station, with markers of patterns detected by nodes 2 – 7 is shown in Figure 5.4.

## Findings

The main finding of this experiment is that savings in node workload attributed to DSFM amount to 64% fewer timer ticks and related sensor data acquisition. Taking into account that WSN nodes typically execute tasks in a constant loop dictated by their timers, reducing the frequency of task execution can consequently conserve resources.

Per-node results including the number of true and false positives reported are shown in Table 5.5. If we use node 4 as an example, without DSFM its timers would have fired 604,800 times, assuming a constant sampling frequency of 0.5Hz. With DSFM, its timers fired 216,059 times. There was a total of 495 sampling frequency adjustments by DSFM that were verified correct, as they would either follow the end of the learning phase or a detected pattern event.

Overall the hypothesis that DSFM can reduce the MCU workload was confirmed in this deployment. The majority of reported patterns coincided with the thunderstorm event, suggesting that pattern detection is not adversely affected by automatic sampling frequency adjustments.

---

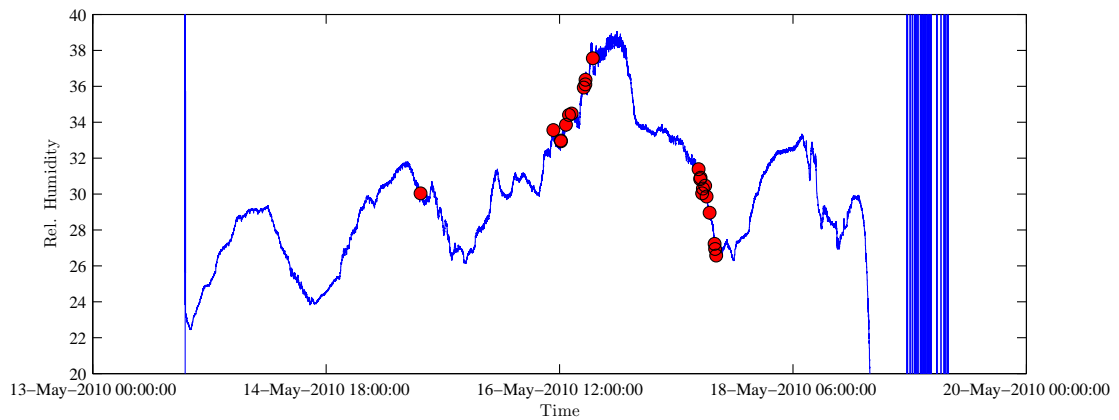
<sup>3</sup>The BMS cannot monitor relative humidity.

	Node ID					
	3	6	4	5	2	7
Window Length	128		256		512	
True Patterns (RH)	9	6	1	3	2	0
False Patterns (RH)	1	0	0	0	0	0
True Patterns (T)	0	0	0	1	1	1
False Patterns (T)	2	0	0	0	0	0
DSFM Adjustments	195	105	30	75	60	30
Total Timer ticks	216378	216204	216059	216146	216117	216064
Ticks Saved (as %)	64.22%	64.25%	64.27%	64.26%	64.26%	64.27%

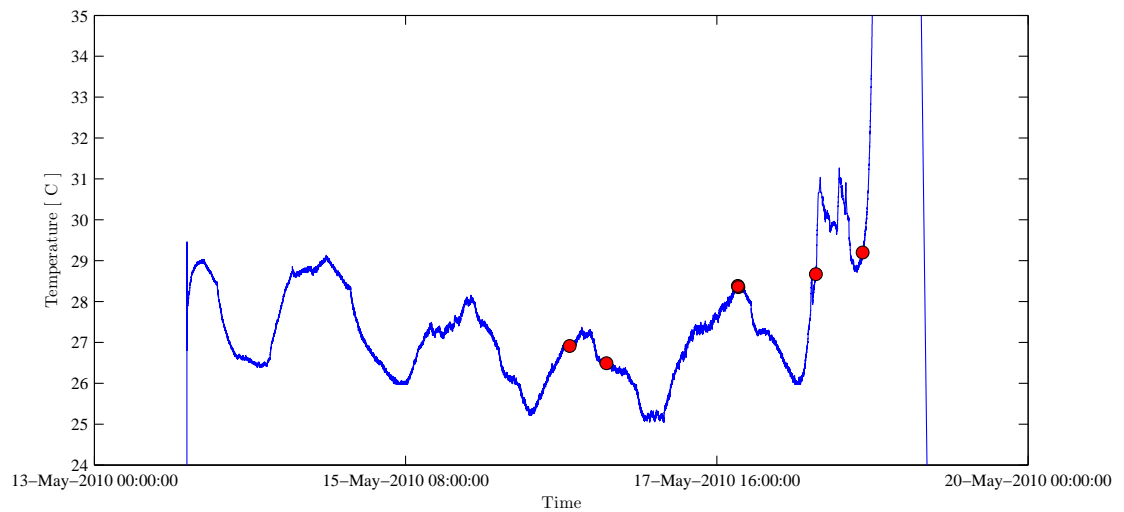
Table 5.5: Summary of true and false positives, and DSM timer adjustments from data centre deployment. (RH) stands for Relative Humidity and (T) stands for Temperature.

Figure 5.4: Observations of relative humidity and temperature recorded by Node 1 of the data centre deployment. Detected pattern events are shown as circles.

(a) Relative Humidity as recorded by Node 1. Circles represent detected patterns.



(b) Temperature as recorded by Node 1. Circles represent detected patterns.



### 5.3 Integration with Publish/Subscribe

The proposed pattern matching and detection algorithms are accessible via a Publish/Subscribe (Pub/Sub) interface that serves two purposes:

- It allows users to express interests in events as subscriptions [EFGK03].
- It allows nodes to notify users upon pattern event occurrences.

A subscription for a pattern of interest is disseminated in the WSN, stored by nodes and compared against sensor produced strings according to matching operators described in Section 3.1.3. A notification is a message destined for the subscriber when a pattern event is detected or matched against a template by a WSN node. We refer the reader to the Pub/Sub literature [DGH<sup>+</sup>06, HGM04, EFGK03, CJ02] for a detailed discussion of the Pub/Sub communication paradigm.

The pattern matching and detection algorithms are integrated with a Publish/Subscribe (Pub/Sub) interface by extending the TinyCOPS [HHK<sup>+</sup>08] framework which provides a content-based Pub/Sub service for WSN nodes. This integration of pattern matching and detection with Publish/Subscribe was tested in the data centre deployment of Section 5.2.1 where the notification delivery protocol [HHK<sup>+</sup>08] was responsible for delivering pattern event notifications from nodes to the base station.

TinyCOPS allows additional functionality to be introduced into the framework with Service Extension Components (SECs) without modification of the existing Pub/Sub core. The temporal pattern matching and detection algorithms follow this mechanism and provide their functionality through an Attribute Service Extension Component (ASEC) that processes WSN observations in the manner described in the algorithms of Chapter 3.

The pattern matching and detection algorithms employ default initialisation values for alphabet size, compression ratio and numeric sensor window length, however users can override these values by sending *subscription metadata* messages to WSN nodes. Such messages are widely used in TinyCOPS and interact

with our algorithms via the developed ASEC. Subscription metadata is represented as attribute-value pairs, for example  $\langle \textit{CompRatio}, 4 \rangle$  instructs one or more nodes to set their symbolic conversion compression ratio to 4/1.

TinyCOPS employs TinyOS protocols such as Trickle [LPCS04] for dissemination of subscriptions and Collection Tree Protocol (CTP) for collection of notifications. The integration of our pattern matching and detection algorithms through the developed ASEC with the communication mechanisms of TinyCOPS, confirms that our algorithms are compatible with standard TinyOS protocols and do not require any code modifications in the underlying networking layers. This means that pattern matching and detection algorithms are agnostic of lower layer protocols and decoupled from both the WSN naming/addressing schemes and the choice of subscription/notification delivery protocols.

## 5.4 Observations from Further Deployments

In order to show that our algorithms can operate in a new class of extremely resource constrained devices, we select the Wireless Identification and Sensing Platform (WISP) node developed by Intel Research [Res08]. The WISP is a node that combines the capabilities of RFID tags with those of WSN nodes. Its distinctive feature is that it lacks on-board power supply. Instead, it harvests power from an off-the-shelf RFID reader to operate its MSP430 MCU and sensors. This execution environment poses the challenge of achieving a computational goal with intermittently powered hardware resources.

To verify operation in this battery-free platform, we ported the NPPD algorithm and demonstrated<sup>4</sup> pattern detection during a 2009 Knowledge Transfer Network (KTN) event. The demonstration [ZR09c] tasked the algorithm to classify accelerometer patterns in a system used for teaching primary education pupils the basic laws of motion (cf. [PSFR08] for more information on the project).

We found the NPPD algorithm suited this challenging environment as it does not require prior configuration and takes approximately 13ms to classify new

---

<sup>4</sup>This demonstration won the Best R&D award [ZR09e].

patterns. The algorithm spent 10 seconds to learn normal motions from on-board accelerometer observations and subsequently classified other motions — induced by users shaking and moving the WISP — as unusual. For this demonstration, a window of 80 data points was employed with a sampling frequency of 20Hz and a compression ratio of 2/1.

To alleviate the effects of intermittent and unpredictable power resources, we installed a supercapacitor that stores accumulated power and prolongs the lifetime of the WISP, by up to 30 seconds, when it is not within the range of the RFID reader.

Other past deployments include a small testbed of four nodes installed in one of our laboratory buildings for five weeks during December 2008. Having processed over one million temperature observations, two nodes were running probabilistic pattern detection and the other two were running non-parametric pattern detection with the first day of deployment used as learning period.

Nodes converted numeric sequences of 40 observations to strings using a 4/1 compression ratio and a 10 letter alphabet. Neither true nor false positives were detected, in line with expectations as temperature observations were normal in comparison with the first day of deployment that was used as training period.

## 5.5 Summary of Findings

We described practical work and findings from implementing our temporal pattern matching and detection algorithms and deploying on real resource constrained sensor networks. We found the following:

- (i) The precise implementation of pattern matching and detection algorithms incorporating integer arithmetic and related optimisations showed a factor of ten runtime improvement in comparison with a floating point implementation.
- (ii) The Dynamic Sampling Frequency Management (DSFM) algorithm was assessed in a data centre deployment where it resulted in 64% fewer timer

ticks in comparison with constant sampling frequency. The company that commissioned the work decided to deploy a further WSN (scheduled for summer 2011) comprised of Zolertia Z1 [Zol10] nodes.

- (iii) Integration with a Publish/Subscribe framework shows that the proposed pattern matching and detection algorithms are compatible with standard TinyOS communication protocols and do not require modifications of lower networking layers.
- (iv) NPPD execution profile was sufficiently low to support use in a new class of energy harvesting nodes powered from RFID readers.

These findings provide evidence that the family of algorithms introduced in Chapter 3 are well-suited to extremely resource constrained nodes since they require minimal processing time and modest RAM for the task of pattern matching and detection.

## Chapter 6

# Pattern Location Estimation in the Spatial Domain

We introduce an algorithm that operates on the spatial domain and computes a coarse estimate of a spatial pattern event location. We focus on a particular type of pattern event, the dispersion of a plume from a pollutant-emitting point source in space. In contrast to the temporal algorithms of Chapter 3 that operate autonomously without radio communication, the spatial algorithm relies on exchanging information with local neighbours in order to collaboratively solve the location estimation problem.

Section 6.1 provides a more detailed description of the problem and Section 6.2 reviews the Kalman filter which forms the statistical foundation for the solution. The proposed algorithm, presented in Section 6.3, introduces a geometric computation which is combined with the Kalman filter to estimate the location and intensity of the source.

### 6.1 The Location Estimation Problem

As sensor technologies mature, costs are reduced and wireless connectivity becomes ubiquitous, it is possible to have dense in-situ networks of sensor nodes in urban centres for people protection from terrorists detonating “dirty bombs”

[CYR<sup>+</sup>08]. WSN nodes can sense the presence of pollutants in the atmosphere and collaborate to estimate the location, intensity and type of threat. Notifications can be sent to emergency personnel that use the information to evacuate citizens from the affected area and neutralise the threat to the general public.

The focus of this chapter is the problem of estimating the location and intensity of the “dirty bomb” inside the network. This is an instance of the *Inverse Problem* [ATB05] where dispersion parameters must be estimated from sensor-observed data.

Specifically, the problem is characterised by the following parameters: a single static point source emits a pollutant of chemical or radiological nature. The source is located at the unknown coordinates  $(x_s, y_s)$  in two dimensional space. The presence and intensity of the pollutant in the atmosphere is sensed by  $N$  sensor nodes located at  $(x_i, y_i)$  coordinates with  $i = 1, 2, \dots, N$ . The problem is the distributed, collaborative and iterative estimation of the pollutant source coordinates  $(\hat{x}_s, \hat{y}_s)$  and intensity  $I$  from  $z_i$  sensor observations collected at coordinates  $(x_i, y_i)$ .

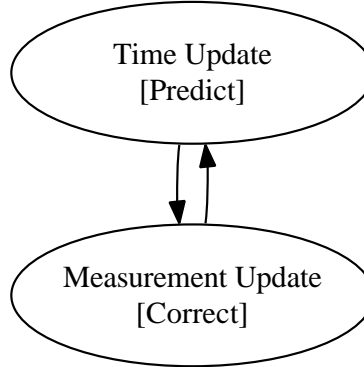
Coarse-grained estimation is chosen on the basis that it requires lower resource consumption [Kri05], at the expense of reduced estimate accuracy, in comparison with fine-grained approaches such as Time Difference of Arrival (TDOA) that usually rely on strict time synchronisation. We limit the scope to an in-network solution, in order to avoid the high energy costs associated with transmitting observations across multihop paths to far located sinks [WDWS10, FCG10, ZG09, GJV<sup>+</sup>05].

## 6.2 Kalman Filter Properties

The foundation for the pattern location estimation algorithm of this chapter is a *Kalman Filter* which is an optimal estimator of the true state of a dynamic linear system whose observations may be corrupted by noise [Sim06].

The operation of a Kalman filter is based on a *Predict-Correct* cycle shown in Figure 6.1. In its simplest form, it incorporates five equations, with the first

Figure 6.1: The Kalman filter loop (Reproduced from [WB95]). A prediction of the state is made together with a projection of the error covariance. Once an observation becomes available the estimate and error covariance are updated.



two (*Time Update* — Equations 6.1 and 6.2) — predicting the system’s varying quantities (state) which in our case comprise the source location and intensity, and the remaining three (*Measurement Update* — Equations 6.3 to 6.5) — correcting the prediction when sensor observations become available.

Project the state ahead:

$$\hat{x}_k^- = A\hat{x}_{k-1} + w_{k-1} \quad (6.1)$$

Project the error covariance ahead:

$$P_k^- = AP_{k-1}A^T + Q \quad (6.2)$$

Compute the Kalman Gain:

$$K_k = P_k^- H^T (HP_k^- H^T + R)^{-1} \quad (6.3)$$

Update estimate with observation  $z_k$ :

$$\hat{x}_k = \hat{x}_k^- + K_k(z_k - H\hat{x}_k^-) \quad (6.4)$$

Update the error covariance:

$$P_k = (I - K_k H) P_k^- \quad (6.5)$$

- $\hat{x}_k^-$  is the a priori state estimate.
  - $\hat{x}_k$  is the a posteriori state estimate.
  - $A$  is the state transition matrix.
  - $w$  is the white, zero-mean, uncorrelated noise.
  - $P_k^-$  is the a priori error covariance.
- Where:
- $P_k$  is the a posteriori error covariance.
  - $Q$  is the process covariance.
  - $R$  is the observation (measurement) noise covariance.
  - $H$  is the observation (measurement) matrix.
  - $z_k$  is the observation taken at time  $k$ .
  - $K$  is the Kalman Gain.

The goal of the Kalman filter is to formulate an *a posteriori* estimate  $\hat{x}_k$  as a linear combination of an *a priori* estimate  $\hat{x}_k^-$  and a weighted difference between an actual observation  $z_k$  and a predicted observation  $H\hat{x}_k^-$ , as shown in Equation 6.4 [WB95]. The optimal nature of the filter stems from the fact that as the observation noise covariance  $R$  approaches zero the matrix (or scalar)  $K$  weighs the innovation (the term  $(z_k - H\hat{x}_k^-)$  — also referred to as the residual or the error) more heavily. Conversely, as the a priori estimate error covariance  $P_k^-$  approaches zero, the gain  $K$  weighs the residual less heavily.

The Kalman filter has several advantages that make it a suitable estimator for our context:

- It is an optimal estimator, under the least square errors criterion.
- It is designed to tolerate measurement noise and process errors, both common properties of chemical and radiological sensors [CYR<sup>+</sup>08].
- There exist efficient integer-only implementations from the DSP community [TK88] that can be adapted for WSN nodes.

Lastly, the Kalman filter operates in a recursive manner suitable for in-network implementation since it only requires the last estimate instead of the entire estimate history to produce the next estimate.

### 6.3 Spatial Pattern Location Estimation (SPLE) Algorithm

Assuming a WSN deployed in an urban area, the estimation process initiates independently at nodes that detect the presence of pollutant in the atmosphere using the algorithms of Chapter 3. To avoid congestion effects from having all the nodes in a WSN transmitting simultaneously upon detection, we assume that the WSN is clustered with an approach such as LEACH [HCB02] or HEED [YF04]. Nodes that are assigned the role of cluster head at detection time initiate the estimation process.

An initiating node that detects the event, estimates the state of the pattern event as it would be observed by the neighbours of its immediate vicinity (line 2, Algorithm 6.1). This estimate is a linear transformation of the local observation (Equation 6.1). Next, the node tasks its nearest *unvisited* neighbours to report their observations (line 4). This is shown in Figure 6.2a and is achieved by a local broadcast. At each information exchange, the objective of the sender node is to select a receiver located closer to the source than itself.

Neighbours receiving the message, take a current observation of the gas concentration and transmit it as a response to the initiating node. This is shown in Figure 6.2b. For each response received, the Kalman filter innovation  $Z_n = (z_k^{(i)} - H\hat{x}_k^-)$  is calculated (lines 5-7). Note that  $\hat{x}$  is the estimate of the initiating node and each observation  $z_k^{(i)}$  has a superscript  $i$  to indicate which neighbour reported it. The initiating node calculates the minimum innovation  $\underset{z}{\operatorname{argmin}}(z_k^{(i)} - H\hat{x}_k^-)$  and selects the neighbour  $i$  who reported the error-minimising observation as the next hop (line 8). This is shown in Figure 6.2c.

During node selection, the selecting node changes its state to **visited** and

---

**Algorithm 6.1** Spatial Pattern Location Estimation (SPLE) Algorithm

---

- 1: **variables** Estimate Error Covariance  $P$ , Measurement Noise Variance  $R$ , Process Variance  $Q$ , State Transition Matrix  $A$ , Measurement Matrix  $H$ , Initial Estimate  $\hat{x}_k^-$ , maxhopcount=1, netpath[], observations[], counter  $c = 0$ ;
  - 2: Project state estimate  $\hat{x}_k^-$  ahead (Eq. 6.1).
  - 3: Project error covariance  $P_k^-$  ahead (Eq. 6.2).
  - 4: Task *unvisited* neighbours within maxhopcount to report observations.
  - 5: **for** (each of replies received) **do**
  - 6:   calculate innovations  $(z_k^{(i)} - H\hat{x}_k^-)$
  - 7: **end for**
  - 8: Select as next hop the node that minimises the innovation.
  - 9: Compute the Kalman gain (Eq. 6.3).
  - 10: Correct (Update) estimate with observation  $z_k$  (Eq. 6.4).
  - 11: Correct (Update) the error covariance  $P_k$  (Eq. 6.5).
  - 12: Compute relative error.
  - 13: **if** abs(relative error)  $\geq$  multiple  $\cdot$  ( $\mathbb{E}[Rel\ Error]$ ) **then**
  - 14:   **exit**
  - 15: **else**
  - 16:   Set state to visited, add local address to netpath[c], add  $z_k$  to observations[] and increment  $c$ .
  - 17:   Send command message to selected node (line 8) and task it to start at Line 1.
  - 18: **end if**
- 

sends the selected node a command message with necessary Kalman filter parameters so the latter can continue the estimation process (line 17).

The stopping condition of the estimation process is bound to the relative estimation error (Algorithm 6.1 — line 13) such that when the relative estimation error exceeds a multiple of the mean relative error, the process stops. Typically, the relative error diminishes after a few iterations as more available observations increase confidence in estimates. A sharp rise in the relative error reveals the estimation process moved to a node outside the plume or to an area where observations differ significantly given the initial estimates and observations.

A successful estimation process ends at a node that is as close to the real

pollutant source as possible. The coordinates and observation of that node, become the final estimate and are transmitted to the application user together with the `netpath` and `observations` arrays. The former is a trajectory sequence of coordinates that indicate the path of the estimation process and the latter is a sequence of observations taken by nodes participating in the estimation process.

To enhance the quality of the estimates we introduce a geometric computation that operates in the following manner: at initiation of the estimation process, the cluster heads (or initiating nodes) communicate with each other to establish the centroid of the Convex Hull formed by their coordinates. The convex hull is the boundary of the minimal convex set containing a finite set of points, representing WSN nodes. This is shown in Figure 6.3a. The coordinates of the centroid are stored for later use.

After four<sup>1</sup> hops nodes carrying out the estimation task re-evaluate the centroid of the convex hull formed by their current coordinates. By differencing the coordinates of the previously evaluated convex hull centroid with those of the current centroid, a *quadrant direction* is established. This is one of the four Cartesian space regions in which the majority of nodes participating in the process estimate the source location. This region becomes the consensus and is used to directionally propagate estimates. If a node does not have neighbours in the mean direction of movement quadrant, it aborts the estimation run. An example of the geometric computation is shown in Figure 6.3b: the mean direction of movement has been established as the top-right quadrant, therefore estimates are only propagated towards that direction.

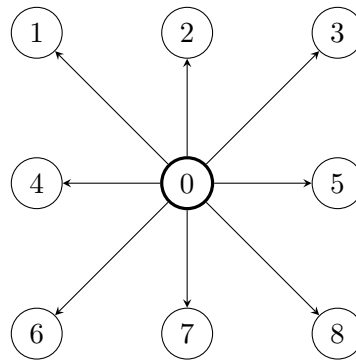
The following chapter evaluates the geometric computation and finds that estimation accuracy of the algorithm is improved as minority errors made by individual nodes cannot affect the overall estimation decision.

---

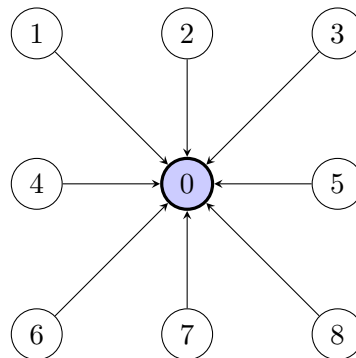
<sup>1</sup>This parameter is configurable, but we empirically found that four hops represents a good choice for re-evaluating the mean direction of movement.

Figure 6.2: An example of SPLE estimate propagation: first, an estimate is transmitted to 1-hop neighbours. Second, the neighbours report their observations. Third, the neighbour whose reading minimises the estimation error is selected as next hop, and repeats the process

(a) Step 1 — Transmit estimate to 1-hop neighbours



(b) Step 2 — Collect Observations



(c) Step 3 — Select Node for Next Hop

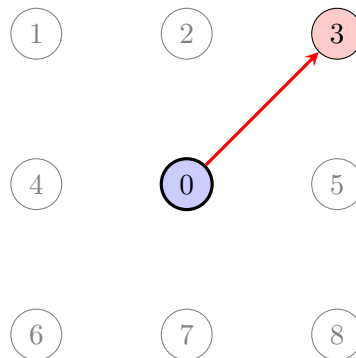
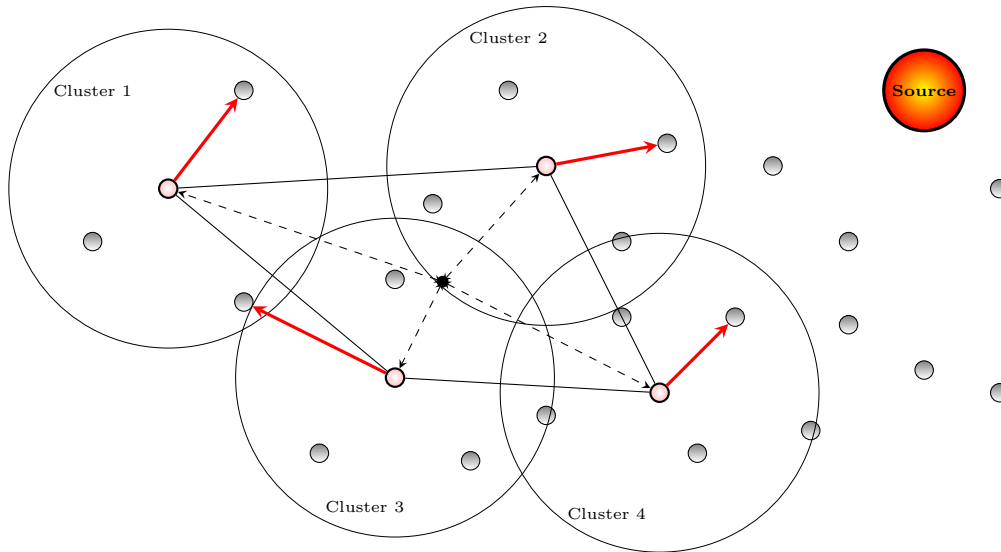
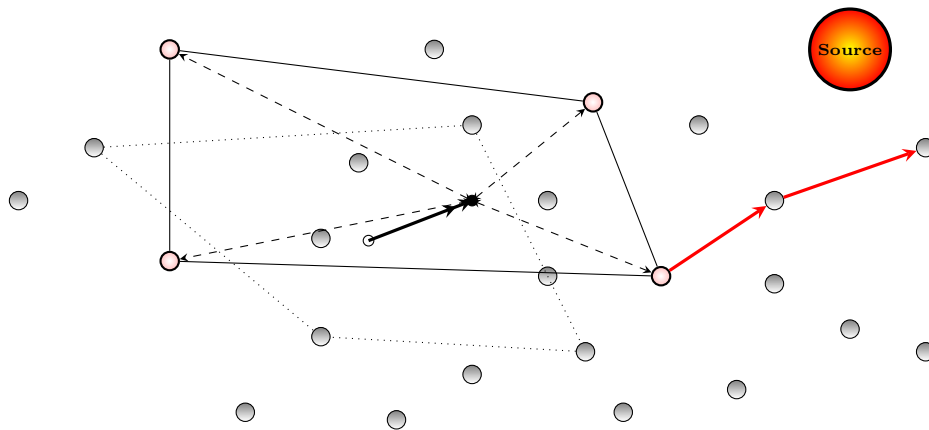


Figure 6.3: Example of the geometric computation to establish the mean direction of movement

- (a) Nodes initiating an estimation process. The dashed lines inside the polygon point to the current centroid of the Convex Hull formed by the four cluster heads. The thick arrow lines point to neighbours selected individually by the initiating nodes as next hops.



- (b) The centroid is re-evaluated after one iteration. Differencing the coordinates of the previous centroid with those of the current results to the mean quadrant direction of movement. Note that the incorrect decision of the bottom-left node (in Cluster 3 of the above figure) does not affect the overall estimation. Once the top-right quadrant has been established as consensus, the only node that has valid choices for next hops, is the one on the bottom right of the figure.



## 6.4 Summary

We presented an iterative coarse-grained location estimation algorithm of a point source emitting a pollutant plume. The algorithm operates in-the-network and provides an alternative to techniques that rely on network-wide observation harvesting and offline processing. A Kalman filter supplies the optimal estimation functionality and an in-network localised information exchange builds a collaborative solution to the problem.

In addition, we described a geometric computation employed to augment the estimation accuracy by adding a consensus or majority rule to the estimation proceedings. The consensus assumes that a group of collaborating nodes establish mean direction of movement in order to preclude estimation deviations made by incorrect individual node decisions.

# Chapter 7

## Spatial Algorithm: Evaluation through Simulation

The purpose of this chapter is to evaluate the estimation accuracy, with respect to varying parameters such as WSN density and node placement, of the proposed Spatial Pattern Location Estimation (SPLE) algorithm through simulation.

Section 7.1 outlines the evaluation methodology and the setup of the simulation environment including the gas dispersion model. The evaluation study of Section 7.2 is categorised according to WSN topology of both grid and random node placements. A summary of findings is presented in Section 7.3.

### 7.1 Methodology and Simulation Set-up

The experiments described in this chapter were conducted using a MATLAB [Mat10] implementation of the SPLE algorithm. MATLAB is selected on the basis that it offers an environment where the behaviour of the SPLE algorithm can be tested and compared against a baseline algorithm in relatively large WSNs fields of varying densities.

### 7.1.1 Maximum Selection Algorithm

In order to compare the estimation accuracy of SPLE against a competitive approach, we use the *Maximum Selection* algorithm. The choice of this algorithm as a baseline for comparison was made on the basis of its application [HMG03, SLV93] in contexts similar to ours and its relative simplicity. It is inspired from the biological approach *chemotaxis* [ZSST04, Ate96] where animals and insects iteratively locate odours by moving to spatial regions where their receptors sense a higher intensity odour than their previous position.

Similar to SPLE, the maximum selection algorithm is iterative and operates in the following manner: the estimation process starts when one or more initiating nodes sense the spatial pattern event. The assumptions made in Section 6.3 hold, in particular that WSN nodes participate in a cluster scheme with the cluster heads initiating the estimation process. Upon sensing the spatial pattern event using the algorithms of Chapter 3, nodes send a message to their local neighbours tasking them to report their observations. The initiating node collects the observations of its neighbours and selects the neighbour with the maximum observation as the next hop, as it represents a node closer to the source. The selected node changes its state to `visited` and repeats the process until it runs out of `unvisited` local neighbours with higher intensity observations than itself.

The procedural steps for maximum selection are shown in Appendix D, Algorithm D.1.

### 7.1.2 Dispersion Model

We use the gas dispersion and sensor response model proposed in [INM97] due to the similarity of the investigated problem, namely a sensing system with the capacity to locate a gas or odour source.

The model assumes one-directional wind field, constant wind speed, homogeneous turbulence and single pollutant source emitting gas at a constant rate. The dimensionality of the problem is reduced by not taking height into account and assuming that the source is placed on the floor. The resultant gas distribution

$C_0$  and sensor response  $r_0$  are governed by the following two equations:

$$C_0(x, y) = p_1 \frac{1}{d_s} \exp[-p_2(d_s - \Delta x)] \quad (7.1)$$

$$r_0(x, y) = [1 + 0.2309C_0(x, y)]^{-0.6705} \quad (7.2)$$

where:

- $C_0(x, y)$  is the time-averaged gas concentration at coordinates  $(x, y)$
- $p_1$  is given by  $p_1 = \frac{q}{2\pi K}$
- $q$  is the gas emission rate (in  $g/sec$ )
- $K$  is the turbulent diffusion coefficient
- $p_2$  is given by  $p_2 = \frac{U}{2K}$
- $U$  is the wind speed (in  $m/sec$ )
- $d_s$  is given by  $d_s = \sqrt{(x_s - x)^2 + (y_s - y)^2}$
- $(x_s, y_s)$  are the true coordinates of the source
- $\Delta x$  is given by  $(x_s - x) \cos \theta + (y_s - y) \sin \theta$
- $\theta$  is the angle from the  $x$ -axis to the upwind direction

The experiments of Section 7.2, use the parameter values shown in Table 7.1.

### 7.1.3 Kalman Filter Initial Parameters

As described in the previous chapter, the estimation functionality of the SPLE algorithm is realised by the combination of a geometric computation with a Kalman filter. The filter was optimised using the functions `fminsearch` [Mat08b] and

Parameter	Description	Value
$q$	Gas-emission rate	45,000
$K$	Turbulent diffusion coefficient	17.463
$U$	Wind speed	3.1
$\theta$	Upwind direction angle	1
$(x_s, y_s)$	True source coordinates	(95, 95)

Table 7.1: Parameter values for gas dispersion model

KF Parameter	Description	Value
$A$	State transition scalar	1.0315
$P$	Estimation error covariance	0.1021
$Q$	Process error covariance	0.0503
$R$	Measurement noise covariance	0.1

Table 7.2: Kalman filter initial parameters obtained by MATLAB functions `fminsearch` and `fminbnd`. For a more detailed discussion of their role to the Kalman filter, refer to Section 6.2 and references therein.

`fminbnd` [Mat08a] of MATLAB in order to obtain necessary initialisation parameters for state transition scalar, error covariance, process covariance and observation noise covariance.

Minimisation was performed by repeatedly executing the SPLE algorithm for simulated nodes with different coordinates. Function minimisation selects appropriate Kalman filter parameter values such that the estimation error, in terms of distance and intensity of the real source, is minimised. The final set of parameter values is shown in Table 7.2 and is used globally for all nodes in the WSN field and all experiments described in this chapter. Adaptation of Kalman filter parameters is often necessary and common in estimation tasks, for example [GRG88] describes a similar optimisation process.

#### 7.1.4 Topology Generation

We use the Link Layer model and topology generator<sup>1</sup> described in [ZK05] to generate the network topologies. The same model is used by TinyOS and generates topologies and network links, as a collection of coordinates and Packet Reception Rates (PRR) respectively. For simplicity, we do not explicitly model radio communications and only use the topology coordinates generated by the software.

<sup>1</sup>Distributed as MATLAB and Java software.

## 7.2 Evaluation of Spatial Pattern Location Estimation

For this study, we classify an estimation run as *accurate* if it terminates at a WSN node located no farther than six meters from the true source. We refer to this measure as *proximity accuracy* and impose the limit of six meters (Euclidean distance) because we are targeting a coarse-grained estimation technique.

An *estimation run* is the estimation process of Section 6.3, from the starting point where a node first senses the pattern event until one (or more) of its neighbours, tasked with continuing the estimation process, decide to terminate because either the terminating condition has been met or there are no more unvisited local neighbours to continue the estimation process.

The topology terrain is a plane of 100-by-100 meters with the true source located at coordinates (95, 95).

### 7.2.1 Metrics

To evaluate the estimation accuracy of SPLE, we use the following metrics:

- The Euclidean distance, in meters, between the estimated source coordinates and the true source coordinates.
- The error, in relative terms, between the final intensity estimate and the true intensity of the source.
- The length of the path, in hops, followed from beginning to end of an estimation run.

The first two parameters determine estimation accuracy and the third parameter offers a coarse indication of communication cost and detection latency.

### 7.2.2 Grid Topology

To conduct an initial investigation on the impact of WSN density to the performance of the SPLE algorithm, we consider two grid topologies of 4,900 and 1,024

nodes.

### **Hypothesis**

The SPLE algorithm can perform competitively against a maximum selection algorithm with respect to estimation accuracy as distance from the true source, error in intensity estimate and path length as the number of nodes visited during an estimation run.

### **Experiments**

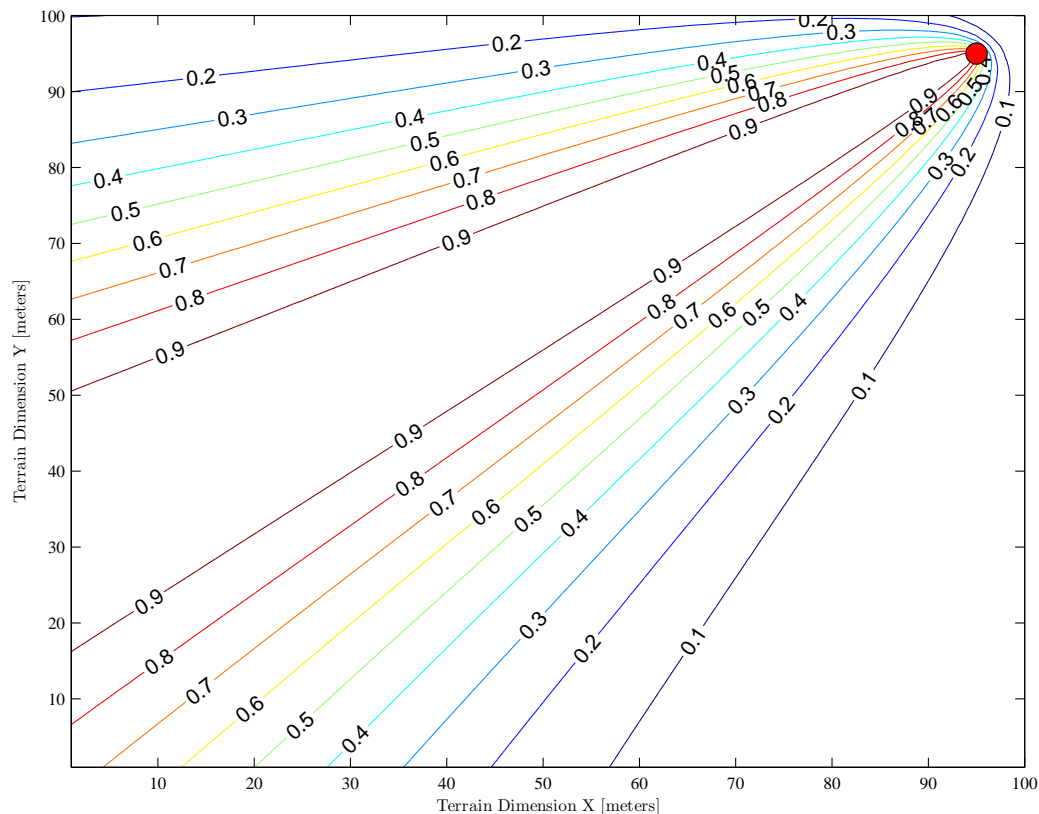
We cover the WSN by initiating our SPLE algorithm without the geometric computation at every simulated node in the field. In the 4,900 topology, we exclude 192 nodes as they were placed within a region of less than 16 meters to the source and they would bias the results in favour of the SPLE algorithm. For the same reason, we exclude 33 nodes in the 1,024-node topology. An example of the dispersion plume labelled with gas concentration intensities is shown in Figure 7.1.

### **Findings**

A summary of the results over both topologies is shown in Tables 7.3 and 7.4: out of 4,708 nodes that initiated a SPLE run, 2,905 or 61.7% estimated the source location within six meters in the 4,900-node topology. For the 1,024-node topology, 54.59% or 541 nodes estimated the source within six meters.

The maximum selection algorithm underperformed with respect to both estimation accuracy and path lengths: 53.29% and 50.01% of nodes terminated within six meters of the source in the 4,900 and 1,024 node topologies respectively. On the basis of these experiments the hypothesis that SPLE can perform competitively against a maximum selection algorithm was confirmed.

Figure 7.1: The dispersion plume considered by the experiments. Gas concentration intensities are labelled on the contour lines. The source is located at the top right of the figure at coordinates (95, 95) marked with a circle.



### 7.2.3 Random Topology

Similar to the previous experiment, we consider two topologies of different densities: a 5,000-node and a 1,000-node topology.

#### Hypothesis

The SPLE algorithm is capable of computing accurate estimates — within six meters of the true source — with random placement and selection of initiating nodes.

	SPLE	Max Selection
<i>Proximity Accuracy</i> (% of nodes ending an estimation run within six meters of the source)	61.7 %	53.29 %
<i>Mean Distance</i>	3.26	2.87
<i>Median Distance</i>	3	3
<i>Intensity Accuracy</i> (Mean Relative Error)	6.73 %	8.17%
<i>Mean Path Length</i> (hops)	72.16	77.01
<i>Median Path Length</i> (hops)	74	79

Table 7.3: Baseline comparison of our SPLE algorithm with the Maximum Selection algorithm over 4,900-node grid topology. 4,708 WSN nodes initiate the estimation run and their results are summarised.

## Experiments

We assume a WSN that arranges nodes in clusters using a method like LEACH [HCB02] or HEED [YF04]. As described in Section 6.3, the role of a cluster head is to initiate an estimation run and to collaborate with neighbouring cluster heads in order to compute the geometric mean direction of movement.

Similar to the previous experiments, to avoid bias of results in favour of the SPLE algorithm nodes placed within 16 meters of the true source are not considered as candidates for initiating an estimation run.

The experiments are divided into eight trials testing 1,000 possible clusters with 4 and 5 nodes per cluster.

## Findings

For reference, we perform an initial evaluation of the SPLE algorithm without its geometric computation component. The results were comparable with those of the grid topologies: 50.74% and 46.09% of nodes computed an accurate proximity estimate, for the 5,000 and 1,000 topologies respectively.

The strength of the geometric computation is demonstrated by achieving improved mean proximity accuracy of 87.24% and 90.91% with four and five cluster

	<b>SPLE</b>	<b>Max Selection</b>
<i>Proximity Accuracy</i> (% of nodes ending an estimation run within six meters of the source)	54.59 %	50.01 %
<i>Mean Distance</i>	4.13	3.99
<i>Median Distance</i>	4	4
<i>Intensity Accuracy</i> (Mean Relative Error)	9.11 %	10.33%
<i>Mean Path Length</i> (hops)	39.52	41.91
<i>Median Path Length</i> (hops)	38	43

Table 7.4: Baseline comparison of our SPLE algorithm with the Maximum Selection algorithm over 1,024-node grid topology. 991 WSN nodes initiate the estimation run and their results are summarised.

heads participating in the geometric computation respectively. This means that over eight trials, the geometric computation with SPLE maintained estimation accuracy over 85%; that is over 85% of nodes were successful in estimating the true source coordinates within six meters. In addition, mean distance to the source and path lengths also improve with results for the 5,000-node topology summarised in Table 7.5.

The experiments were repeated on five 1,000-node topologies and the results are shown in Table 7.6. It can be seen that proximity accuracy is affected by topology with a worst case of 86.53% of nodes successfully estimating the true source coordinates within six meters. Results for five cluster heads participating in the geometric computation (not shown on the table for clarity) are slightly higher with a maximum of 98.21% of nodes successfully estimating the true source within six meters of its actual location.

An example of the geometric computation with multiple evaluations of the convex hull centroids is shown in Figure 7.2. Overall the hypothesis that SPLE can compute estimates accurate within six meters of the true source location without relying on particular initiating node selection or placement was confirmed.

Trials	4 cluster heads	5 cluster heads
	# of Accurate Clusters (At least one node terminates within 6m)	
Trial #1 :	897/1000	918/1000
Trial #2 :	873/1000	916/1000
Trial #3 :	862/1000	894/1000
Trial #4 :	891/1000	909/1000
Trial #5 :	865/1000	924/1000
Trial #6 :	874/1000	906/1000
Trial #7 :	855/1000	900/1000
Trial #8 :	862/1000	906/1000
<i>Proximity Accuracy</i> (Average over 8 trials)	<b>87.24%</b>	<b>90.91%</b>
<i>Mean distance</i>	2.7811	2.7263
<i>Median distance</i>	2.6861	2.6681
<i>Intensity Accuracy</i> (Mean Relative Error)	5.28 %	5.24%
<i>Mean Path Length</i>	26.79	20.09
<i>Median Path Length</i>	21	21

Table 7.5: The general performance of the SPLE algorithm over the 5,000-node random topology. In total, we average the results for the eight trials with a cluster considered accurate if at least one of the member nodes terminates the estimation run within six meters to the true source.

Topology	Overall performance				
	#1	#2	#3	#4	#5
<i>Proximity Accuracy</i> (Average over 8 trials)	<b>86.53%</b>	<b>97.33%</b>	<b>94.45 %</b>	<b>94.5%</b>	<b>86.71</b>
<i>Mean distance</i>	3.66	5.12	5.64	3.2	2.29
<i>Median distance</i>	3.44	5.16	5.92	3.07	2.19
<i>Intensity Accuracy</i> (Mean Relative Error)	6.91%	8.12%	8.19%	6.07%	5.1%
<i>Mean Path Length</i>	23.71	25.68	23.2	26.11	27.02
<i>Median path Length</i>	21	23	21	22	24

Table 7.6: The performance of the SPLE algorithm over five 1,000-node topologies with 4-node clusters initiating the estimation run.

### 7.3 Summary of Findings

We conducted evaluation through simulation of the Spatial Pattern Location Estimation (SPLE) algorithm. We found that, under certain assumptions, the SPLE algorithm is accurate at the task of locating the pollutant source coordinates within six meters. Specifically we found the following:

- (i) The SPLE algorithm is competitive against a maximum selection algorithm. The latter follows the maximum sensor observations in an attempt to locate the pollutant source.
- (ii) Four cluster heads collaborating in the geometric computation improve the proximity accuracy of SPLE with 86%-97% of nodes estimating the source location within six meters of its actual coordinates on the random topologies.
- (iii) The overall performance of the SPLE algorithm is not significantly affected by placement and selection of initiating nodes with a worst-case accuracy of over 85% across the random topologies.

Finally, the study described in this chapter opens several directions for future work further explored in Section 8.4.

Figure 7.2: SPLE algorithm with geometric computation of the mean direction of movement shown as the arrow joining the two convex hull centroids (denoted by the 'X'). Solid points represent node locations and the polygon surrounding them is the convex hull. True source is located at coordinates (95,95).

- (a) First evaluation of the geometric computation. Nodes form a cluster in order to establish the current centroid of the polygon formed by the edge node coordinates.

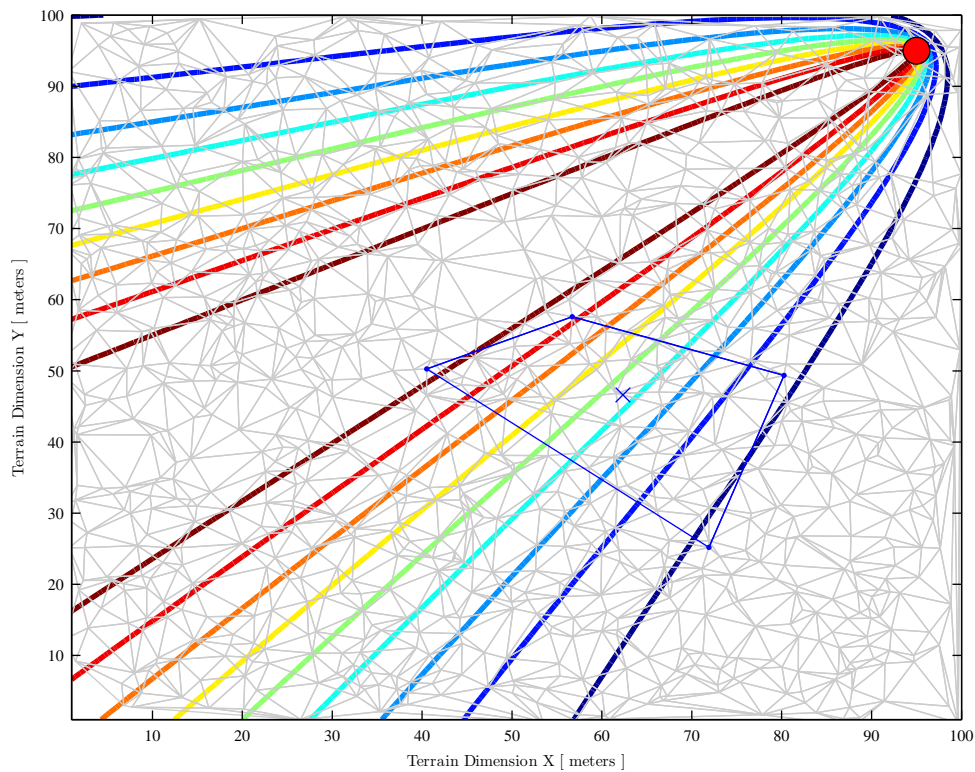


Figure 7.2: SPLE algorithm with geometric computation of the mean direction of movement shown as the arrow joining the two convex hull centroids (denoted by the 'X'). Solid points represent node locations and the polygon surrounding them is the convex hull. True source is located at coordinates (95,95).

- (b) Second evaluation of the geometric computation. Cluster heads establish consensus by determining the mean direction of movement, as difference between the previous and the current convex hull centroids. The centroids are marked with 'X' and the direction of movement is marked with an arrow.

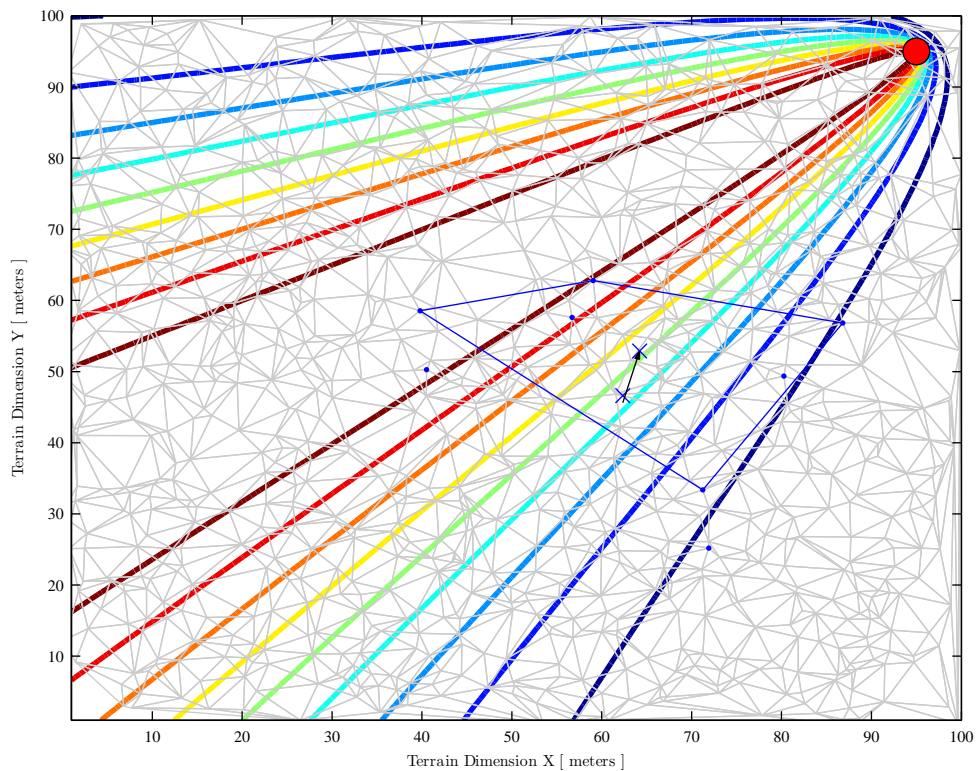
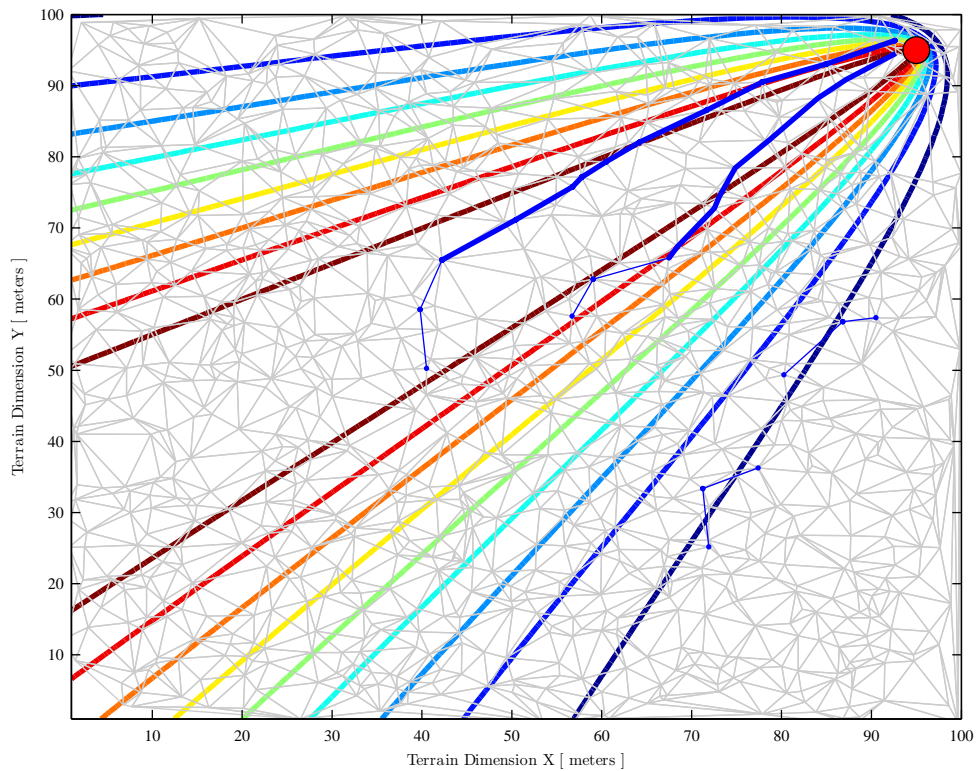


Figure 7.2: SPLE algorithm with geometric computation of the mean direction of movement shown as the arrow joining the two convex hull centroids (denoted by the 'X'). Solid points represent node locations and the polygon surrounding them is the convex hull. True source is located at coordinates (95,95).

- (c) Final outcome of the estimation run: two (out of 4) nodes achieve estimates of 2.364 and 2.7431 (Euclidean) distance to the true source. Their paths are shown by the thick solid lines. Two of the other nodes (shown in the bottom right of the figure) cannot identify neighbours in the consensus direction of movement and terminate the process. Their paths are shown by the normal weight solid lines.



# Chapter 8

## Conclusions and Future Work

In this thesis, we introduced methods and algorithms that provide pattern matching and detection in extremely resource constrained Wireless Sensor Networks (WSNs). Specifically, we presented temporal domain algorithms that process streaming sensor observations to classify patterns that reveal interesting or unusual activity in the monitored process, phenomenon or structure (*monitored object*). Moreover, we designed a spatial domain iterative algorithm, based on a geometric computation and a Kalman filter that estimates the location of a gas emitting source.

This final chapter, summarises the thesis in Section 8.1 and reviews the contributions in Section 8.2. A critical appraisal of the thesis is presented in Section 8.3 and directions for future work are explored in Section 8.4.

### 8.1 Summary of the Thesis

**Target Platform Constraints** As discussed in Chapter 1, this thesis introduces methods and algorithms that target extremely resource constrained WSN nodes. A characteristic of such devices is that they are limited in power resources and computational capabilities. In particular, Section 1.1.1 identified the high power draw of radio in relation to other components in agreement with the view [ZG09, MGH09, TE07, CES04, GKW<sup>+</sup>02] that locally processing sensor data to

determine the presence of interesting or unusual activity can reduce the number of unnecessary transmissions and, as a consequence, prolong node lifetime.

**Problem Formulation** The problem investigated is the provision of computationally efficient in-network pattern matching and detection algorithms that involve solely local processing for temporal patterns and localised communication for location estimation of spatial patterns.

A *pattern* was defined as an ordered list of potentially non-unique sensor observations revealing interesting or unusual activity in the monitored object. *Interesting* and *unusual* are class labels [CBK09] defined in terms of distance, probability or string searching.

**Rationale** Motivation for selecting this problem was twofold: first, pattern matching and detection can benefit a number of reactive applications from different domains reviewed in Chapter 2. Second, after examining related literature, we found a number of approaches either lacked evidence of implementation for resource constrained WSNs or assumed an out-of-network processing model that relies on radio communication for transmitting observations to base stations.

**Temporal domain patterns** Chapter 3 introduced temporal domain pattern matching and detection algorithms. The basis for the algorithms is symbolic aggregate approximation (SAX [LKLC03]) that converts windows of streaming sensor observations to strings. Pattern matching is performed by computing the distance between a sensor produced pattern (*sensor string*) with a user submitted template pattern (*template*), or by determining whether the sensor string appears in the collection of templates. Non-parametric detection compares two temporally adjacent sensor strings to a maximum learnt distance and probabilistic detection computes the path probability of a sensor string, given learning data.

Evaluation was conducted in two parts: the first part (Chapter 4) emulated the timer, sensor and ADC components of a node to simulate sensor data acquisition. Experiments investigated the impact of symbolic conversion parameters

— such as alphabet size, window length and compression ratio — to false positives. Further experiments compared Non-Parametric Pattern Detection against two alternative event detection techniques. Findings confirmed that our approach was competitive with 92.7% sensitivity (cf. Section 4.3.1). In addition, findings from a preliminary study into the effects of measurement noise were encouraging: detection accuracy degraded gracefully in relationship to increasing signal noise (cf. Section 4.3.2).

The second part (Chapter 5) of evaluation validated the operational profile of the algorithms through deployments and full implementation. The algorithms were refactored to ensure computationally efficient pattern matching and detection runtime (cf. Section 5.1). The runtime cost is known at compile-time and depends only on the window length of sensor observations. To achieve a reduction of MCU active time, an algorithm that automatically adjusts sampling frequency according to the perceived activity level of the monitored object was introduced (cf. Section 5.2). For validation, a WSN was deployed in a data centre and findings showed that both automatic sampling frequency management and non-parametric detection are feasible (cf. Section 5.2.1).

The temporal algorithms are made available to users of a reactive system via a Publish/Subscribe (Pub/Sub) interface. Integration with Pub/Sub through implementation (cf. Section 5.3) shows that the proposed methods and algorithms are compatible with standard TinyOS communication protocols and do not require modifications in the underlying networking layers.

**Spatial Domain Patterns** Spatial patterns are events with position and direction in physical space. Chapter 6 introduces a localised communication algorithm that combines a geometric computation with a Kalman filter to solve the problem of estimating the location and intensity of a pollutant emitting source. The motivating scenario is urban deployment of WSNs for in-network detection of dirty bombs as an alternative to transmitting observations across multihop paths to base stations.

Initial evaluation of the spatial pattern location estimation algorithm, shows

it is competitive (cf. Section 7.2.2) compared to a maximum selection algorithm. Furthermore, evaluation of estimation performance on a number of random WSN topologies provides evidence that the collaborative geometric computation component of the algorithm improves location estimation accuracy (cf. Section 7.2.3).

## 8.2 Summary of Contributions

This thesis makes the following contributions:

- (i) Introduces five temporal domain in-network pattern matching and detection algorithms (Chapter 3).
- (ii) Provides evidence (Chapter 4) that the algorithms produce consistent results across three case studies and are competitive against other pattern event detection methods.
- (iii) Demonstrates suitability for extremely resource constrained WSN nodes by verifying the modest runtime requirements through implementation (Chapter 5).
- (iv) Introduces a geometric computation combined with a Kalman filter into a collaborative algorithm (Chapter 6) that iteratively estimates the location of a spatial pattern event inside-the-network.
- (v) Provides evidence (Chapter 7) that the spatial algorithm is competitive against a maximum selection approach without relying on node placement.

Overall, we believe our findings contribute towards WSN-related research in the field of reactive systems by proposing computationally efficient algorithms for in-network pattern matching and detection.

### 8.3 Critical Appraisal

Despite the findings from evaluation of the proposed algorithms through deployments and simulation, further work is required to establish their general applicability and competitiveness with other approaches across a number of domains. There are several directions for improving the findings and extending the work, explored in the next section.

### 8.4 Directions for Future Research

**Temporal Algorithms** In order to demonstrate that the algorithms can generalise beyond the range of domains already tested, that are resilient to signal noise and competitive against a number of other event detection approaches, we propose the following actions:

- (i) Conduct a comparative evaluation of all five temporal algorithms of Chapter 3 against additional competitive techniques on a range of data sets with varying characteristics.
- (ii) Investigate the noise model of different hardware sensors and extend the preliminary study of Section 4.3.2 with respect to accuracy of temporal domain algorithms under varying magnitudes and types of noise.
- (iii) Perform a matching and detection accuracy comparison between the proposed algorithms and a straightforward thresholding technique. The latter will require adaptation to data sets and specification of threshold values and predicates, nevertheless shortcomings of such a technique can be quantified, for instance with an investigation into the effect of outliers on false positives.
- (iv) Compare the execution profile of the proposed algorithms to competitive techniques and evaluate the runtime of the probabilistic pattern detection algorithm.

- (v) Conduct a study into the effects of dynamic sampling frequency management (Section 5.2) with respect to false negatives that may occur as a side effect of reduced sensor data acquisition frequency.

**Spatial Algorithm** The plume dispersion scenario of Chapter 6 makes a number of simplifying assumptions to study and understand the problem parameters, common with related research by others [GRG88, INM97, CYR<sup>+</sup>08]. To address properties of the real world problem and extend evaluation of the proposed solution, the following directions can be pursued:

- (vi) Alter the gas dispersion model assumptions and investigate the performance of the algorithm with respect to multiple sources, variations in wind speed and atmospheric turbulence and irregular topologies with sparse or disconnected regions.
- (vii) Evaluate against competitive techniques such as TDOA and comparatively investigate the communication cost and estimation latency of the algorithm.
- (viii) Implement the proposed spatial algorithm for resource constrained WSN nodes and conduct a processing measurement evaluation to verify execution efficiency. Moreover, consider and evaluate the operational cost of a range of filters to cater for different situations. Runtime cost analysis will contribute towards operational predictability of the spatial algorithm.

**Additional opportunities** Further to the above directions that extend the findings of this thesis in the short term, we aim to explore the following longer term issues:

- (ix) Extension of pattern matching and detection to automated diagnosis systems. In the past, we conducted data analysis from breath samples of cystic fibrosis patients collected using a Cyranose 320 [Det07] electronic nose comprising an array of 32 sensors, each one responding to a particular gas. The objective was to aid diagnosis of bacterial lung infections using samples from

the electronic nose. Although the device is accompanied by classification algorithms such as PCA and nearest neighbour, other classification algorithms can be applied in vertical applications designed with a particular objective. Research in the use of the electronic nose for classification (cf. [DD06, SMD<sup>+</sup>04, ATH03]), indicates this is an application area where the algorithms of Chapter 3 can apply.

- (x) Development of an integer-only library comprising functions defined in the `math.h` C header specification [KR78], such as `sqrt`, `sin`, `cos`, `tan`. A software library with fixed-point implementation of varying precision for these functions can be a valuable tool to applications that perform target tracking or data analysis. The temporal domain algorithms rely on square root and an integer version has already been implemented, however extending the implementation to functions outside the scope of this thesis can benefit practitioners in the wider WSN community.
- (xi) Continue to adapt the algorithms to devices with intermittent power such as the battery-free Intel WISP [Res08] that has been used as a target platform for deployment (cf. Section 5.4). A related platform [Alb08], combines RFID tags with chemically or biologically sensitive films capable of detecting chemical vapours in scenarios similar to the one considered by spatial pattern location estimation. These devices introduce a new paradigm where computation is intermittent and dictated by the presence of power sources such as RFID readers. Scavenged energy is usually available in short bursts and fluctuations can cause abrupt changes in power levels, interrupting ongoing operations. We intend to investigate the possibility and associated cost of intermittent checkpoints to save pattern matching and detection state in case of power failures.

Overall, we will continue to pursue deployment of WSNs targeting reactive applications since the practical work involved often uncovers issues deeply intertwined with the restricted functionality of nodes and extend empirical application-level research in WSNs.

# Glossary

**ADC** An Analog-to-Digital Converter is a hardware component responsible for converting continuous analog signals to discrete digital numbers. It is typically found as the interfacing component between the sensors and the processor in a wireless sensor node. 76, 119

**AIS** An Artificial Immune System (AIS) is a biologically inspired system that mimics the human immune system to solve a problem. 28, 35

**BMS** A Building Management System (BMS) is a computer-based system that aims to monitor a building's mechanical and electrical equipment such as cooling, heating, lighting and power. 83

**BSN** A more specific type of WSN that employs various sensors to provide continuous monitoring and analysis of physiological parameters of human subjects. 26, 27

**Convex Hull** A Convex Hull for a set of points  $P$  in a real vector space  $V$  is the minimal convex set containing  $P$ . It represents the boundary of the minimal convex set containing the set of points  $P$  in the plane. 100

**EWMA** An Exponentially Weighted Moving Average (EWMA) is a statistical technique used to analyse a set of data points by creating an average of one subset of the full data set at a time, with each number in the subset given a weighting factor that decreases exponentially giving more importance to

recent observations while still not discarding older observations entirely. 24, 35, 58–60

**FPU** The floating point unit (FPU) is a computer chip that has been designed to carry out arithmetic operations involving floating point numbers. Modern desktop and server-class processors integrate the FPU in the main CPU, however a number of embedded devices lack an FPU altogether and operations involving floating-point numbers must be carried out in software. 15

**MAC** The Medium (or Media) Access Control sublayer provides access control mechanisms that make it possible for nodes to communicate in a network. It is responsible for framing, medium access, reliability, flow control and error detection. 29

**MCU** A Microcontroller Unit (MCU) is a small computer on a single integrated circuit consisting of a relatively simple CPU combined with support functions such as a crystal oscillator, timers, watchdog, serial and analog I/O and so on. 15, 20, 73, 76, 77, 81, 84, 91, 120, 152

**OSI** The Open Systems Interconnection (OSI) is a joint effort to standardise networking protocols started by the International Organisation for Standardisation. 29

**PCA** Principal Component Analysis (PCA) aims to reduce dimensionality of a data set consisting of a large number of interrelated variables while retaining as much information as possible on the variations present in the data set [Jol02]. 29, 36, 124

**PRR** The Packet Reception Rate (PRR) is the ratio of packets received by a receiving node to packets sent by a transmitting node. A PRR of 1 indicates a perfect link while a PRR of 0 indicates no path between source and destination. 107

- Pub/Sub** Publish/Subscribe (Pub/Sub) is a loosely-coupled communication paradigm that is primarily used to deliver interests in events (subscriptions) to event producers and to disseminate event notifications from producers (publishers) to interested parties (event consumers). 20, 90, 120
- RAM** Random-Access Memory (RAM) is a form of computer data storage with constant access time regardless of the location of the data. 15
- RFID** Radio-frequency identification (RFID) is an automatic identification method, relying on storing and remotely retrieving data using devices called RFID tags or transponders. 91, 93
- RLE** Run Length Encoding (RLE) is a technique that reduces the the size of a repeating string of characters by replacing one long string of consecutive characters with a single data value and count. 25, 26
- RSAM** Real-time Seismic Amplitude Measurement (RSAM) sums the average amplitude of a seismic signal during an interval to output a measure of the overall level of seismic activity. 59
- SHM** Structural Health Monitoring (SHM) is the process of implementing a damage detection strategy for aerospace, civil and mechanical engineering infrastructure. 36
- SNR** The Signal-to-Noise Ratio (SNR or S/N) is the ratio of the signal power to the noise corrupting this signal. In the context of WSNs it is sometimes used as a Link Estimation metric. 65, 70
- SPoF** A Single Point of Failure (SPoF) is a network node whose failure compromises or even stops the operation of the entire system. 36
- SVM** The original Support Vector Machine (SVM) is a non-probabilistic linear classifier that aims to predict one of two appropriate classes for given input data. SVMs are collections of related classifiers used, among other purposes, for pattern classification. 27, 30, 36

**TDOA** Time Difference Of Arrival (TDOA) is a localisation method based on combining the time of arrival of a signal emitted from a source and received by three, or more, receivers. 32, 36, 123

**WSAN** A Wireless Sensor Actuator Network (WSAN) is a kind of control system in which sensing, actuation and decision making are distributed while resource-constrained system components communicate with each other [KC08].  
25

**WSN** A Wireless Sensor Network (WSN) is a wireless network consisting of spatially distributed autonomous devices using sensors to cooperatively monitor physical or environmental conditions, such as temperature, sound, vibration, pressure, motion or pollutants, at different locations. 14, 15, 50, 118

# Bibliography

- [AK04] Ian F. Akyildiz and Ismail H. Kasimoglu. Wireless sensor and actor networks: research challenges. *Ad Hoc Networks*, 2(4):351–367, 2004.
- [Alb08] Brian Albright. RFID Sensor Platform from GE Breaks New Ground. <http://www.rfidupdate.com/articles/index.php?id=1691>, October 2008.
- [ASSC02] I. F. Akyildiz, W. Su, Y. Sankarasubramaniam, and E. Cayirci. Wireless sensor networks: a survey. *Computer Networks*, 38(4):393–422, 2002.
- [ATB05] R. C. Aster, C. H. Thurber, and B. Borchers. *Parameter estimation and inverse problems*. Academic Press, 2005.
- [Ate96] J. Atema. Eddy chemotaxis and odor landscapes: exploration of nature with animal sensors. *Biological Bulletin*, 191(1):129–138, 1996.
- [ATH03] Anna Aronzon, Erica R. Thaler, and C. William Hanson. Differentiation between cerebrospinal fluid and serum with electronic nose. *Otolaryngology - Head and Neck Surgery*, 129(2):–204, 2003. Annual Meeting of the American Academy of Otolaryngology-Head and Neck Surgery Foundation, Inc.

- [AY05] Kemal Akkaya and Mohamed Younis. A survey on routing protocols for wireless sensor networks. *Ad Hoc Networks*, 3(3):325–349, 2005.
- [BCFL09] Yingyi Bu, Lei Chen, Ada Wai-Chee Fu, and Dawei Liu. Efficient anomaly monitoring over moving object trajectory streams. In *KDD '09: Proceedings of the 15th ACM SIGKDD international conference on Knowledge discovery and data mining*, pages 159–168, 2009.
- [Ben99] Jon Bentley. *Programming Pearls (2nd Edition)*. Addison-Wesley, 1999.
- [BGG09] J. Brusey, E. Gaura, D. Goldsmith, and J. Shuttleworth. FieldMAP: A Spatio-Temporal Field Monitoring Application Prototyping Framework. *IEEE Sensors Journal*, 9(11):1378–1390, 2009.
- [BHL07] L. M. A. Bettencourt, A. A. Hagberg, and L. B. Larkey. Separating the wheat from the chaff: practical anomaly detection schemes in ecological applications of distributed sensor networks. *Lecture Notes in Computer Science*, 4549:223–239, 2007.
- [BPC<sup>+</sup>07] Paolo Barontib, Prashant Pillaia, Vince W. C. Chooka, Stefano Chessab, Alberto Gottab, and Y. Fun Hu. Wireless Sensor Networks: A Survey on the State of the Art and the 802.15.4 and ZigBee Standards. *Computer Communications*, 30(7):1655–1695, 2007.
- [BRR08] Elizabeth A. Basha, Sai Ravela, and Daniela Rus. Model-based monitoring for early warning flood detection. In *SenSys '08: Proceedings of the 6th ACM conference on Embedded network sensor systems*, pages 295–308, New York, NY, USA, 2008. ACM.

- [Byr05] C. L. Byrne. *Signal Processing: a mathematical approach*. AK Peters Ltd, 2005.
- [CBK09] Varun Chandola, Arindam Banerjee, and Vipin Kumar. Anomaly Detection: A Survey. *ACM Computing Surveys*, 2009.
- [CES04] David E. Culler, Deborah Estrin, and Mani B. Srivastava. Guest Editors' Introduction: Overview of Sensor Networks. *IEEE Computer*, 37(8):41–49, 2004.
- [CJ02] Gianpaolo Cugola and H. Arno Jacobsen. Using publish/subscribe middleware for mobile systems. *SIGMOBILE Mob. Comput. Commun. Rev.*, 6(4):25–33, 2002.
- [CLD08] Kenan Casey, Alvin Lim, and Gerry Dozier. A Sensor Network Architecture for Tsunami Detection and Response. *International Journal of Distributed Sensor Networks*, 4(1):28–43, 2008.
- [CMY05] Jiansheng Chen, Yiu Sang Moon, and Hoi-Wo Yeung. Palmprint Authentication Using Time Series. In Takeo Kanade, Anil K. Jain, and Nalini K. Ratha, editors, *AVBPA*, pages 376–385. Springer, 2005.
- [CP07] Joseph Cox and Michael Partensky. Spatial Localization Problem and the Circle of Apollonius. <http://arxiv.org/abs/physics/0701146>, January 2007.
- [CPGM06] V. Chatzigiannakis, S. Papavassiliou, M. Grammatikou, and B. Maglaris. Hierarchical Anomaly Detection in Distributed Large-Scale Sensor Networks. In *ISCC '06: Proceedings of the 11th IEEE Symposium on Computers and Communications*, pages 761–767, Washington, DC, USA, 2006. IEEE Computer Society.
- [CWC<sup>+</sup>07] Rebecca Castano, Kiri L. Wagstaff, Steve Chien, Timothy M. Stough, and Benyang Tang. On-board analysis of uncalibrated

- data for a spacecraft at mars. In *KDD '07: Proceedings of the 13th ACM SIGKDD international conference on Knowledge discovery and data mining*, pages 922–930, 2007.
- [CYR<sup>+</sup>08] Jren-Chit Chin, David K. Y. Yau, Nageswara S. V. Rao, Yong Yang, Chris Y. T. Ma, and Mallikarjun Shankar. Accurate localization of low-level radioactive source under noise and measurement errors. In *SenSys '08: Proceedings of the 6th ACM conference on Embedded network sensor systems*, pages 183–196, New York, NY, USA, 2008. ACM.
- [DD06] Ritabrata Dutta and Ritaban Dutta. "Maximum Probability Rule" based classification of MRSA infections in hospital environment: Using electronic nose. *Sensors and Actuators B: Chemical*, 120(1):156–165, 2006.
- [Det07] Smiths Detection. Cyranose 320 Electronic Nose. [http://www.smithsdetection.com/eng/Cyranose\\_320.php](http://www.smithsdetection.com/eng/Cyranose_320.php), 2007.
- [DFN06] Wenliang Du, Lei Fang, and Peng Ning. LAD: localization anomaly detection for wireless sensor networks. *Journal of Parallel and Distributed Computing*, 66(7):874–886, 2006.
- [DGH<sup>+</sup>06] Alan J. Demers, Johannes Gehrke, Mingsheng Hong, Mirek Riedewald, and Walker M. White. Towards Expressive Publish/Subscribe Systems. In *EDBT*, pages 627–644. Springer, 2006.
- [DGL<sup>+</sup>05] P. Desnoyers, D. Ganesan, H. Li, M. Li, and P. Shenoy. PRESTO: A predictive storage architecture for sensor networks. In *Tenth Workshop on Hot Topics in Operating Systems (HotOS X)*, 2005.
- [DSS07] M. Drozda, S. Schaust, and H. Szczerbicka. Is AIS based misbehavior detection suitable for wireless sensor networks. In *Proc. IEEE Wireless Communications and Networking Conference (WCNC)*. Citeseer, 2007.

- [DTP91] J. Durkin, D. Tallo, and E. J. Petrik. FIDEX: An expert system for satellite diagnostics. In *In its Space Communications Technology Conference: Onboard Processing and Switching p 143-152 (SEE N92-14202 05-32)*, pages 143–152, 1991.
- [EFGK03] Patrick Th. Eugster, Pascal A. Felber, Rachid Guerraoui, and Anne-Marie Kermarrec. The many faces of publish/subscribe. *ACM Comput. Surv.*, 35(2):114–131, 2003.
- [EM91] E. T. Endo and T. Murray. Real-time seismic amplitude measurement (RSAM): a volcano monitoring and prediction tool. *Bulletin of Volcanology*, 53(7):533–545, 1991.
- [FCG10] P. A. Forero, A. Cano, and G. B. Giannakis. Consensus-based distributed support vector machines. *Journal of Machine Learning Research*, 11:1663–1707, 2010.
- [GJV<sup>+</sup>05] L. Gu, D. Jia, P. Vicaire, T. Yan, L. Luo, A. Tirumala, Q. Cao, T. He, J. A. Stankovic, and T. Abdelzaher. Lightweight detection and classification for wireless sensor networks in realistic environments. In *SenSys' 05*, pages 205–217. Citeseer, 2005.
- [GKW<sup>+</sup>02] D. Ganesan, B. Krishnamachari, A. Woo, D. Culler, D. Estrin, and S. Wicker. Complex Behavior at Scale: An Experimental Study of Low-Power Wireless Sensor Networks. Technical report, 2002.
- [GN03] E. Gaura and R. M. Newman. Microsensors, arrays and automatic diagnosis of sensor faults. In *IEEE International Conference on Advanced Intelligent Mechatronic (AIM2003)*, pages 360–366, 2003.
- [Gol91] D. Goldberg. What every computer scientist should know about floating-point arithmetic. *ACM Computing Surveys (CSUR)*, 23(1):5–48, 1991.

- [GRG88] Ajith Gunatilaka, Branko Ristic, and Ralph Gailis. Radiological Source Localisation, 1988. DSTO-TR-1988.
- [Gus97] Dan Gusfield. *Algorithms on Strings, Trees and Sequences: Computer Science and Computational Biology*. Cambridge University Press, 1997.
- [Han02] D. Hand. Pattern detection and discovery. *Pattern Detection and Discovery*, pages 161–173, 2002.
- [HCB02] W. B. Heinzelman, A. P. Chandrakasan, and H. Balakrishnan. An application-specific protocol architecture for wireless microsensor networks. *Wireless Communications, IEEE Transactions on*, 1(4):660–670, Oct 2002.
- [HCM08] Simon J. Haggett, Dominique F. Chu, and Ian W. Marshall. Evolving a dynamic predictive coding mechanism for novelty detection. *Knowledge-Based Systems*, 21(3):217–224, 2008.
- [HGH<sup>+</sup>06] Ling Huang, Minos Garofalakis, Joseph Hellerstein, Anthony Joseph, and Nina Taft. Toward sophisticated detection with distributed triggers. In *MineNet '06: Proceedings of the 2006 SIGCOMM workshop on Mining network data*, pages 311–316, New York, NY, USA, 2006. ACM.
- [HGM04] Yongqiang Huang and Hector Garcia-Molina. Publish/Subscribe in a Mobile Environment. *Wireless Networks*, 10(6):643–652, 2004.
- [HHB<sup>+</sup>03] Tian He, Chengdu Huang, Brian M. Blum, John A. Stankovic, and Tarek Abdelzaher. Range-free localization schemes for large scale sensor networks. In *MobiCom '03: Proceedings of the 9th annual international conference on Mobile computing and networking*, pages 81–95, New York, NY, USA, 2003. ACM.

- [HHK<sup>+</sup>08] Jan-Hinrich Hauer, Vlado Handziski, Andreas Köpke, Andreas Willig, and Adam Wolisz. A Component Framework for Content-Based Publish/Subscribe in Sensor Networks. In *EWSN*, pages 369–385. Springer, 2008.
- [HHM03] Joseph M. Hellerstein, Wei Hong, and Samuel Madden. The sensor spectrum: technology, trends, and requirements. *SIGMOD Record*, 32(4):22–27, 2003.
- [Hig02] N. J. Higham. *Accuracy and stability of numerical algorithms*. Society for Industrial Mathematics, 2002.
- [HJCX08] Fei Hu, Meng Jiang, Laura Celentano, and Yang Xiao. Robust medical ad hoc sensor networks (MASN) with wavelet-based ECG data mining. *Ad Hoc Netw.*, 6(7):986–1012, 2008.
- [HMBE06] Raffay Hamid, Siddhartha Maddi, Aaron Bobick, and Irfan Essa. Unsupervised analysis of activity sequences using event-motifs. In *VSSN '06: Proceedings of the 4th ACM international workshop on Video surveillance and sensor networks*, pages 71–78, 2006.
- [HMG03] Adam T. Hayes, Alcherio Martinoli, and Rodney M. Goodman. Swarm robotic odor localization: Off-line optimization and validation with real robots. *Robotica*, 21(4):427–441, 2003.
- [INM97] Hiroshi Ishida, Takamichi Nakamoto, and Toyosaka Moriizumi. Remote sensing of gas/odor source location and concentration distribution using mobile system. *Solid State Sensors and Actuators*, 1(16):559–562, 1997.
- [Ins06] Texas Instruments. MSP430x2xx Family: User’s guide, 2006.
- [Int04] Intel. Lab Data (Berkeley). <http://db.csail.mit.edu/labdata/labdata.html>, 2004.

- [IPV07] Tsuyoshi Idé, Spiros Papadimitriou, and Michail Vlachos. Computing Correlation Anomaly Scores Using Stochastic Nearest Neighbors. In *ICDM*, pages 523–528. IEEE Computer Society, 2007.
- [Jai91] R. Jain. *The art of computer systems performance analysis*. Wiley New York, 1991.
- [Jol02] I. Jolliffe. *Principal component analysis*. Springer Series in Statistics. Springer-Verlag, 2002.
- [KC08] Marcin Karpiński and Vinny Cahill. Stream-based macro-programming of wireless sensor, actuator network applications with SOSNA. In *DMSN '08: Proceedings of the 5th workshop on Data management for sensor networks*, pages 49–55, New York, NY, USA, 2008. ACM.
- [KDS05] Andrea Kulakov, Danco Davcev, and Georgi Stojanov. Learning patterns in wireless sensor networks based on wavelet neural networks. In *ICPADS '05: Proceedings of the 11th International Conference on Parallel and Distributed Systems - Workshops*, pages 373–377, Washington, DC, USA, 2005. IEEE Computer Society.
- [KHW<sup>+</sup>07] Eleftheria Katsiri, Mel Ho, Lei Wang, Benny Lo, and Chris Toumazou. Embedded Real-Time Heart Variability Analysis. In *4th International Workshop on Wearable and Implantable Body Sensor Networks (BSN 2007)*, pages 128–132, 2007.
- [KLF05] Eamonn Keogh, Jessica Lin, and Ada Fu. HOT SAX: Efficiently Finding the Most Unusual Time Series Subsequence. *Data Mining, IEEE International Conference on*, pages 226–233, 2005.
- [KLK<sup>+</sup>05] N. Kumar, N. Lolla, E. Keogh, S. Lonardi, C. Ratanamahatana, and L. Wei. Time-series bitmaps: A practical visualization tool for working with large time series databases. In *SIAM 2005 Data Mining Conference*, pages 531–535. Citeseer, 2005.

- [KLR04] Eamonn Keogh, Stefano Lonardi, and Chotirat Ann Ratanamahatana. Towards parameter-free data mining. In *KDD '04: Proceedings of the tenth ACM SIGKDD international conference on Knowledge discovery and data mining*, pages 206–215, New York, NY, USA, 2004. ACM.
- [KR78] B. W. Kerningham and D. M. Ritchie. *Programming in C*. Prentice Hall, 1978.
- [Kri05] Bhaskar Krishnamachari. *Networking Wireless Sensors*. Cambridge University Press, 2005.
- [KSW<sup>+</sup>08] S. Kasetty, C. Stafford, G. P. Walker, X. Wang, and E. Keogh. Real-time classification of streaming sensor data. In *Tools with Artificial Intelligence, 2008. ICTAI'08. 20th IEEE International Conference on*, volume 1, pages 149–156, 2008.
- [LBC<sup>+</sup>08] Philip Levis, Eric Brewer, David Culler, David Gay, Samuel Madden, Neil Patel, Joe Polastre, Scott Shenker, Robert Szewczyk, and Alec Woo. The Emergence of a Networking Primitive in Wireless Sensor Networks. *Communications of the ACM*, 51(7):99–106, 2008.
- [LGH<sup>+</sup>05] P. Levis, D. Gay, V. Handziski, J. H. Hauer, B. Greenstein, M. Turon, J. Hui, K. Klues, C. Sharp, and R. Szewczyk. T2: A second generation os for embedded sensor networks. *Telecommunication Networks Group, Technische Universitat Berlin, Technical Report TKN-05-007*, 2005.
- [LKLC03] Jessica Lin, Eamonn Keogh, Stefano Lonardi, and Bill Chiu. A symbolic representation of time series, with implications for streaming algorithms. In *DMKD '03: Proceedings of the 8th ACM SIGMOD workshop on Research issues in data mining and knowledge discovery*, pages 2–11, New York, NY, USA, 2003. ACM.

- [LKQ<sup>+</sup>03] M. Lin, A. Kumar, X. Qing, S. J. Beard, S. S. Russell, J. L. Walker, and T. K. Delay. Monitoring the integrity of filament-wound structures using built-in sensor networks. In *Society of Photo-Optical Instrumentation Engineers (SPIE) Conference Series*, volume 5054, pages 222–229, 2003.
- [LLC07] Mo Li, Yunhao Liu, and Lei Chen. Non-Threshold based Event Detection for 3D Environment Monitoring in Sensor Networks. In *ICDCS '07: Proceedings of the 27th International Conference on Distributed Computing Systems*, page 9. IEEE Computer Society, 2007.
- [LLWC03] P. Levis, N. Lee, M. Welsh, and D. Culler. TOSSIM: Accurate and scalable simulation of entire TinyOS applications. In *Proceedings of the 1st international conference on Embedded networked sensor systems*, pages 126–137. ACM New York, NY, USA, 2003.
- [LNLP06] C. E. Loo, M. Y. Ng, C. Leckie, and M. Palaniswami. Intrusion detection for routing attacks in sensor networks. *International Journal of Distributed Sensor Networks*, 2(4):313–332, 2006.
- [LPCS04] Philip Levis, Neil Patel, David Culler, and Scott Shenker. Trickle: a self-regulating algorithm for code propagation and maintenance in wireless sensor networks. In *NSDI'04: Proceedings of the 1st conference on Symposium on Networked Systems Design and Implementation*, pages 2–2, Berkeley, CA, USA, 2004. USENIX Association.
- [Mat08a] Mathworks. fminbnd — Find minimum of single-variable function on fixed interval. Matlab R2008b Function Reference, 2008.
- [Mat08b] Mathworks. fminsearch — Find minimum of unconstrained multivariable function using derivative-free method. Matlab R2008b Function Reference, 2008.

- [Mat08c] Mathworks. `randn` — Normally distributed pseudorandom numbers. MATLAB R2008b Function Reference, 2008.
- [Mat08d] Mathworks. `Timer` — Function Reference. MATLAB 2008b Documentation, 2008.
- [Mat10] Mathworks. MATLAB — The Language Of Technical Computing. <http://www.mathworks.com/products/matlab/>, 2010.
- [MFHH03] Samuel Madden, Michael J. Franklin, Joseph M. Hellerstein, and Wei Hong. The design of an acquisitional query processor for sensor networks. In *SIGMOD '03: Proceedings of the 2003 ACM SIGMOD international conference on Management of data*, pages 491–502, New York, NY, USA, 2003. ACM.
- [MFjWM04] David Malan, Thaddeus Fulford-jones, Matt Welsh, and Steve Moulton. CodeBlue: An ad hoc sensor network infrastructure for emergency medical care. In *International Workshop on Wearable and Implantable Body Sensor Networks*, 2004.
- [MGH09] Alexandra Meliou, Carlos Guestrin, and Joseph Hellerstein. Approximating Sensor Network Queries Using In-Network Summaries. In *IPSN*, 2009.
- [MM90] Udi Manber and Gene Myers. Suffix arrays: a new method for on-line string searches. In *SODA '90: Proceedings of the first annual ACM-SIAM symposium on Discrete algorithms*, pages 319–327, Philadelphia, PA, USA, 1990. Society for Industrial and Applied Mathematics.
- [MP03] Junshui Ma and Simon Perkins. Online novelty detection on temporal sequences. In *KDD '03: Proceedings of the ninth ACM SIGKDD international conference on Knowledge discovery and data mining*, pages 613–618, New York, NY, USA, 2003. ACM.

- [MPL<sup>+</sup>07] Ian W. Marshall, Mark C. Price, Hai Li, N. Boyd, and Steve Boult. Multi-sensor Cross Correlation for Alarm Generation in a Deployed Sensor Network. In *EuroSSC*, pages 286–299. Springer, 2007.
- [MPR03] G Mellen, M Pachter, and J Raquet. Closed-form solution for determining emitter location using time difference of arrival measurements. *IEEE Transactions on Aerospace and Electronic Systems*, 39(3):1056–1058, 2003.
- [MRK<sup>+</sup>07] Amy McGovern, D. H. Rosendahl, A. Kruger, M. G. Beaton, R. A. Brown, and K. K. Droegemeier. Anticipating the formation of tornadoes through data mining. In *Fifth Conference on Artificial Intelligence Applications to Environmental Science*, 2007.
- [Nor97] James R. Norris. *Markov Chains*. Cambridge University Press, 1997.
- [OF02] S. F. Oberman and M. J. Flynn. Design issues in division and other floating-point operations. *Computers, IEEE Transactions on*, 46(2):154–161, 2002.
- [PHCL06] Tran Van Phuong, Le Xuan Hung, Seong Jin Cho, and Young-Koo Lee and Sungyoung Lee. An Anomaly Detection Algorithm for Detecting Attacks in Wireless Sensor Networks . In *Intelligence and Security Informatics*, pages 735–736, 2006.
- [PK00] G. J. Pottie and W. J. Kaiser. Wireless integrated network sensors. *Communications of the ACM*, 43(5):51–58, 2000.
- [PLPG06] S. Phoha, T. F. La Porta, and C. Griffin. *Sensor network operations*. Wiley-IEEE Press, 2006.
- [PMSR09] Debprakash Patnaik, Manish Marwah, Ratnesh Sharma, and Naren Ramakrishnan. Sustainable operation and management of

- data center chillers using temporal data mining. In *KDD '09: Proceedings of the 15th ACM SIGKDD international conference on Knowledge discovery and data mining*, pages 1305–1314, 2009.
- [PSFR08] S. Price, J. G. Sheridan, T. P. Falcao, and G. Roussos. Towards a framework for investigating tangible environments for learning. *International Journal of Arts and Technology*, 1(3):351–368, 2008.
- [Rao06] Nageswara Rao. Identification of simple product-form plumes using networks of sensors with random errors. *9th International Conference on Information Fusion*, pages 1–8, 2006.
- [RBLP09] Sutharshan Rajasegarar, James C. Bezdek, Christopher Leckie, and Marimuthu Palaniswami. Elliptical anomalies in wireless sensor networks. *ACM Trans. Sen. Netw.*, 6(1):1–28, 2009.
- [Res08] Intel Research. WISP: Wireless Identification and Sensing Platform. <http://seattle.intel-research.net/wisp/>, 2008.
- [Sen08] MoteIV (later renamed to Sentilla). TMote Sky Datasheets and Downloads. <http://www.sentilla.com/pdf/eol/tmote-sky-datasheet.pdf>, 2008.
- [Sen10] Sensirion. Datasheet SHT1x — Temperature and Humidity Sensor. [http://www.sensirion.com/en/pdf/product\\_information/Datasheet-humidity-sensor-SHT1x.pdf](http://www.sensirion.com/en/pdf/product_information/Datasheet-humidity-sensor-SHT1x.pdf), 2010.
- [SG07] Yan Shen and Bing Guo. Dynamic Power Management based on Wavelet Neural Network in Wireless Sensor Networks. In *NPC '07: Proceedings of the 2007 IFIP International Conference on Network and Parallel Computing Workshops*, pages 431–436, Washington, DC, USA, 2007. IEEE Computer Society.
- [Sim06] Dan Simon. *Optimal State Estimation: Kalman, H Infinity, and Nonlinear Approaches*. WileyBlackwell, 2006.

- [SLLM09] M. Salson, T. Lecroq, M. Léonard, and L. Mouchard. Dynamic extended suffix arrays. *Journal of Discrete Algorithms*, 2009.
- [SLV93] G. Sandini, G. Lucarini, and M. Varoli. Gradient driven self-organizing systems. In *Intelligent Robots and Systems' 93, IROS'93. Proceedings of the 1993 IEEE/RSJ International Conference on*, volume 1, pages 429–432. IEEE, 1993.
- [SMD<sup>+</sup>04] M. E. Shykhon, D. W. Morgan, R. Dutta, E. L. Hines, and J. W. Gardner. Clinical evaluation of the electronic nose in the diagnosis of ear, nose and throat infection: a preliminary study. *The Journal of Laryngology & Otology*, 118(09):706–709, 2004.
- [SMP<sup>+</sup>04] R. Szewczyk, A. Mainwaring, J. Polastre, J. Anderson, and D. Culler. An analysis of a large scale habitat monitoring application. In *Proceedings of the 2nd international conference on Embedded networked sensor systems*, pages 214–226. ACM, 2004.
- [SOM07] M Schwabacher, N Oza, and B Matthews. Unsupervised Anomaly Detection for Liquid-Fueled Rocket Propulsion Health Monitoring. *Journal of Aerospace Computing, Information, and Communication*, 6(7):464–482, 2007.
- [SOSM05] Demetri P. Spanos, Reza Olfati-Saber, and Richard M. Murray. Approximate distributed Kalman filtering in sensor networks with quantifiable performance. In *IPSN '05: Proceedings of the 4th international symposium on Information processing in sensor networks*, page 18, Piscataway, NJ, USA, 2005. IEEE Press.
- [SRT07] Thomas Stiefmeier, Daniel Roggen, and Gerhard Tröster. Gestures are strings: efficient online gesture spotting and classification using string matching. In *BodyNets '07: Proceedings of the ICST 2nd international conference on Body area networks*, pages 1–8, 2007.

- [STG07] Cory Sharp, Martin Turon, and David Gay. TinyOS Enhancement Proposal (TEP) 102: Timers. <http://tinycvs.sourceforge.net/tinycvs/tinycvs-2.x/doc/html/tep102.html>, 2007.
- [STKC09] Minh Shin, Patrick Tsang, David Kotz, and Cory Cornelius. DEAMON: Energy-efficient Sensor Monitoring. In *Sensor, Mesh and Ad Hoc Communications and Networks, 2009. SECON '09. 6th Annual IEEE Communications Society Conference on*, pages 1–9, June 2009.
- [SWJR07] Xiuyao Song, Mingxi Wu, Christopher Jermaine, and Sanjay Ranka. Statistical change detection for multi-dimensional data. In *KDD '07: Proceedings of the 13th ACM SIGKDD international conference on Knowledge discovery and data mining*, pages 667–676, New York, NY, USA, 2007. ACM.
- [TE07] Y. Tian and E. Ekici. Cross-layer collaborative in-network processing in multihop wireless sensor networks. *IEEE Transactions on Mobile Computing*, pages 297–310, 2007.
- [TK88] Jimfron Tan and Nicholas Kyfuakopoulos. Implementation of a Tracking Kalman Filter on a Digital Signal Processor. *IEEE Transactions on Industrial Electronics*, 35(1):126–134, 1988.
- [UoC08] Riverside University of California. The UCR Time Series Data Mining Archive. <http://www.cs.ucr.edu/~eamonn/TSDMA>, 2008.
- [WADHW08] Geoffrey Werner-Allen, Stephen Dawson-Haggerty, and Matt Welsh. Lance: optimizing high-resolution signal collection in wireless sensor networks. In *SenSys '08: Proceedings of the 6th ACM conference on Embedded network sensor systems*, pages 169–182, New York, NY, USA, 2008.
- [WALJ<sup>+</sup>06] Geoffrey Werner-Allen, Konrad Lorincz, Jeff Johnson, Jonathan Lees, and Matt Welsh. Fidelity and Yield in a Volcano Monitoring

- Sensor Network. In *OSDI*, pages 381–396. USENIX Association, 2006.
- [WB95] Greg Welch and Gary Bishop. An Introduction to the Kalman Filter. Technical Report 95-041, Chapel Hill, NC, USA, 1995.
- [WDWS10] Georg Wittenburg, Norman Dziengel, Christian Wartenburger, and Jochen Schiller. A system for distributed event detection in wireless sensor networks. In *Proceedings of the 9th ACM/IEEE International Conference on Information Processing in Sensor Networks*, pages 94–104, New York, NY, USA, 2010.
- [WF05] I. H. Witten and E. Frank. *Data Mining: Practical machine learning tools and techniques*. Morgan Kaufmann Pub, 2005.
- [WYC<sup>+</sup>06] S. Wang, J. Yang, N. Chen, X. Chen, and Q. Zhang. Human activity recognition with user-free accelerometers in the sensor networks. In *Neural Networks and Brain, 2005. ICNN&B'05. International Conference on*, volume 2, pages 1212–1217. IEEE, 2006.
- [XLCL06] Wenwei Xue, Qiong Luo, Lei Chen, and Yunhao Liu. Contour map matching for event detection in sensor networks. In *SIGMOD '06: Proceedings of the 2006 ACM SIGMOD international conference on Management of data*, pages 145–156, New York, NY, USA, 2006. ACM.
- [XRC<sup>+</sup>04] Ning Xu, Sumit Rangwala, Krishna Kant Chintalapudi, Deepak Ganesan, Alan Broad, Ramesh Govindan, and Deborah Estrin. A wireless sensor network For structural monitoring. In *SenSys '04: Proceedings of the 2nd international conference on Embedded networked sensor systems*, pages 13–24, New York, NY, USA, 2004. ACM.

- [XRS07] Xiaochun Xu, Nageswara Rao, and Sartaj Sahni. A computational geometry method for DTOA triangulation. In *10th International Conference on Information Fusion*, pages 1–7, 2007.
- [YF04] O. Younis and S. Fahmy. HEED: a hybrid, energy-efficient, distributed clustering approach for ad hoc sensor networks. *Mobile Computing, IEEE Transactions on*, 3(4):366–379, Oct.–Dec. 2004.
- [ZG09] F. Zhao and L. Guibas. Wireless sensor networks. *Communications Engineering Desk Reference*, page 247, 2009.
- [ZK05] Marco Zuniga and Bhaskar Krishnamachari. Link Layer Models for Wireless Sensor Networks. <http://ceng.usc.edu/~anrg/downloads/LinkModellingTutorial.pdf>, December 2005.
- [Zol10] Zolertia. Z1 WSN Module. <http://www.zolertia.com/products/Z1>, 2010.
- [ZR] M. Zoumboulakis and G. Roussos. Complex Event Detection in Extremely Resource-Constrained Wireless Sensor Networks. *Mobile Networks and Applications*, pages 1–20.
- [ZR07] Michael Zoumboulakis and George Roussos. Escalation: Complex Event Detection in Wireless Sensor Networks. In Gerd Kortuem, Joe Finney, Rodger Lea, and Vasughi Sundramoorthy, editors, *EuroSSC*, pages 270–285. Springer, 2007.
- [ZR09a] Michael Zoumboulakis and George Roussos. Efficient pattern detection in extremely resource-constrained devices. In *SECON'09: Proceedings of the 6th Annual IEEE communications society conference on Sensor, Mesh and Ad Hoc Communications and Networks*, pages 10–18, 2009.
- [ZR09b] Michael Zoumboulakis and George Roussos. Estimation of Pollutant-Emitting Point-Sources Using Resource-Constrained

- Sensor Networks. In *GSN '09: Proceedings of the 3rd International Conference on GeoSensor Networks*, pages 21–30, 2009.
- [ZR09c] Michael Zoumboulakis and George Roussos. In-network Pattern Detection on Intel WISPs. (Demo Abstract) in Proceedings of Wireless Sensing Showcase, 2009.
- [ZR09d] Michael Zoumboulakis and George Roussos. Integer-Based Optimisations for Resource-Constrained Sensor Platforms . In *First International ICST Conference, S-CUBE 2009*, pages 144–157, 2009.
- [ZR09e] Michael Zoumboulakis and George Roussos. SIKTN 2009 wireless sensing winners, 2009.
- [ZR11] Michael Zoumboulakis and Geoge Roussos. *Pattern Recognition in Extremely Resource Constrained Devices*. Reasoning in Event-based Distributed Systems. Springer, 2011.
- [ZRP04a] M. Zoumboulakis, G. Roussos, and A. Poulouvassilis. Active rules for sensor databases. In *Proceedings of the 1st international workshop on Data management for sensor networks: in conjunction with VLDB 2004*, pages 98–103. ACM, 2004.
- [ZRP04b] M. Zoumboulakis, G. Roussos, and A. Poulouvassilis. Active rules for wireless networks of sensors & actuators. In *Proceedings of the 2nd international conference on Embedded networked sensor systems*, pages 263–264. ACM, 2004.
- [ZSST04] Dimitri Zarzhitsky, Diana F. Spears, William M. Spears, and David R. Thayer. A Fluid Dynamics Approach to Multi-Robot Chemical Plume Tracing. In *AAMAS '04: Proceedings of the Third International Joint Conference on Autonomous Agents and Multiagent Systems*, pages 1476–1477, Washington, DC, USA, 2004. IEEE Computer Society.

# Appendix A

## Publications

Our peer reviewed publications related to this thesis are shown in reverse chronological order in Table A.1. Publication [ZR11] is a critical review of recent advances in the fields of anomaly and novelty detection in extremely resource constrained systems (related to Chapter 2), together with a presentation of the spatial pattern location estimation algorithm of Chapter 6. Publication [ZR] presents the temporal domain algorithms of Chapter 3. [ZR09d] describes the implementation and deployment work (Chapter 5) involved in refactoring the temporal domain algorithm. The spatial algorithm of Chapter 6 are described in [ZR09b]. An implementation and demonstration of the non-parametric pattern detection algorithm on the battery-free Intel WISP nodes is described in [ZR09c]. Publications [ZR09a] and [ZR07] describe the temporal domain algorithms and related findings. Finally, publications [ZRP04a] and [ZRP04b] cover earlier work and involve adapting active database technologies to reactive WSNs; a direction not pursued further in this thesis.

Ref. Key	Title	Appeared in:	Year
[ZR11]	Pattern Detection in Extremely Resource Constrained Devices	Book chapter in: Reasoning in Event-based Distributed Systems	2011 (to appear)
[ZR]	Complex Event Detection in Extremely Resource-Constrained Wireless Sensor Networks	Article in: ACM Mobile Networks and Applications	2010
[ZR09d]	Integer-based Optimisations for Resource-constrained Sensor Platforms	in Proceedings of: First International Conference on Sensor, Systems and Software (S-CUBE)	2009
[ZR09b]	Estimation of Pollutant Emitting Point-Sources using Resource Constrained Sensor Networks	in Proceedings of: Third International Conference on Geosensor Networks (GSN3)	2009
[ZR09c]	In-network Pattern Detection on Intel WISPs	(Demo Abstract) in Proceedings of: Wireless Sensing Showcase (KTN)	2009
[ZR09a]	Efficient Pattern Detection in Extremely Resource Constrained Devices	in Proceedings of: Sixth Annual IEEE Communications Society Conference on Sensor, Mesh and Ad Hoc Communications and Networks (SECON)	2009
[ZR07]	Escalation: Complex Event Detection in Wireless Sensor Networks	in Proceedings of 2nd European Conference on Smart Sensing and Context (EuroSSC)	2007
[ZRP04a]	Active Rules for Sensor Databases	Proceedings of: 1st international workshop on Data management for sensor networks: in conjunction with VLDB	2004
[ZRP04b]	Active rules for wireless networks of sensors & actuators	(Demo abstract) Proceedings of the 2nd international conference on Embedded networked sensor systems, ACM SenSys	2004

Table A.1: Publications related to this thesis

# Appendix B

## Example of Multiple Pattern Matching

This is a simplified example of a suffix array construction for the three user submitted templates `abbbcdbb`, `eeeghaahe`, `hgaaiaab`. In practice, we anticipate longer templates to be supplied by users. The first step involves the construction of the individual arrays. Although for the sake of the example all the suffixes are shown in the table, in practice we prune the Suffix Array as we construct it. Pruning involves the removal of suffixes with length smaller than the minimum length of the user submitted template. This examples assumes that the smaller template has a length of 5, therefore any suffixes smaller than 5 characters are removed.

The resulting Suffix Array is shown in table B.2 with an example of the binary search positions. In this instance the binary search identifies the suffix with two comparisons.

String 1: abbbcdbb	String 2: eeeghaahe	String 3: hgaaiiab
<b>Step 1 (Build Individual Arrays)</b>		
Suffix Array 1	Suffix Array 2	Suffix Array 3
abbbcdbb	aahe	aab
b	ahe	aaiaab
bb	e	ab
bbbcdbb	eeeghaahe	aiaab
bbcdbb	eeghaahe	b
bcdbb	eghaahe	gaaiiab
cdbb	ghaahe	hgaaiiab
dbb	haahe	iaab
	he	
<b>Step 3 (Prune Structure)</b>		
Pos	Index	Suffix
0	(19)	aaiaab
1	(00)	abbbcdbb
2	(20)	aiaab
3	(01)	bbbcdbb
4	(02)	bbcdbb
5	(03)	bcdbb
6	(08)	eeeghaahe
7	(09)	eeghaahe
8	(10)	eghaahe
9	(18)	gaaiiab
10	(11)	ghaahe
11	(12)	haahe
12	(17)	hgaaiiab

Table B.1: Outline of merging and pruning of the array structures involved in Multiple Pattern Matching.

Pos	Index	Suffix	Search Order	Match
0	(19)	aaiaab		
1	(00)	abbbcd		
2	(20)	aiaab	(2)	(√)
3	(01)	bbcd		
4	(02)	bcd		
5	(03)	cd		
6	(08)	eeeghaahe	(1)	(X)
7	(09)	eeghaahe		
8	(10)	eghaahe		
9	(18)	gaiaab		
10	(11)	ghaahe		
11	(12)	haahe		
12	(17)	hgaaiaab		

Table B.2: Example of Binary Search over a (Pruned) Suffix Array. The template of interest is “aiaab”.

# Appendix C

## Software Development Timing Model

We construct a timing model for WSN nodes, analogous to the one introduced by Bentley [Ben99] for guiding software development, by investigating program performance according to implementation choices of data types and operations.

Timing measurements in milliseconds per 5,000 trials are presented in Table C.1 and the impact of floating point arithmetic is illustrated by a factor of 432 slow-down for addition in comparison with integer addition. Integer arithmetic operations larger than the MCU word size require more time than their 16-bit counterparts. 64-bit integer division is almost as slow as floating point division, while other 64-bit operations require less time than floating point operations. Bitwise operations are slower than addition and subtraction but bitwise shifts are faster than division and multiplication. TinyOS tasks, which are placed in separate FIFO queues, are slower — almost by a factor of 2 — than C or TinyOS functions. Hardware-specific results show sampling light and internal voltage sensors slower than sampling temperature and humidity; the similarity between temperature and humidity access times is attributed to sensors located on the same chip (Sensirion SHT1x — [Sen10]).

	<b>Arithmetic (Integer)</b>		
<i>Operation</i>	<i>16-bit</i>	<i>32-bit</i>	<i>64-bit</i>
Increment	6,734	12,824	67,271
Addition	7,955	15,319	88,301
Subtraction	7,969	15,310	87,985
Multiplication	145,020	159,060	316,755
Division	226,265	709,720	3,519,055
Remainder	225,375	706,875	3,540,080
	<b>Bitwise</b>		
AND	7,965	15,285	88,095
OR	7,985	15,325	88,360
XOR	7,955	15,315	88,310
SHIFT	56,735	62,880	573,665
	<b>Floating Point Arithmetic</b>		
Assignment & Cast	2,687,535		
Addition	3,438,530		
Subtraction	3,499,920		
Multiplication	4,841,490		
Division	4,041,785		
	<b>Array Comparisons &amp; Swaps</b>		
Straight Comp	104,095		
Comp C Fcn	83,315		
Comp TOS Fcn	83,335		
Comp TOS task	159,055		
Swap C Macro	93,085		
Swap C Function	83,320		
	<b>Max Function</b>		
Straight Max	137,565		
Max C Macro	137,075		
Max C Function	79,110		
	<b>Built-in Sensors</b>		
ReadLight	327,510		
ReadTemperature	154,125		
ReadHumidity	154,175		
ReadIVoltage	321,635		
	<b>External Flash Chip IO</b>		
Reads (4-bytes)	158,750		
Writes (4-bytes)	191,280		

Table C.1: Performance Times (in ms) for various operations executed by the TMote Sky (measured using TinyOS 2.x and msp430-gcc 3.2.3).

# Appendix D

## Maximum Selection Spatial Location Algorithm

The procedural steps of the Maximum Selection Spatial Location Estimation Algorithm, used as a baseline comparison in the evaluation of Chapter 6 are shown in Algorithm D.1.

---

**Algorithm D.1** Maximum Location Estimation Algorithm

---

- 1: **variables** maxhopcount=1, maxpathlength, netpath[], observations[], counter  $c = 0$ ;
  - 2: **if**  $c \geq \text{maxpathlength}$  **then**
  - 3:   **exit**
  - 4: **end if**
  - 5: Task *unvisited* neighbours within maxhopcount to report measurement.
  - 6: **for** (each of replies received) **do**
  - 7:   calculate maximum observation  $\max(z_k^{(i)})$
  - 8:   **break** and exit if remote observation  $\max(z_k^{(i)})$  is less than local observation.
  - 9: **end for**
  - 10: Select as next hop the node that maximises the observation.
  - 11: Set state to visited, add local address to netpath[c], add  $z_k$  to observations[] and increment  $c$ .
  - 12: Send command message to selected node (line 8) and task it to start at Line 1.
-